Supplementary Materials for

Liquid-liquid phase separation drives skin barrier formation

Felipe Garcia Quiroz, Vincent F. Fiore, John Levorse, Lisa Polak, Ellen Wong, H. Amalia Pasolli, Elaine Fuchs*

*Corresponding author. Email: fuchslb@rockefeller.edu

Published 13 March 2020, *Science* **367**, eaax9554 (2020)
DOI: 10.1126/science.aax9554

This PDF file includes:

Other Supplementary Materials for this manuscript include the following:
(available at science.sciencemag.org/content/367/6483/eaax9554/suppl/DC1)

Supplementary Text

Engineering of clients that function as phase separation sensors

"Phase separation sensors" are a new class of clients optimally designed to interrogate dynamic liquid-liquid phase separation events in a way that does not perturb the process. As we define them, phase separation sensors do not bind specific domains on the scaffold protein. Rather, they engage in ultra-weak molecular interactions with key residues of the scaffold (in this case filaggrin). Consequently, only upon a liquid-liquid phase separation do we expect these proteins to become sufficiently concentrated to enable the sensors to appreciably interact with the scaffold. As our data show, these sensors can exhibit a uniquely high signal:noise ratio and participate innocuously without altering the phase separation process (Fig 4E and fig. S14). This design permits sensitive and innocuous probing of the evolving dynamics of liquid-phase transitions, which as we show in this manuscript, can profoundly impact tissue processes in vivo. Importantly, designing "phase separation sensors" does not require prior knowledge of scaffold protein binding domains.

By contrast, conventional clients were initially defined as macromolecules that are recruited to a condensate by binding to free sites in its protein scaffold (*30*). The underlying assumption has been that clients bind to specific domains within the scaffold protein and engage in specific protein-protein interactions between a domain in the client and a domain in the scaffold protein. Such clients have been successful in directing cargo to test-tube and/or phase separated compartments in cell lines *in vitro*. However, these traditional clients that bind domains within scaffolds have caveats as probes for endogenous phase behavior. They may, for instance, bind to the scaffold prior, regardless of the phase separation process. Moreover, as with fluorescently tagged scaffold proteins (fig. S7G), client binding may alter both the biological features of the scaffold and its phase separation properties. Finally, one-to-one binding of a client to its target limits the client's partition coefficient as binding sites in the scaffold become saturated. This is a common scenario, since clients are often smaller than scaffolds and are thus expressed at higher levels.

We illustrate these critical differences between phase separation sensors and conventional clients by providing a direct experimental comparison with a conventional client that we engineered to bind a small domain within a filaggrin-like protein (figs. S11 and S14). While the conventional client was recruited into filaggrin condensates, it perturbed the normal liquid-like dynamics of the filaggrin scaffold even at concentrations that were well below those at which our phase separation sensors innocuously reported the true liquid-like dynamics of the system. Finally, our engineered client only achieved a partition coefficient of 2.1 (similar to that of other such clients in cells as reported in the literature). By contrast, our phase separation sensors achieved an order of magnitude higher partition coefficient (P=21 for sensor A).

We anticipate the development and utilization of new client-based technologies to study native phase separation processes. This will be important to move beyond protein-tagging and into complex biological systems like tissues and living organisms.

Implementation of phase separation sensors to study phase separation dynamics in skin

Genetically-encoded phase separation sensors feature two domains: a sensing domain proper and a fluorescent reporter consisting of a fluorescent protein with suitable surface characteristics. The overall rationale is well explained above, in the main manuscript and in Fig. S12. The main manuscript also explains in sufficient detail the rationale for the selection and optimization of the fluorescent reporter domain. Here we explain in detail the strategy for the

design of phase separation sensors that are highly sensitive to the phase separation behavior of filaggrin and filaggrin-like proteins.

Considering that a single filaggrin repeat does not drive phase separation in keratinocytes (Fig. 2B), and that non-synonymous human filaggrin mutations often involve His to Tyr mutations (fig. S12B-C), we designed Tyr-high single repeat unit variants (r8H1 and r8H2) to optimize their phase separation propensity (Fig. S12D) and test them as potential phase separation sensors (Fig. S13). Notably, we focused on these mutations as Tyr residues promote the phase separation behavior of IDPs (*22*). Specifically, to generate r8H1, we introduced into the r8 sequence (Table S1) all 11 His to Tyr mutations in GnomAD that specifically mapped to the r8 repeat. Then, to generate r8H2, we further introduced additional His to Tyr mutations that occurred in r9, resulting in a total of 21 His to Tyr mutations. Notably, despite the increasing mutational burden on r8H2, the sensing domain remains His-rich (5.9%) compared with the mean abundance of His in the human proteome (2.3%). We also note that mouse filaggrin has a His content of about 7.7% (significantly lower than human filaggrin or filaggrin from non-human primates). These initial variants shared high sequence identity with the original human r8 filaggrin repeat *(%I* in Fig. 4B). To generate sensor variants with low sequence identity as to avoid using sensor sequences that may have other potential sequence-encoded features of filaggrin —other than its potential for phase-separation-specific interactions—, we used two simple strategies: (i) sequence-reversal and (ii) scrambling of residues. Our preferred strategy is sequence-reversal. Sequence-reversal is interesting because the resulting sensor sequence is identical to the parent sequence when the new variant is read from C- to N-terminus (as opposed to the proper N- to C-terminal direction), so that the overall composition and other physicochemical properties remain unaltered. In our experience this strategy tends to preserve the overall biophysical properties of low complexity IDPs (*22*), unlike scrambling, which can introduce unusual amino acid motifs that are non-native and potentially aggregation-prone. Specifically, we generated the sensor variant ir8H2 by sequence-reversal and the sensor variant pr8H2 by permutation of the r8H2 sequence. As shown in Fig. 4B, these new variants have low sequence identity with respect to the original r8 repeat. Notably, while the phase separation propensity of ir8H2 is nearly identical to that of r8H2, pr8H2 has higher phase separation propensity and in our preliminary experiments showed signs of non-liquid-like behavior, unlike the canonical liquid-like behavior of r8H2-based sequences that we forced into phase separating through the addition of a trimerization domain (Fig. S11C).

We also generated additional (distant) sensor variants that are smaller than a filaggrin repeat but with similar compositional biases (eFlg1, ieFlg1 and eFlg2). Specifically, while the original filaggrin repeat is 324 amino acid resides in length and lacks a clearly discernable internal repeat structure (though low complexity in nature), we engineered a new sensor domain (eFlg1) composed of 5 repeats of a minimal filaggrin repeat that is only 40 amino acid residues in length (GRDGSHSYQGDRSGHSHQRQGYHEQSDRAGHGDSGHRGYS). This minimal repeat does not occur in filaggrin, but some short motifs do occur within r8 (RQGYH, DRAGHG, EQS, RDGS, DSGHRGYS) and the overall design is modeled after a canonical UCST phase transition protein-polymer with low phase separation propensity (*22*). We then generated ieFlg1 by sequence-reversal of eFlg1. eFlg2 corresponds to a sensor domain that approximates the size of r8 by directly fusing a 4-mer of the eFlg1 repeat with a 4-mer of the ieFlg1 repeat (Table S3).

Overall, we suggest that the use of naturally-occurring non-pathogenic mutations within specific domains of human phase-sensitive proteins followed by sequence-reversal constitutes a straightforward and likely general approach to the design of highly sensitive phase separation

sensors that are tailored for specific biological systems. As our knowledge of phase separation behavior in IDPs increases, other strategies will likely become feasible, as we also demonstrate here with the design of fully engineered sensor domains (e.g. ieFlg1 in Sensor B, Fig. 4C).

Script to analyze mutational profiles in human filaggrin

The MATLAB script below handles SNP data from GnomAD browser. The Script is nearly identical to handle SNPs from dsSNPs. The resulting data (Fig. S12B-C) was plotted using OriginPro.

```
%Script to handle data from the GnmomAD Browser (similar to dsSNP data)
clear all
file=tdfread('Flg_GenomeADv1.txt'); %downloaded Flg SNPs

%Assignment of GnomAD data to specific MATLAB variables
ids=file(1).VariantID(:,:);
mut=file(1).Proteinchange(:,:);
mtype=file(1).Type;
misse=find(mtype(:,1)=='m');


%Filtering of data to eliminate repeated entries in dataset
misid=ids(misse,:);
mispc=mut(misse,:);
[umisid,nn,nn2]=unique(misid(:,:),'rows'); %seems like all missense are unique in EVS (so this step may be unncessary).
umispc=mispc(nn,:);

%Processing of mutational data to identify coding mutations
ns=1;
for i=1:length(umispc) %create vector res1 (X1Y1) with original residue (X1) and its mutated form (Y1)
  aux=strtok(umispc(i,:));
  res(1,:)=aux(3:5); %original residue
  res(2,:)=aux(length(aux)-2:end); %mutant residue
  position(ns,1)=str2double(aux(6:length(aux)-3));
  for j=1:2
  if strcmp('Ala',res(j,:));res1(ns,j)='A';end
  if strcmp('Val',res(j,:));res1(ns,j)='V';end
  if strcmp('Leu',res(j,:));res1(ns,j)='L';end
  if strcmp('Ile',res(j,:));res1(ns,j)='I';end
  if strcmp('Met',res(j,:));res1(ns,j)='M';end
  if strcmp('Phe',res(j,:));res1(ns,j)='F';end
  if strcmp('Tyr',res(j,:));res1(ns,j)='Y';end
  if strcmp('Trp',res(j,:));res1(ns,j)='W';end
  if strcmp('Ser',res(j,:));res1(ns,j)='S';end
  if strcmp('Thr',res(j,:));res1(ns,j)='T';end
```

```
    if strcmp('Cys',res(j,:));res1(ns,j)='C';end
    if strcmp('Gln',res(j,:));res1(ns,j)='Q';end
    if strcmp('Asn',res(j,:));res1(ns,j)='N';end
    if strcmp('Lys',res(j,:));res1(ns,j)='K';end
    if strcmp('His',res(j,:));res1(ns,j)='H';end
    if strcmp('Arg',res(j,:));res1(ns,j)='R';end
    if strcmp('Asp',res(j,:));res1(ns,j)='D';end
    if strcmp('Glu',res(j,:));res1(ns,j)='E';end
    if strcmp('Pro',res(j,:));res1(ns,j)='P';end
    if strcmp('Gly',res(j,:));res1(ns,j)='G';end
    end
    ns=ns+1;

end

%Start of section that calculates global (non-syn) mutaional frequencies
[allm,nn0,n1]=unique(res1(1:end,1)); %freq of mutations at all X residues

for i=1:length(allm)
   freqX(i,1)=length(find(n1==i))/(length(n1)); %non-synonymous mut-only
  end
%end of section to calculate global frequencies

LmutS=find(res1(1:end,1)=='H'); %select (S) mutated residue to analyze (e.g. His)
StoX=res1(LmutS,2);
lss=length(find(StoX=='H')); %finds syn mutations
[u,nn,n2]=unique(StoX); %finds all unique residues
ln2=length(n2);
for i=1:length(u)
   freqStoXwoS(i,1)=length(find(n2==i))/(ln2-lss); %non-synonymous mut-only

end

muttype=[lss; length(StoX)-lss;(length(StoX)-lss)/length(res1); length(res1)]; %total syn
(lss, should be zero) and nonsyn mutations
%note that res1 doesn't contain any syn mutations due to the way it was
%generated
summary=[freqStoXwoS;muttype];
```

Fig. S1.

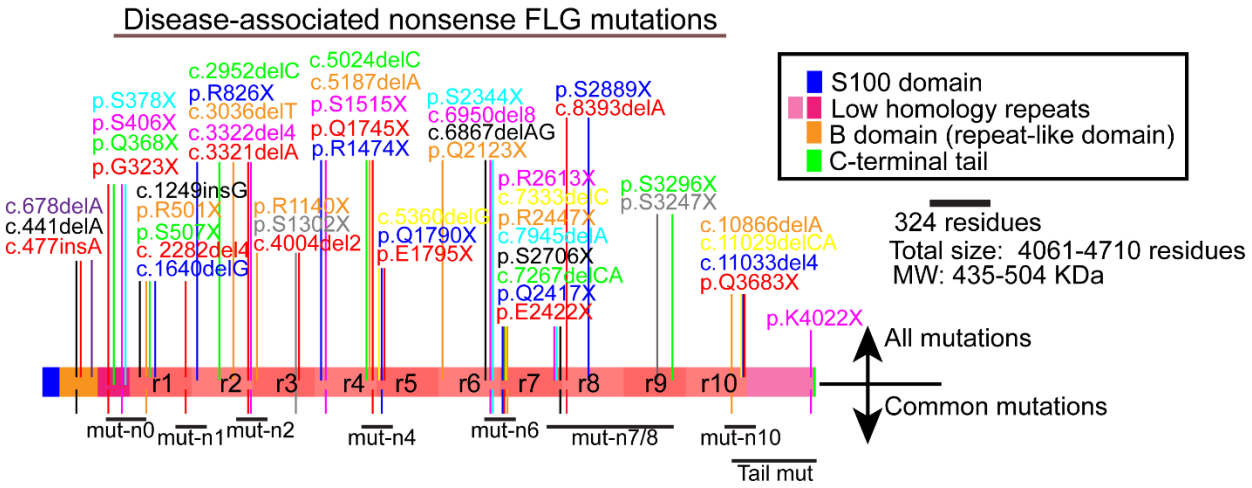

Nonsense human FLG mutations associated with skin barrier disorders A comprehensive list of truncating human FLG mutations [compiled from ref 27 in the main manuscript and (*62*)], with their relative location across the length of the FLG protein denoted by colored lines that cut/truncate the protein. Lines that project below the indicated domains highlight mutations that are most common across European and Asian patients (typically >2% of patients). Because of the wide spectrum of mutations and their apparent clustering at different locations across the protein, we grouped mutations by the number of FLG repeat domains that are spared in each group of truncated variants (mut-n0 to mut-n10, that is mutants left with 0 FLG repeats to 10 repeats). A common variant, p.K4022X, occurs at the C-terminal end of FLG, sparing all repeats but ablating the small 26 a.a. C-terminal tail domain. We refer to this mutant and others that spare all FLG repeats (note that some humans have up to 12 FLG repeats) as 'Tail mutants'.

Fig. S2.

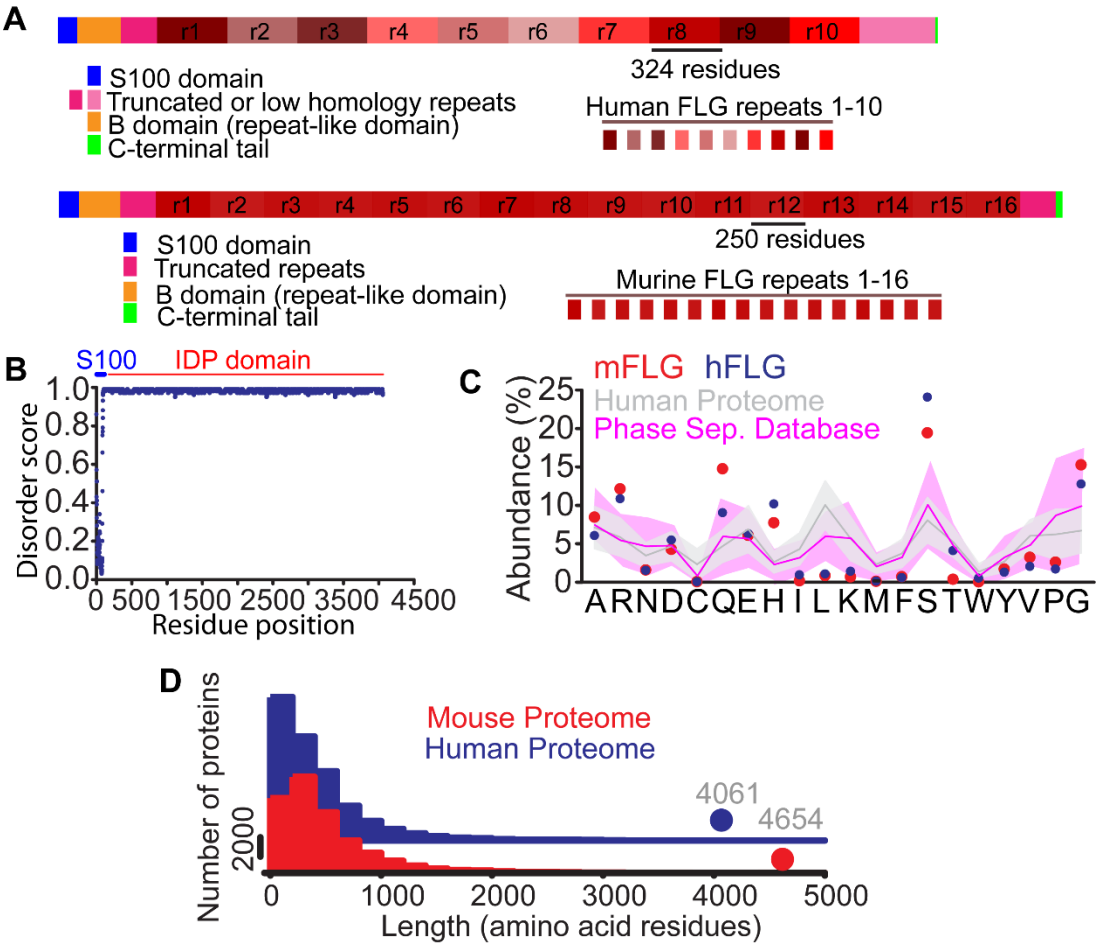

Sequence features of FLG and its paralogs across mammalian species. (A) While both mouse and human FLG share a repeat architecture and similar non-repeat domains, their repeat units and overall repeat domain differ greatly at the sequence and organization levels. Human FLG typically has 10 near perfect copies of a 324-residues repeat (with humans having up to 12 repeats), whereas repeat length in mouse FLG typically spans 16 copies of a near perfect 250-residue repeat. Total number of FLG repeats also varies across mouse strains. Because of this divergence in the repeat domain, FLG sequences are typically identified through sequence conservation in the short S100 domain. Color variations across individual repeats point to subtle changes in repeat identity —mouse FLG has higher repeat identity than human Flg repeats (~95% vs 99%, respective). (B) Disordered regions in human FLG. The disorder score for each residue in the protein was calculated using DISOPRED (*63*)—a score of 1 is characteristic of IDP regions. Note that for human FLG only the first 100 residues (corresponding to the S100 domain) are ordered (folded). (C) Amino acid abundance for all amino acid residues across mouse and human FLG. Only a handful of residues (Fig. 1C) account for the majority of their composition and these biases are well-conserved across mice and humans. The mean proteome-wide abundance of each residue in human proteins is shown as a gray line (the filled area shows the standard deviation). Abundance values are nearly identical for the mouse proteome. We also show the mean abundance (magenta line) of each residue in protein domains that are part of PhaseSePro (a database of manually curated protein drivers of liquid-liquid phase separation)

(*51*) —the filled area (magenta) shows the standard deviation. Note that Pro, Gly and Ser are prominently enriched in FLG and in protein domains found in PhaseSePro, whereas His is uniquely enriched in FLG. (D) Proteome-wide distribution of protein size in mice and humans readily reveals that FLG is among the largest proteins in its corresponding proteome.

Fig. S3.

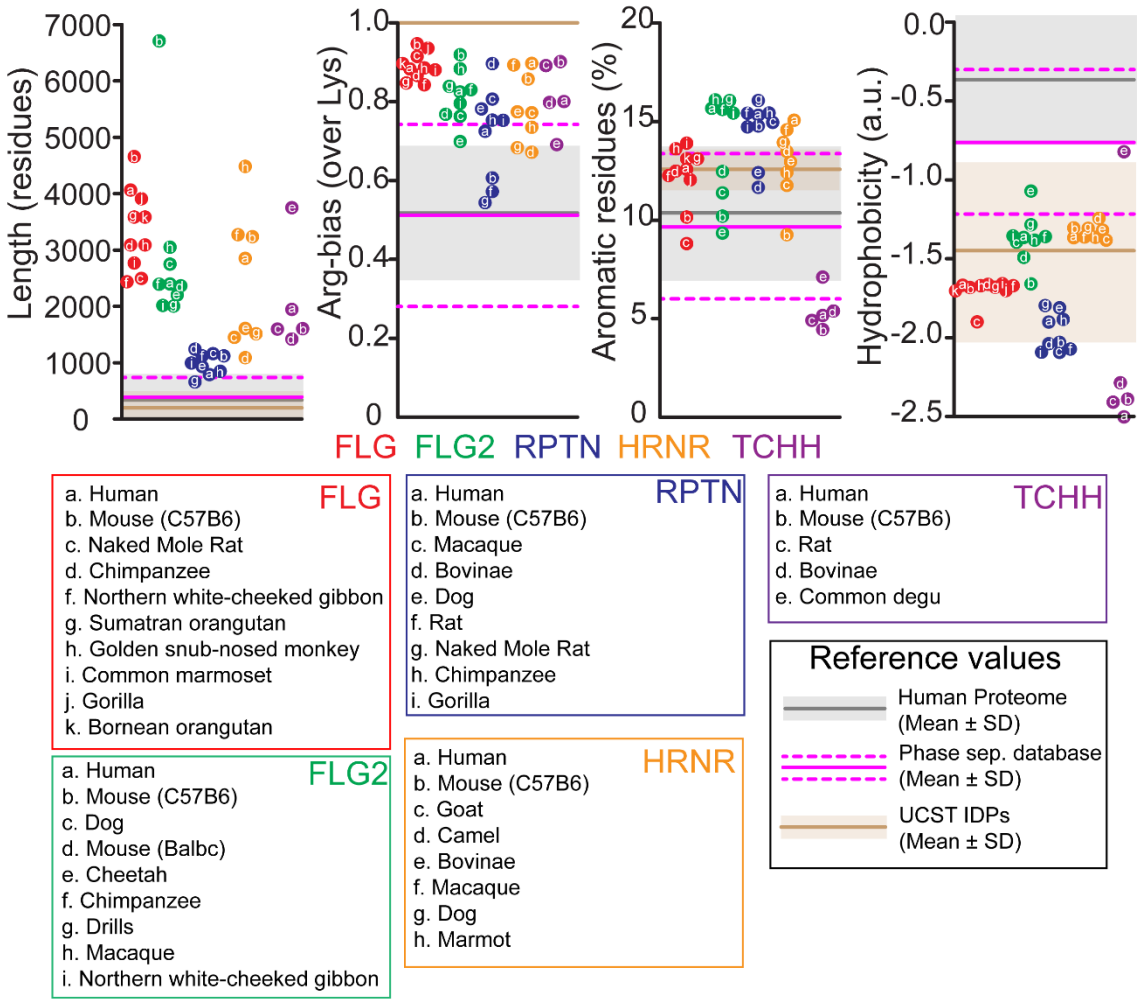

Sequence features of FLG and its paralogs across species. Analysis of sequence-encoded features that are indicators of upper critical solution temperature (UCST) phase separation behavior in low-complexity proteins across of FLG and its paralogs (FLG2, RPNT, HRNR and TCHH) in mice, humans and other mammalian species (see Table S1 for additional details). These indicators were recently proposed as important sequence determinants of UCST-type phase behavior in IDPS (Ref. 18 in the main manuscript). Arginine-bias was calculated as [R/(R+K)]. Percent of aromatic residues corresponds to the sum of Y, H and F residues divided by total number of residues. Hydrophobicity was calculated using the Kyte-Doolittle hydropathy scale (*52*), where increasingly negative values mirror increases in hydrophilicity. As reference values for these sequence features, we have included the mean value and standard deviation of each parameter across (1) all proteins in the human proteome, (2) all protein domains in the PhaSEPro database that were manually curated (as of October 2019) as drivers of liquid-liquid phase separation (*51*), and (3) recently characterized UCST-exhibiting IDPs. We note that FLG is not part of PhaSEPro, and the proteins in PhaSEPro are not discriminated based on sequence-encoded mechanisms of phase separation. As a result, we do not expect PhaSEPro-derived parameters to exactly recapitulate the core sequence-features of canonical UCST-type IDPs. For instance, PhaSEPro encompasses classical LCST-exhibiting IDPs like tropoleastin (LCST is the mirror behavior to UCST and both behaviors are encoded differently in IDPs; see ref 22) as well

as RNA-binding proteins that likely exhibit UCST-type behavior but whose phase separation is RNA-dependent in many cases. Despite these limitations, we observe that the sequence features of FLG and its paralogs are very similar to those of UCST-exhibiting IDPs and that sequence-biases discerned from PhaSEPro align better with UCST-IDPs and with FLG than do the overall distribution of these parameters in the human proteome.

Fig. S4.

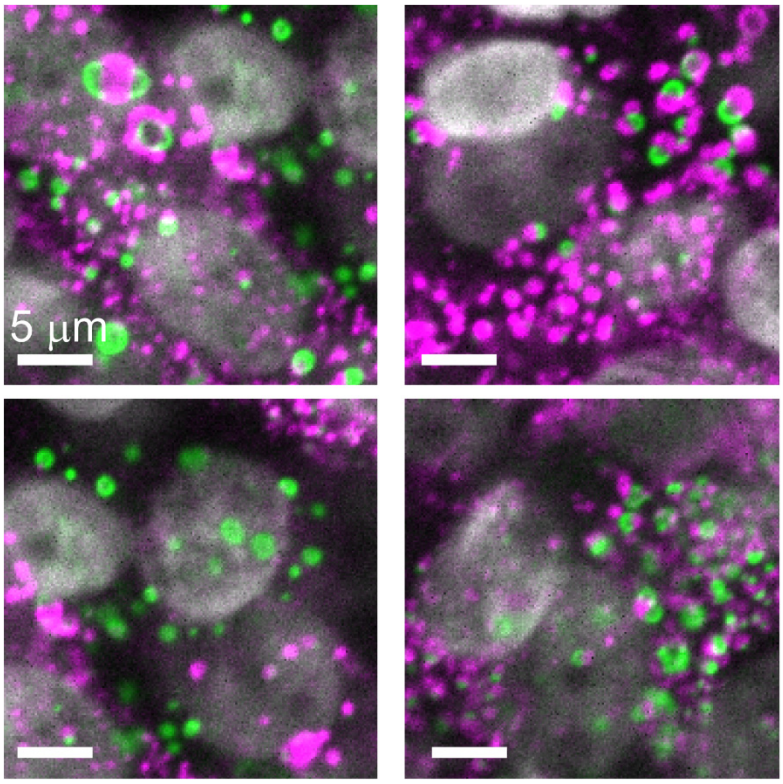

FLG and RPTN (a FLG paralog) form distinct micron-sized granules in HaCATs. Immortalized human keratinocytes (HaCATs) do not form KGs when submerged in medium. However, when cultured at the air-liquid interface for 16 days, as shown here, immunostaining against human FLG (red) or human RPTN (green)reveals endogenous granule formation. Images are close-up views of cells in the granular layer of these cultures. As a note, all other subsequent experiments in this manuscript, we used submerged culture conditions (see methods), where cells remain as progenitors.

Fig. S5.

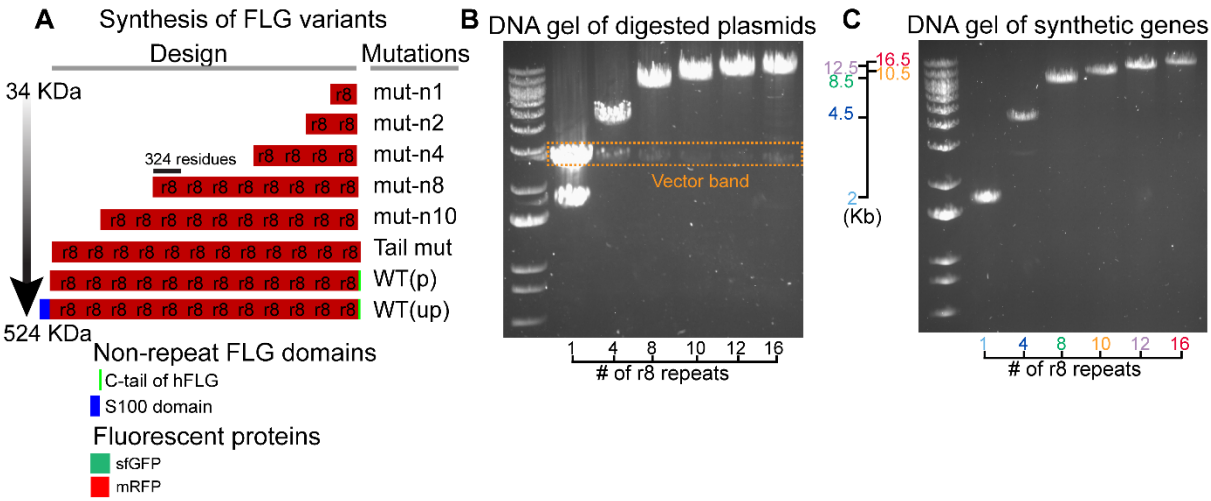

Synthesis of long repetitive DNAs encoding human FLG variants. (A) Efficient iterative synthesis of repetitive FLG-like genes and their fusions to non-repeat FLG domains and fluorescent proteins using a plasmid reconstruction approach (see Table S2 for sequence details) (*53*). These genes are based on the r8 repeat of human FLG (r8 is one of 10 near perfect repeats as shown in Fig. 1B) (B) Electrophoresis of plasmids harboring synthetic Flg genes (fusions to sfGFP in this example) with the indicated number of repeats and digested at NheI and EcoRI sites that flank the genes. Each lane shows a constant fragment that corresponds to the digested vector. The left most lane is a DNA ladder (1Kb plus DNA ladder, Thermofisher Scientific). This gel corresponds to a 0.8% agarose gel (with SYBR Safe) ran over 1.5 h (at 130V) to improve separation between the largest repetitive genes. (C) To better show the size distribution of the synthetic FLG genes we gel purified the corresponding gene bands from (B) and performed a new electrophoresis using similar conditions as in (B). The scale bar (in Kb) shows the precise size of each construct.

Fig. S6.

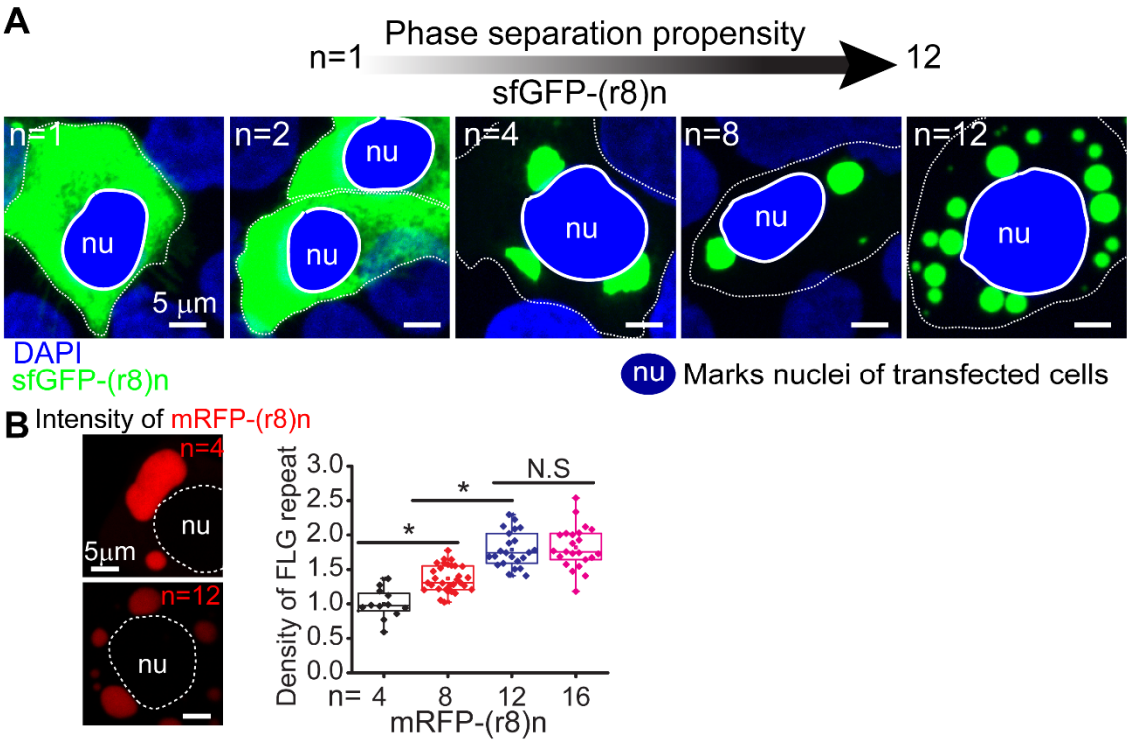

Phase separation properties of FLG repeat proteins. (A) We transfected HaCATs with sfGFP-tagged constructs with increasing number of FLG repeats (n=1 to n=12, where "n" is the number of repeats; see Table S2 for sequence details) and saw that their phase separation propensity (i.e., the ability to form granules or condensates in the cell) was largely dependent on the number of FLG repeats. Below n=4, well-defined granules did not form and sfGFP was cytoplasmic. At n=4, most of the sfGFP fluorescence was compartmentalized into well-defined granules, establishing two phases (dilute and dense) characteristic of phase-separated systems. Constructs with more than 4 repeats typically showed more granules with highly spherical morphologies that were reminiscent of endogenous FLG granules in culture (Fig. S4). Nuclei (nu, DAPI) of transfected cells are circled. (B) Changes in FLG repeat density within cytoplasmic granules that formed *de novo* in HaCATs upon transfection of mRFP1-tagged FLGs with variable numbers of the r8 human FLG repeat (see Fig. S1B). When mRFP1 fluorescence intensities were normalized according to FLG repeat number (e.g. 3X more r8 units per mRFP1 molecule in constructs with n=4 vs n=12), it was clear that the density of repeats was highest within KGs assembled from proteins with the greatest FLG repeat numbers. (B) Fluorescence recovery after photobleaching (FRAP) half-lives of granules composed of FLG repeat variants in (A). Top, representative images of a recovery event; Bottom, quantifications. Dots represent individual FRAP half-life measurements (of granules in different cells) from two experiments. All images correspond to maximum intensity projections of Z stacks spanning the volume of cells in the field of view.

Fig. S7.

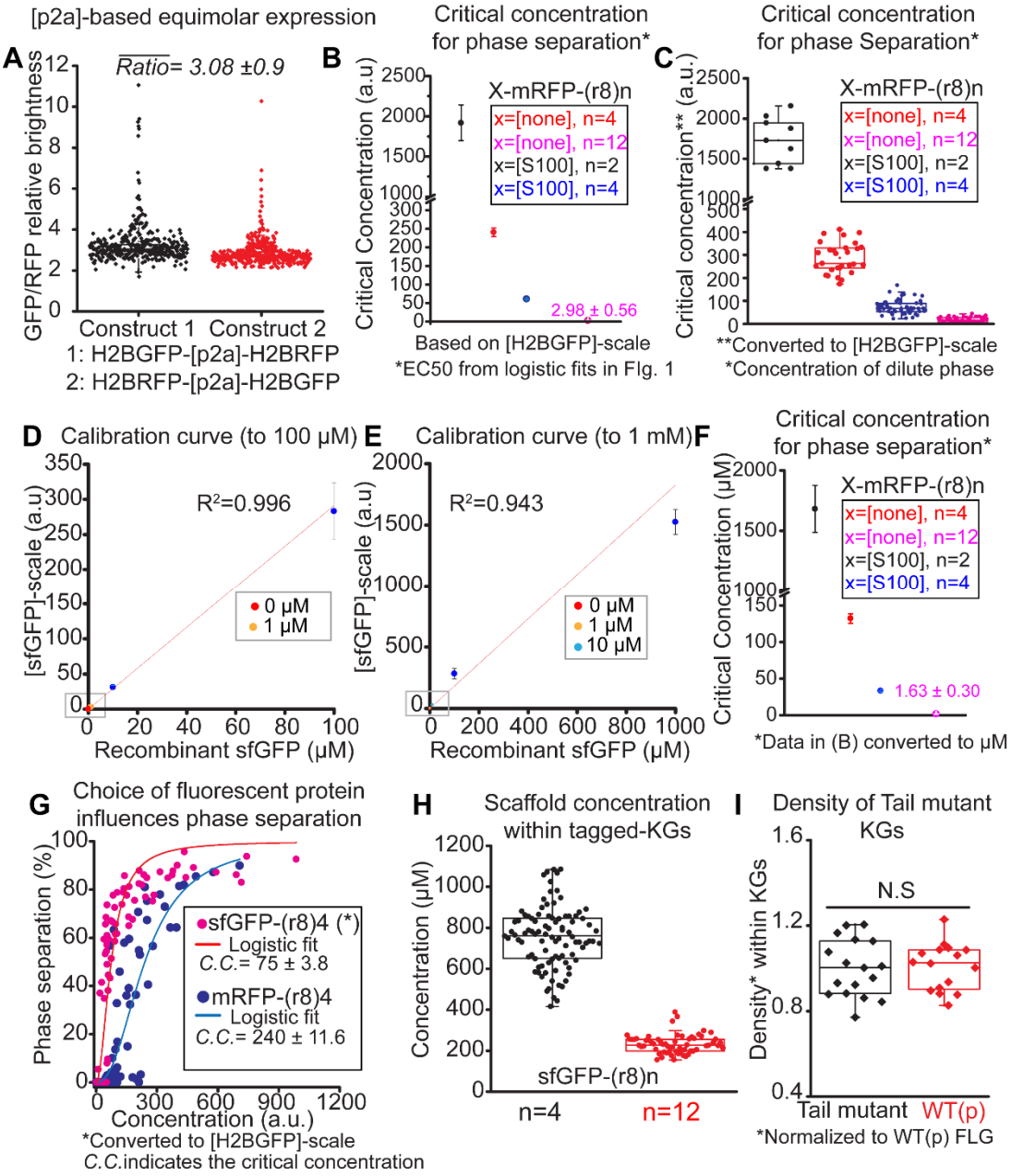

Critical concentration for phase separation and characterization of FLG variants. (A) Relative H2BGFP to H2BRFP brightness for HaCATs that express H2BGFP-[p2A]-H2BRFP or H2BRFP-[p2a]-H2BGFP. [p2a] is an optimized self-cleaving peptide sequence that ensures equimolar synthesis of its N- and C-terminal fusion proteins. Each dot is a measurement from an individual nucleus. The overall average ratio matches the published relative brightness of EGFP and RFP (ratio=3) irrespective of the fusion format, confirming that our strategy works well to produce equimolar amounts of [p2a]-fused constructs upon their expression in HaCATs. The shown average ratio (3.08) and standard deviation accounts for all data acquired for constructs 1 and 2. In subsequent analyses and for conversion between RFP-based and GFP-based concentration values, we use a ratio of 3.0. For clarity, throughout the manuscript, a GFP-based scale is used. (B) Critical concentration for phase separation based on logistic fits from data in

Fig 1G. Operationally, this critical concentration was defined as the *EC50* of the logistic fits, that is the concentration at which most cells achieve a phase separation response of 50% —wherein the total number of molecules in the dilute phase equals the number of molecules in the high density phase. While phase separation happens with a given (low) probability below the EC50 (as can be seen in our data), the concentration fluctuations that potently drive phase separation near the true critical concentration of the system become dominant near the EC50, which justifies its definition as an experimental approximation to the critical value. (C) Critical concentration for phase separation estimated from the concentration of protein in the dilute phase (which exists at the verge of phase separation into the high density phase). Note that these estimates are in excellent agreement with values derived from logistic fits in (B). The advantage of this additional approach to estimate the critical concentration for phase separation is that in this case we only need to consider select cells that already underwent phase separation, whereas for the approach in (B) we need to sample cells that express FLG variants across the entire concentration regime (below and above the critical concentration for phase separation). Note that across the data in Fig 2B and 2D, as well as here in B-C, we consistently see that as the critical concentration for phase separation goes down with S100-fusion or with long repeat domains, the sharpness of the phase transition increases.(D) Purified recombinant sfGFP in PBS at different concentrations (in μM) and its respective concentration values based on fluorescence measurements (reported in arbitrary units). The measurements were done in a similar fashion as in our typical cell-based experiments to account for photobleaching in our imaging protocol. Our limit of detection is ~ 1uM. (E) Linearity is lost for very high sfGFP concentrations (in the order of magnitude found within KGs, ~500 μM-1mM). We use calibration curves in D-E as a rough guideline to gage the range of concentrations (in μM units) at which FLG variants undergo phase separation. We note that based on the intrinsic brightness of EGFP vs sfGFP, [sfGFP]-scale = 1.6 x [H2BGFP]-scale. (F) Critical concentration for phase separation (based on data in B) but converted to μM values based on calibration curves in (D)-(E). (G) Choice of fluorescent protein has a bearing on the measured critical concentration for phase separation for fluorescently-tagged FLG variants. We see that sfGFP-based constructs enhance the phase separation behavior of FLG variants with respect to mRFP-based constructs. The extent of this enhancement is similar to the response measured for constructs with the S100 (dimerizing) domain of human FLG (Fig. 2D), which likely points to weak dimerization of sfGFP (*64*) as a factor that alters the biophysical properties of tagged-FLG. (H) Concentration of the filaggrin scaffold (in μM units) within KGs assembled in HaCATs by transfection of two different sfGFP-tagged FLG variants (one is WT-size, n=12, and the other one is a disease-associated variant with 4 FLG repeats). (I) Quantification of FLG density within KGs studied in Fig. 3B of the main manuscript. Note that changes in FLG density within these KGs are not responsible for the observed changes in FRAP dynamics. N.S, not statistically significant.

Fig. S8.

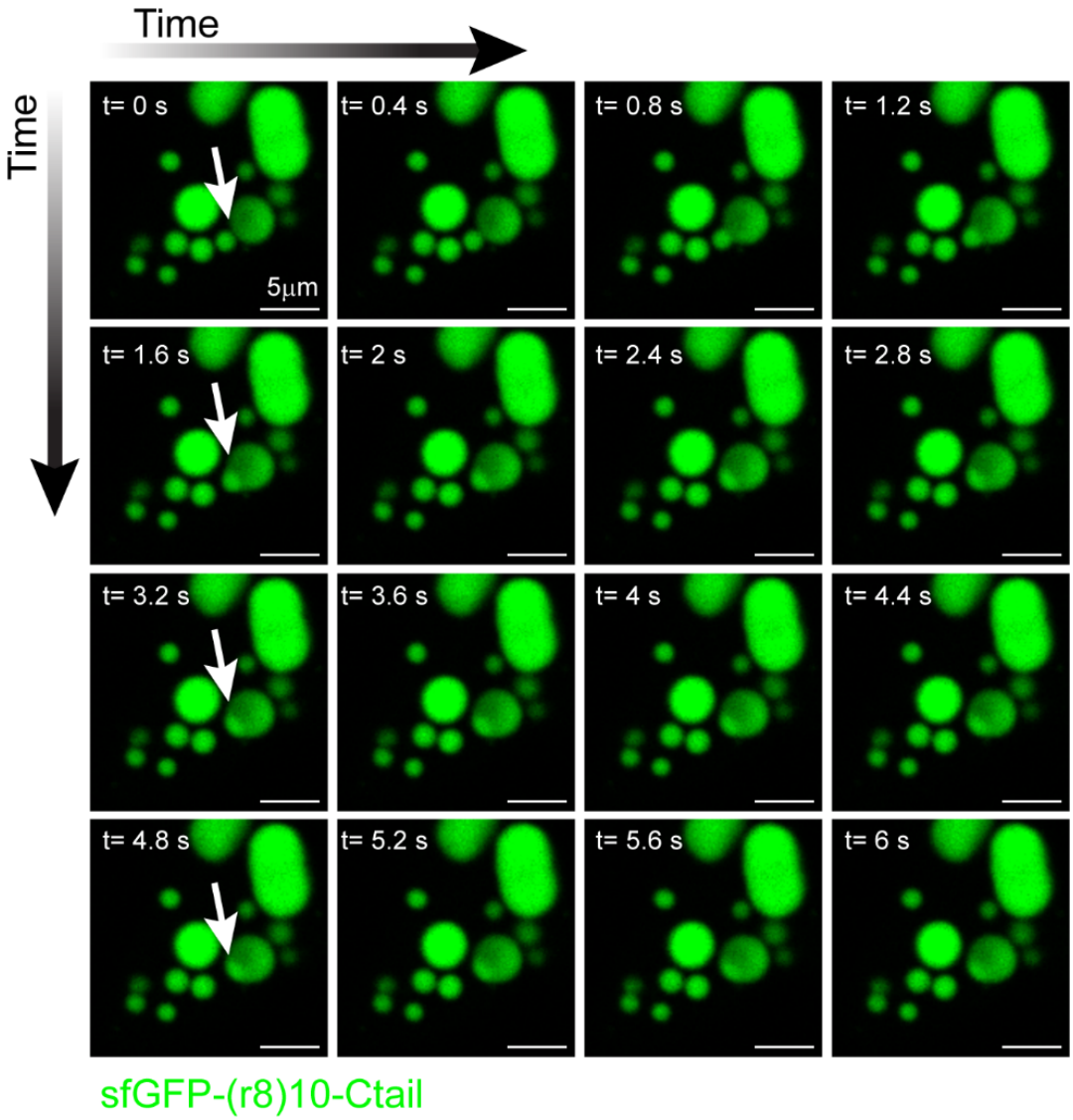

Fusion between two sfGFP-FLG granules at high temporal resolution. Related to Movie S2, these are snapshots 400 ms apart between two sfGFP-tagged FLG granules in HaCATs expressing WT(p) sfGFP-tagged FLG [sfGFP-(r8)10-Ctail]. Arrows point to the resolution of the fusion event over 5 seconds.

Fig. S9.

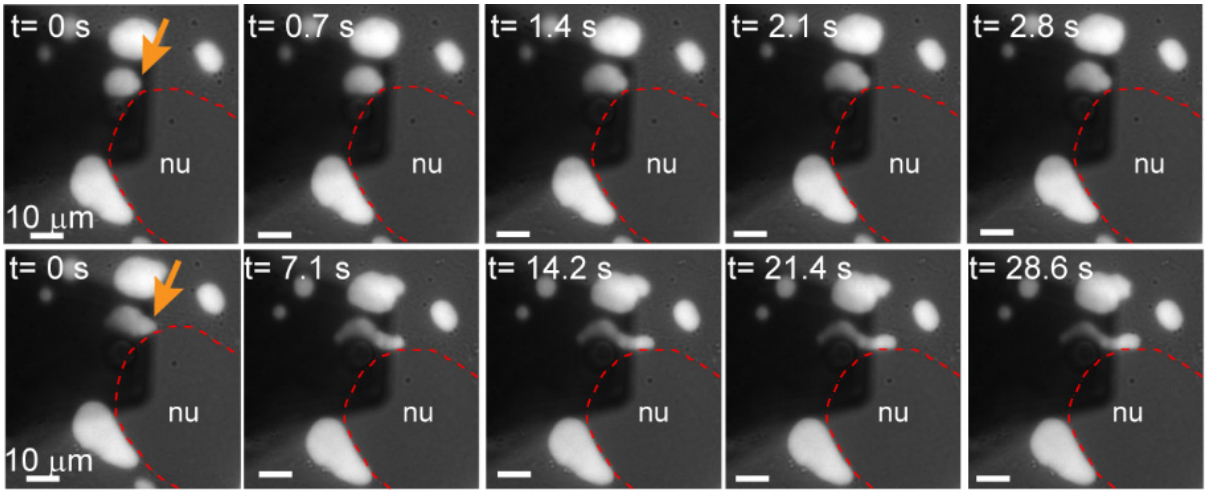

Mechanical deformation of tail mutant FLG granules with an AFM probe. Temporal evolution of granule morphology, in HaCATs cells expressing a tail mutant FLG [sfGFP-(r8)8], upon their mechanical loading with an AFM probe. The AFM probe is seen as a dark shadow over the cell. Images correspond to a combination of bright-field (DIC) and GFP fluorescence, so granules appear white. Granules in this field of view are produced by a single transfected cell, which nuclei was marked with H2B-RFP. For clarity, we outline the nucleus (nu) with a red dashed line. Arrows point to the granule morphology prior to its major deformation. The top and bottom panels show two different short time series as the same granule is pushed by the AFM probe. The bottom panel corresponds to the liquid-like streaming of a granule around the nucleus that is also shown in Fig. 3D of the main manuscript and in Movie S3.

Fig. S10.

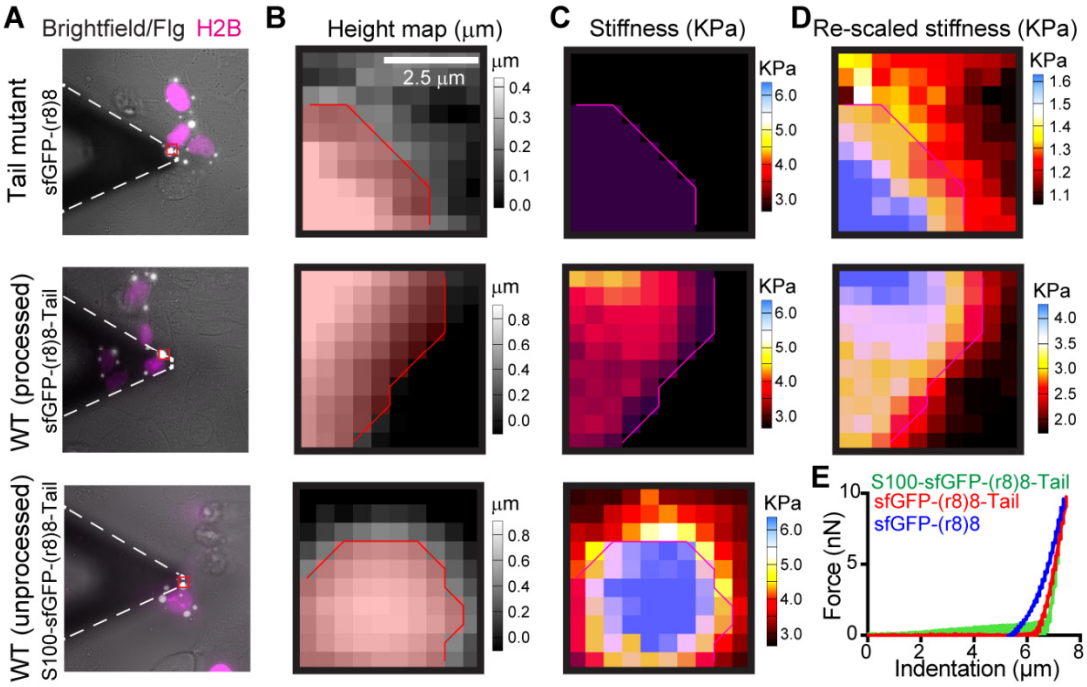

Representative AFM height and stiffness maps for granules assembled from FLG processing variants and tail FLG mutants. (A) Simultaneous bright-field (DIC) and GFP fluorescence of specific, representative granules (marked by a red square) characterized by serial force-indentation measurements using AFM. For this experiment, HaCATs were co-transfected with the indicated FLG variants and a plasmid harboring H2B-RFP. The nuclear mRFP1 signal is shown overlaid over the brightfield/GFP signal. (B) Height maps from the AFM scan readily outline granule morphology, so we used them to create granule masks (labeled in red). We applied those masks to their corresponding stiffness maps (see Methods) (C) in order to average stiffness measurements over all pixels within the granule domain. (C) Note the striking changes in granule stiffness, with tail FLG mutants being particularly soft. FLG processing is clearly important to limit stiffening of granules (see Fig. 3F in main manuscript for average values across several granules per condition). (D) Re-scaled stiffness maps to visualize the full distribution of stiffness values for granules assembled from a tail mutant and its WT (p) counterpart. (E) Raw AFM force measurements for an indentation event within the corresponding granule masks in B.

Fig. S11.

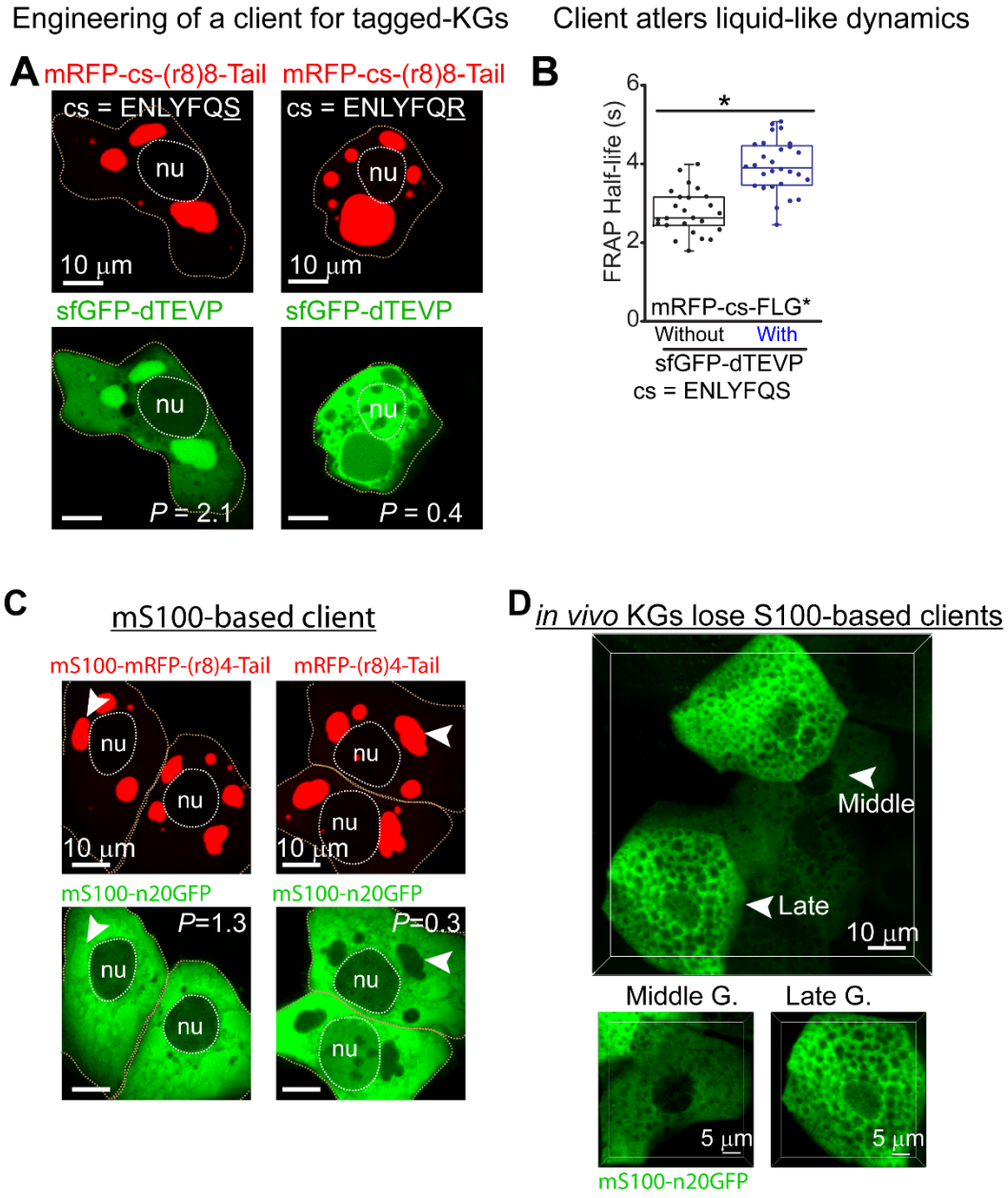

Conventional clients have limitations as *in vivo* probes of endogenous phase separation behavior. (A-B) Conventional clients are typically fluorescently-tagged proteins that bind to phase-separated scaffold proteins. To generate such clients and assess their effects on KGs, we introduced the short peptide ENLYFQS, which corresponds to the canonical TEVP protease cleavage sequence (cs) (*65*), into a mRFP-FLG* construct. The resulting construct [mRFP-cs-(r8)8-Tail] was then expressed in HaCAT cells which were also transfected with a fluorescently-tagged, protease-dead variant of TEVP (*65*) (sfGFP-dTEVP, see Table S5 for sequence details). The engineered client was nicely enriched within the mRFP-cs-FLG* KG-like granules that formed (left panels). However, the partition coefficient of this conventional client (P=2.1) remained low, as compared to the very high partition coefficient (P>20) of the new class of phase separation sensors that we generated (see Fig. 4). Note that the TEVP protease cleaves

ENLYFQR with very low efficiency, serving as a control with very low affinity for the scaffold. This single point mutation in the cleavage sequence was sufficient to abrogate enrichment of the client into cs-containing KGs. (B) Recovery half-lives (in seconds) after photobleaching mRFP1-cs-FLG* signal in granules with or without the dTEVP client. The enrichment of the dTEVP client within tagged-KGs slowed down the liquid-like dynamics of FLG in this system. Taken together, the data in A and B show that although sfGFP-dTEVP can function as a client for phase-separated condensates, it alters the underlying liquid-liquid like dynamics, precluding its use for studying the material properties of endogenous phase transitions *in vivo.* Images are maximum intensity projections. Asterisks, statistically significant ($p<0.05$). (C-D) The S100 domain of FLG is processed relatively early in the epidermal differentiation program. In (C and D), we show that although an S100-based client can be used to detect (albeit weakly) unprocessed FLG assembled into KGs, once it is processed, KGs remain intact but this client no longer recognized KGs. This result points out another potential caveat in designing conventional clients to study liquid phase transitions in tissues, namely the potential modification or processing of client-bound domains in the scaffold that eliminate client-binding but are otherwise nonessential for the scaffold's phase separation behavior. (C) We created tagged-FLG* constructs containing the S100 domain from mouse FLG [mS100-mRFP-(r8)8-Tail, see Table S5 for sequence details], and engineered a corresponding client by fusing the same mS100 domain to -20GFP with a C-terminal nuclear export signal (mS100-n20GFP, see Table S5 for client details). HaCATs transfected with mS100-n20GFP and FLG* with and without the mS100 domain. Note that the enrichment of the mS100-based client, while poor, is entirely dependent on the presence of the mS100 domain in FLG*. "*P*" indicates the partition coefficient for mS100-n20GFP. Dotted lines mark approximate cell boundaries. (D) Live imaging of mouse epidermis *in utero* transduced to drive suprabasal expression of mS100-n20GFP. Note that even relatively immature middle granular cells in mouse E18 skin already exclude mS100-sfGFP, which should be otherwise enriched within mS100-containing KGs (based on the behavior observed in A).

Fig. S12.

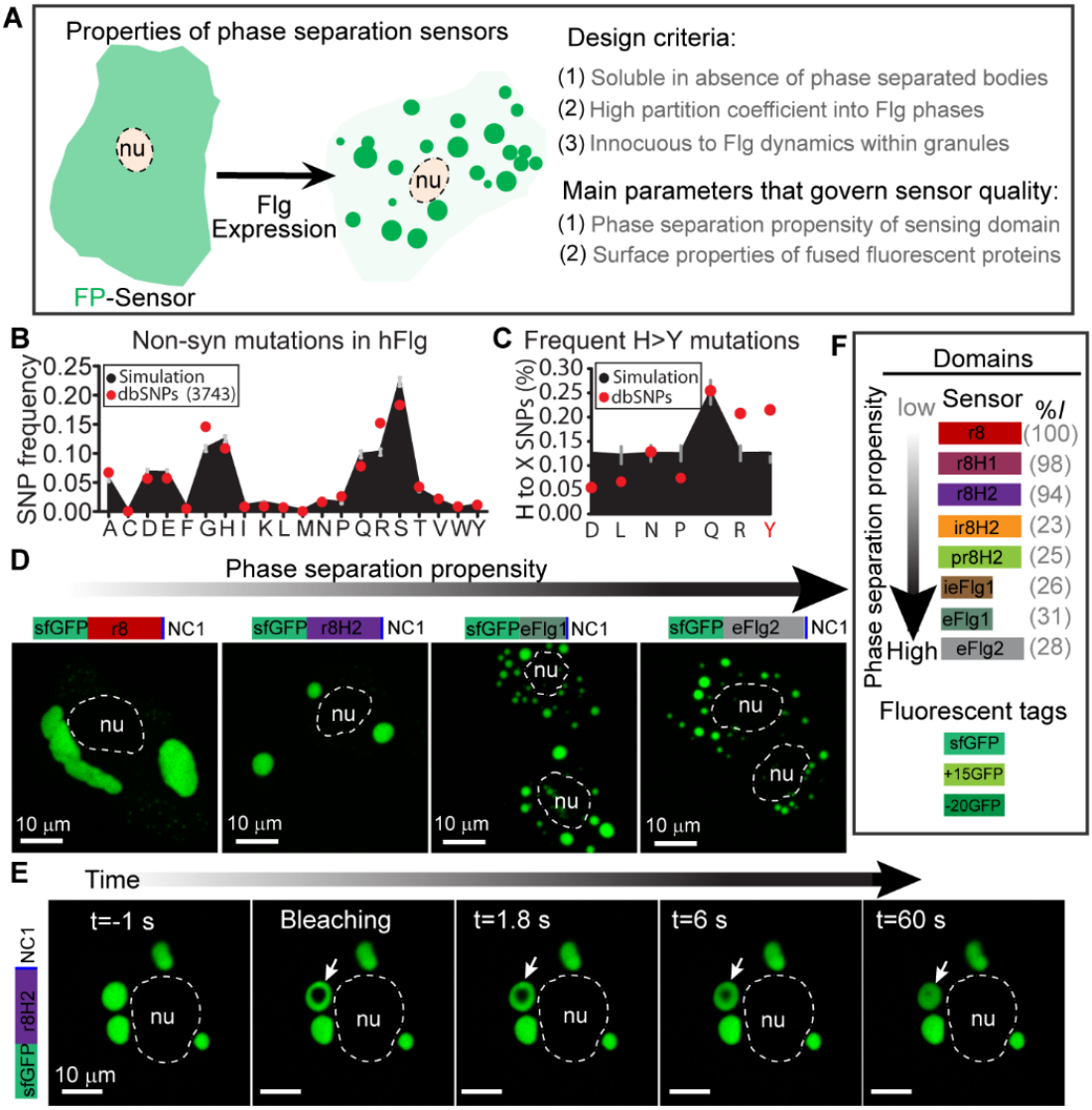

Engineering of phase separation sensors. (A) Concept and design criteria for a phase separation sensor capable of sensing the phase separation behavior of filaggrin. (B) Frequency of non-synonymous mutations for each amino acid in human FLG based on the dbSNPs database (from a total of 3743 SNPs in the *FLG* gene). We show that the observed SNP frequency matches the expected mutational burden from simulations of a random mutational process that targets the most abundant codons in Flg. Histidine codons, being particularly abundant in Flg, are amongst the most commonly mutated. (C) Analysis of non-synonymous mutations involving His residues in human FLG. Note that His codons in *FLG* are frequently mutated to Tyr (Y) codons and that the frequency of these mutations cannot be predicted from simulations of a random mutational process. At the time of our analysis we identified 87 H>Y mutations (from 405 SNPs involving non-synonymous His mutations). We used these mutations to generate Tyr-high variants of a human FLG repeat (r8 in Fig. 1B) (see Fig. 4B in the main manuscript and supplementary text). (D) To qualitatively assess the phase separation propensity of a FLG repeat unit and its Tyr-high variants, we fused them to a fluorescent protein at the N-terminus and a trimerization domain (NC1 domain from human COL18A1) at their C-terminus. Multimerization

is a known mechanism to augment phase separation propensity —we have also confirmed this observation with a bacterial trimerization domain (foldon), see methods and supplementary text. Transfection of HaCATs with these engineered FLG repeat variants allowed us to rank their phase separation propensity based on the morphology and number of observed granules. Note that even after trimerization, the original FLG repeat fails to form compact granules and instead forms very large phases with shapes indicative of protein domains with very low surface tension. (E) Representative photobleaching experiment confirming the liquid-like behavior of Tyr-high variants (upon their trimerization). (F) To identify phase separation sensors with ideal performance (see criteria in A), we fused the original FLG repeat and its Tyr-high variants to three different fluorescent proteins that span a wide range of surface charges (see Table S3 for sequence details). Here we also indicate the sequence identify of each variant with respect to the original FLG repeat (r8).

Fig. S13.

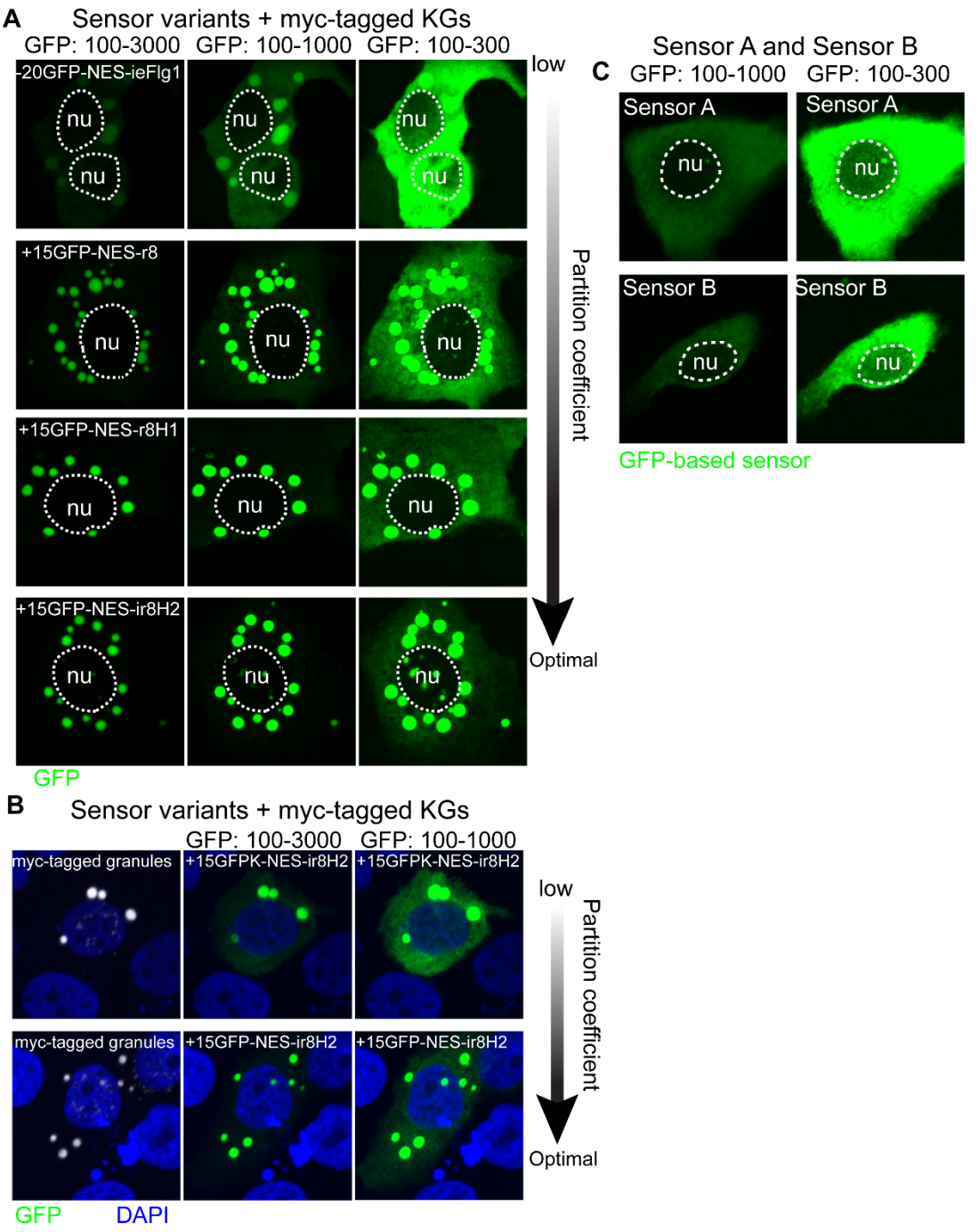

Evaluation of phase separation sensor designs. (A) Live imaging data for HaCATs transfected with a myc-tagged granule forming protein (myc-r8H2-foldon; foldon is a bacterial trimerization domain) and multiple sensor designs. Negatively-charged sfGFP variants lead to low partition coefficients into engineered KGs. Super-positively charged sfGFP provide improved partitioning into myc-tagged KGs and the partition coefficient is further enhanced by selection of a sensing domain with optimal phase separation propensity (ir8H2 in this case). Images correspond to

maximum intensity projections. Each row corresponds to a sensor design and to the same image under different levels of signal saturation (shown in the legend as the range of allowed values for the GFP signal). (B) Immunostaining of HaCATs transfected with a myc-tagged KG-forming protein (myc-eFlg1-foldon) and two sensor designs based on the ir8H2 sensing domain: one based on a variant of +15GFP here referred as +15GFPK (top row), in which we mutated its characteristic surface-exposed Arg residues into Lys residues (Table S3), and one based on +15GFP (as published, see Table S2). Note that while both Arg and Lys are positively charged residues, surface-exposed Arg residues in +15GFP are partly responsible for the outstanding partitioning of +15GFP-based sensors into phase separated FLG-like granules. (C) HaCATs exclusively transfected with Sensor A (+15GFP-NES-ir8H2) or Sensor B (+15GFP-NES-ieFlg1) show fully diffuse signal in the cytoplasm.

Fig. S14.

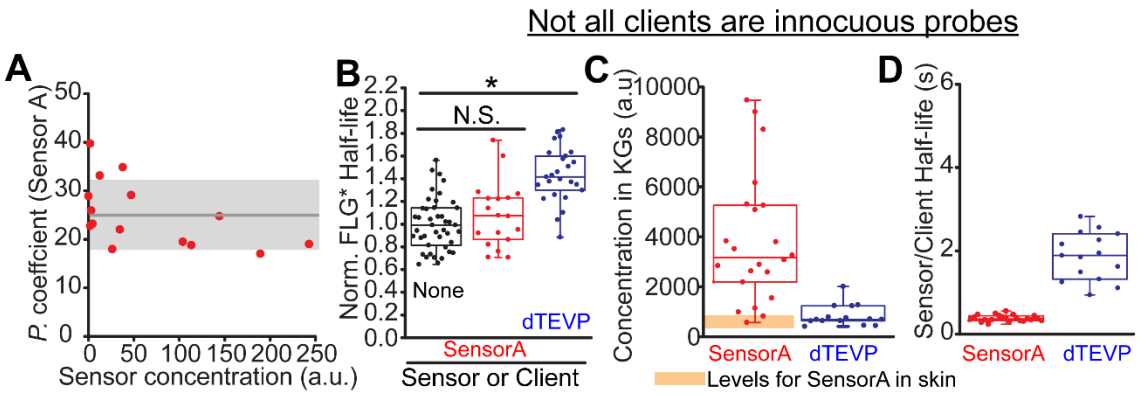

Not all clients serve as ideal probes to study phase separation. In fig. S11, we consider caveats of conventional clients. Here we directly compare the behaviors of the sfGFP-dTEVP client to our new type of client, Sensor A, which recognizes FLG only as it undergoes phase separation and assembles into granules, where it interacts weakly along many different contact sites along the scaffold. (A) Sensor A exhibits a high and stable partition coefficient (*P*, ratio of background corrected signal inside and outside granules) into KGs over a wide range of sensor expression/concentration levels. The average *P* is shown as a gray line (filled area is the standard deviation). Generally, conventional clients engineered to bind a specific domain in the scaffold exhibit progressively lower partition coefficients into condensates as binding sites within the scaffold become saturated (i.e. when client concentration exceeds that of the scaffold; as in fig S11A). Phase separation sensors, in contrast, do not bind a specific domain within the scaffold and may accumulate to higher concentrations than the scaffold itself (particularly in systems like ours in which the scaffold is exceedingly larger than the sensor) while showing a stable partition coefficient over a wide concentration range. (B) To easily compare data between Sensor A and the conventional client in fig. S11(sfGFP-dTEVP), here we show the recovery half-lives (same data as in fig. S11) normalized to the average half-life in the absence of dTEVP. We applied the same normalization procedure for the phase separation sensor data (taken from Fig. 4E). (C) Concentration (based on fluorescence measurements) of the dTEVP client and Sensor A within tagged-KGs analyzed in (B). In these experiments, Sensor A was enriched within tagged-KGs to higher concentrations than dTEVP clients —so even very high levels of Sensor A remain innocuous and these values are well above the concentrations we measure in skin for KGs studied in Fig. 5D-H. (D) Sensor or client recovery half-lives after photobleaching GFP signal within tagged-KGs. The reported affinity for TEVP to ENLYQS is 60 µM (*66*). Thus, despite being a relatively weak binder (µM range), at the very high concentrations of FLG* protein within tagged-KGs (~ 1mM), clients with affinities in the µM range likely exist in a predominantly-bound state. This bound state is reflected in the long FRAP Half-life for sfGFP-dTEVP within tagged-KGs, which is comparable to the FRAP Half-life of tagged-FLG itself (see data in panel B of fig. S11), but nearly an order of magnitude higher than for Sensor A. These data show that relatively to dTEVP, Sensor A within KGs interacts very weakly with tagged-FLG. Note that the observed differences are not due to changes in probe size, since sfGFP-dTEVP has a lower molecular mass (54.8 KDa) than Sensor A (63.5 KDa). Asterisks, statistically significant ($p<0.05$).

Fig. S15.

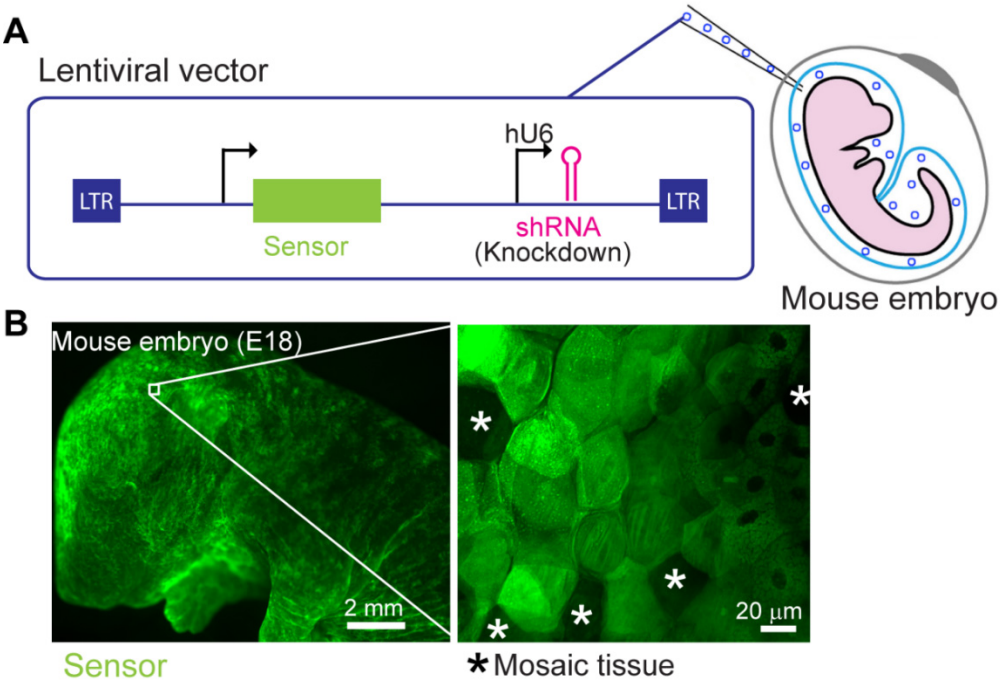

Generation of genetically-modified mice that express phase separation sensors in the epidermis. (A) We synthesized lentiviral vectors harboring genes encoding for Sensors A and B (see Fig. 4C in main manuscript) and under the control of a promoter of interest (see methods). For constitutive expression, we used a PGK promoter, whereas for doxycycline-inducible expression we used a TRE promoter (TRE3G, see methods for details). These vectors also included a human U6 promoter for expression of a shRNA. In most cases, unless indicated in the main manuscript, we used a well-tested *Scramble* (Scr) shRNA that does not target any sequence in the human and mouse genome and that has been validated to have no off-target effects in the skin epidermis (see methods). We produced high titer lentiviruses for *in utero* injection into the amniotic sac of mouse embryos at 9.5 days of development (see methods). This technique exposes the single layer of unspecified epidermal progenitors to the virus, which is taken up, integrated into the progenitor genome and stably propagated into adulthood. (B) Representative example of an *in utero* transduced mouse embryo harvested at 18 days of development. Note bright sensor signal throughout the skin surface. Using confocal spinning disk microscopy (right panel), we resolve Sensor A signal through the epidermis within fields of view of about 0.25 mm^2. The region demarcated in the left panel is simply a guide to the eye. Asterisks denote lack of GFP fluorescence in some (untransduced) cells, which highlights the expected mosaic nature of our *in utero* lentiviral approach.

Fig. S16.

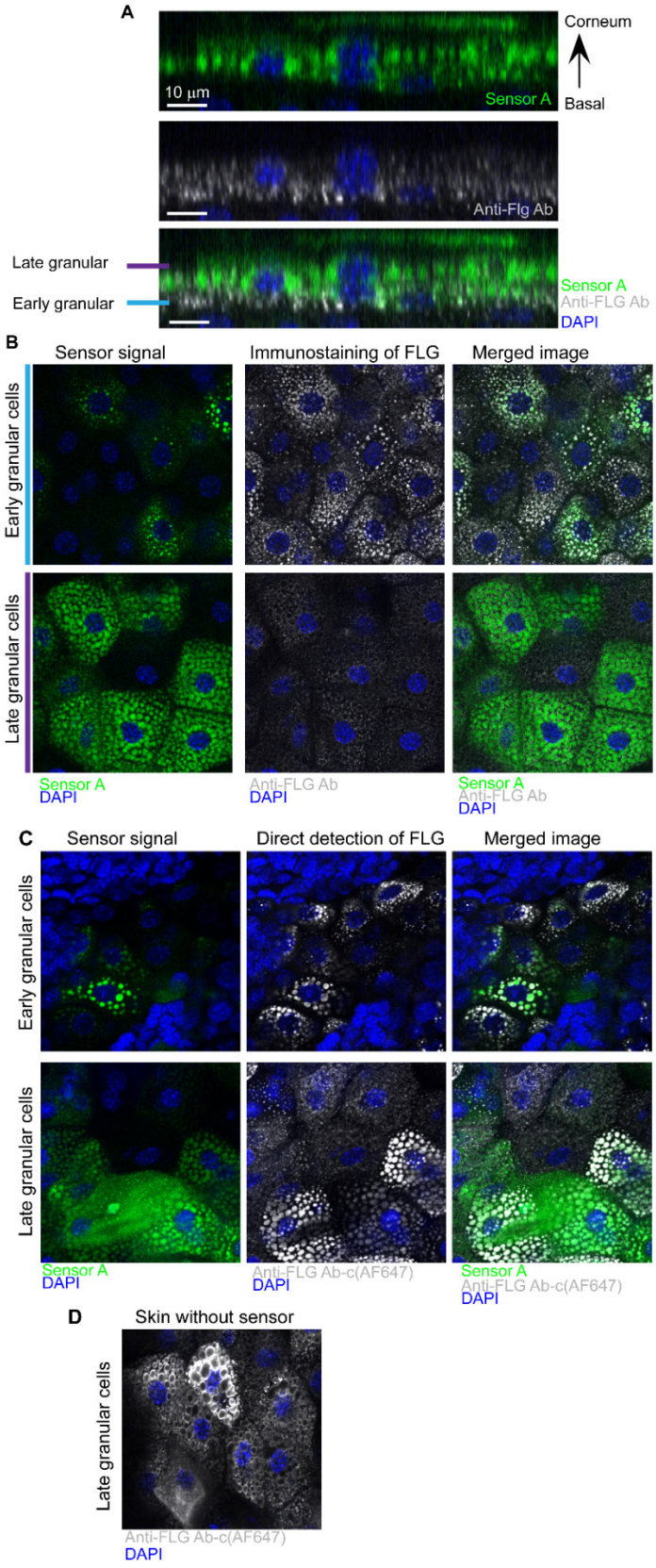
A
Corneum
10 μm
Sensor A
Basal
Anti-Flg Ab
Late granular
Early granular
Sensor A
Anti-FLG Ab
DAPI
B
Sensor signal
Immunostaining of FLG
Merged image
Early granular cells
Late granular cells
Sensor A
DAPI
Anti-FLG Ab
DAPI
Sensor A
Anti-FLG Ab
DAPI
C
Sensor signal
Direct detection of FLG
Merged image
Early granular cells
Late granular cells
Sensor A
DAPI
Anti-FLG Ab-c(AF647)
DAPI
Sensor A
Anti-FLG Ab-c(AF647)
DAPI
D
Skin without sensor
Late granular cells
Anti-FLG Ab-c(AF647)
DAPI

Immunostaining of mouse epidermis expressing Sensor A. (A) Sagittal view of Sensor A (GFP) fluorescence and anti-FLG immunostaining in fixed and whole-mounted mouse epidermis. FLG was detected using a mouse anti-FLG (rabbit) antibody and a conventional anti-rabbit secondary antibody conjugate (see methods). The merged image shows that anti-FLG immunostaining in this whole-mount setting predominantly labels KGs in the early granular layers. (B) Planar views across early and late granular layers marked in (A). Note that Sensor A signal localizes within the rim-like structures that are typically reported upon detection of KGs with anti-FLG antibodies. In late granular cells, however, FLG immunostaining barely outlines prominent mature granules revealed by the phase separation sensor. (C-D) Because primary-secondary antibody complexes, which are larger than the expected mesh size of KGs (3-8 nm as reported for other biomolecular condensates) (*67*), failed to penetrate KGs in (A-B), we directly conjugated a fluorophore to an anti-mFLG antibody (see methods) to facilitate its penetration into and labeling of KGs in whole-mounted epidermis. (C) Using this approach, we show that FLG is prominently accumulated within the very large KGs that crowd the cytoplasm of mature (late) granular cells and which are also readily revealed by the phase separation sensor. Note that these mature KGs were essentially invisible to the primary-secondary antibody complex in (A-B). Note, however, that the primary antibody conjugate still fails to penetrate many KGs and the edges of those KGs are only slightly labeled. The primary antibody conjugate is also altogether excluded from squames (the very thin cells that form after KGs dissolve and granular cells undergo cornification). This exclusion from squames (which feature a protein-reinforced plasma membrane), together with signal amplification due to antibody binding to a repeat sequence in mouse FLG, provides a particularly crisp view of late KGs. While Sensor A enrichment within late KGs is very high, its overall signal is also affected by diffuse Sensor A fluorescence originating from squames that have lost KGs. (D) The immunostaining approach in (C) reveals the same degree of KG crowding for mouse skin that lacks expression of a phase separation sensor.

Fig. S17.

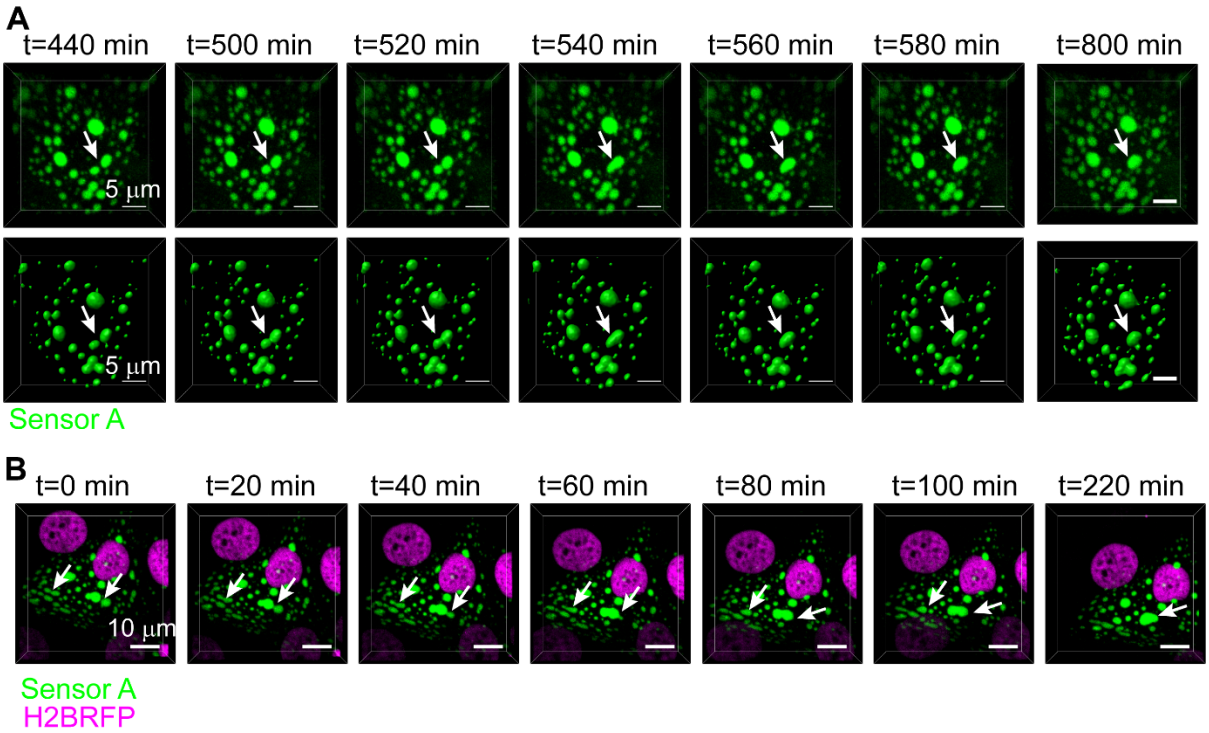

Liquid-like fusions between KGs in skin. (A) Time-lapse images of a granular cell in mouse epidermis in which two KGs undergo fusion events (as indicated by white arrows). The top time series shows 3D projections of raw Sensor A fluorescence, whereas the bottom panels show 3D surface renderings of Sensor A fluorescence to better visualize the 3D morphology of granules. Note that the fused granules eventually relax into a spherical shape (see t= 800 min). (B) Time-lapse images (3D projections) of a human granular cell in which several KGs undergo fusion events (as indicated by white arrows). For this experiment we transduced human primary keratinocytes with two lentiviruses: one harboring a gene that encodes Sensor A and another lentivirus harboring a gene that encodes H2B-RFP to label nuclei. To allow for stratification and *FLG* expression in granular cells, prior to imaging we cultured transduced keratinocytes for 6 days under differentiation conditions (see methods) —we previously optimized this protocol to trigger pronounced *FLG* expression.

Fig. S18.

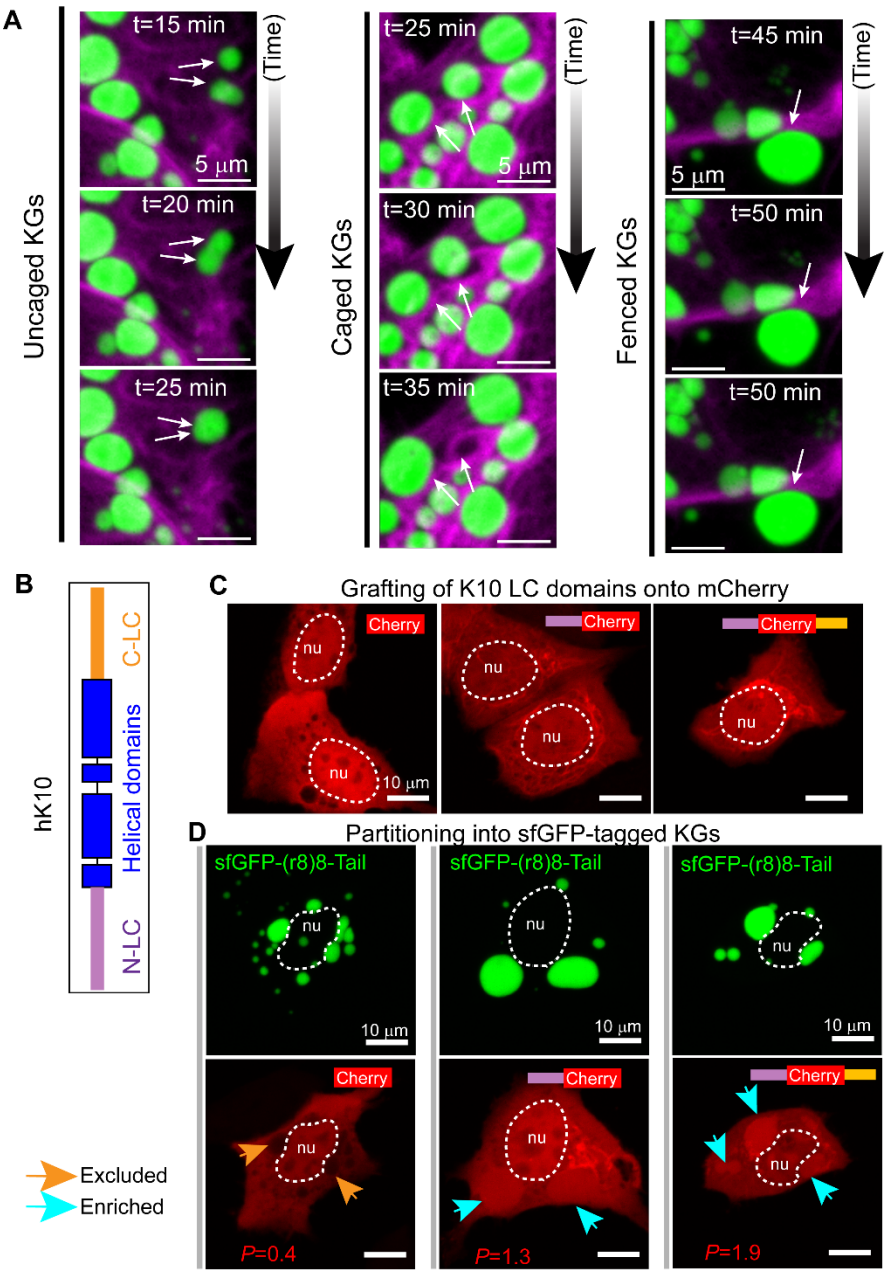

Low complexity domains in human keratin 10 mediate interactions with FLG and its KGs. (A) Live imaging showing three different types of keratin-KG interactions in HaCATs (same cell as in Fig. 6A-B) with an mRFP-tagged K10 network (magenta) and containing sfGFP-tagged FLG* granules (green). Uncaged KGs fuse rapidly, while caged KGs fuse rarely/slowly. Fenced KGs are impeded from fusing. Double arrows depict temporal fusion events; single arrow denotes keratin cable preventing fusion. These images are maximum intensity projections of the same data in Fig. 6B (also movie S7), which shows 3D renderings. (B) Architecture of human keratin 10 drawn with the proper relative size of its domains. While the coiled-coil domain is conserved among type I keratins and is central to its dimerization with type II keratins and assembly into 10 nm filaments, the LC domains vary markedly in size and in sequence. Note the

atypically large low complexity (LC) N- and C- terminal domains that flank the central coiled-coil (helical) rod domain of human K10. (C) We grafted these LC domains onto mCherry and transfected these constructs into HaCATs to assess their behavior. Similar to mCherry itself, mCherry with one or both LC domains does not exhibit phase separation upon overexpression in HaCATs. mCherry grafted with K10 LC domains is predominantly diffuse in the cytoplasm, but occasionally marks perinuclear keratin fibers. (D) Co-expression of mCherry variants and sfGFP-r(8)8-Tail (to form sfGFP-tagged KGs) ―displayed as separate images (top/bottom) for each channel. Note that while mCherry alone is well excluded from KGs (partition coefficient, *P*=0.4), mCherry grafted with one or both K10 LC domain readily partitions into KGs. The mCherry construct with both K10 LC domains exhibited the highest partition coefficient (*P*=1.9 vs *P*=1.3). All images are maximum intensity projections from live imaging data.

Fig. S19.

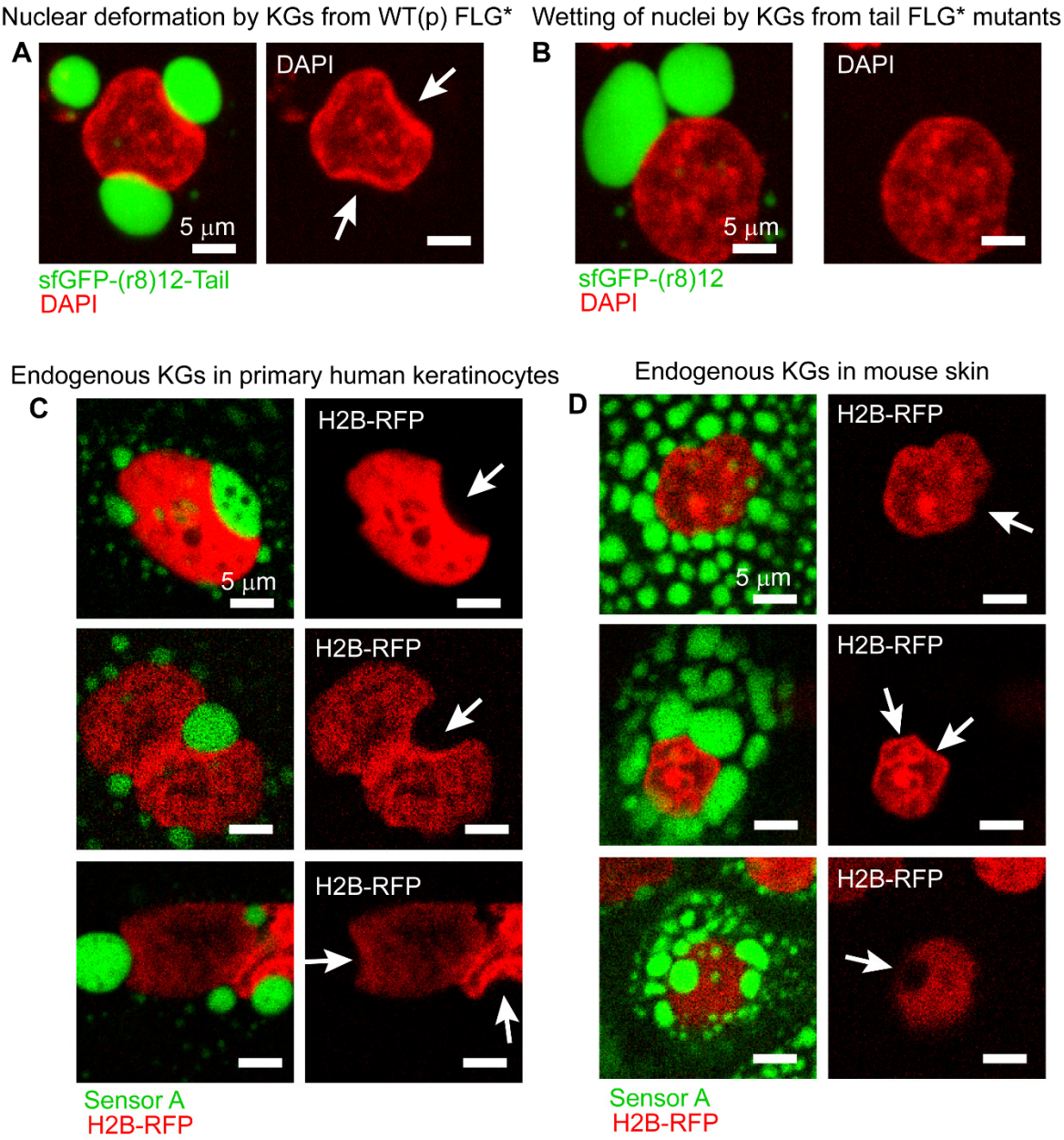

KGs prominently deform the nucleus. (A-B) Nucleus-KG interactions in HaCATs transfected with engineered FLG variants. (A) HaCATs that express synthetic WT(p) FLG [sfGFP-(r8)12-Tail; similar to wild-type FLG in KGs], typically form KGs that can prominently deform the nucleus. (B) In contrast to WT(p) FLG*, mutants without the C-terminal domain [sfGFP-(r8)12] form KGs that fail to deform nuclei and instead change their shape to wet the nuclear surface. (C-D) Nucleus-KG interactions in human primary keratinocytes (C) and mouse skin (D), both of which undergo terminal differentiation and generate a granular layer replete with KGs. (C) Optical sections of individual granular cells from live imaging of primary adult human keratinocytes transduced with constructs for expression of Sensor A and H2BRFP. Primary keratinocytes were cultured for 4 days under differentiation conditions to trigger stratification and KG formation (see methods). (D) Optical sections of individual granular cells

from live imaging of E18.5 mouse skin transduced with constructs for expression of Sensor A and H2B-RFP. Sensor A labels endogenous KGs and H2BRFP labels nuclei. Arrows point to KG-induced nuclear deformations.

Fig. S20.

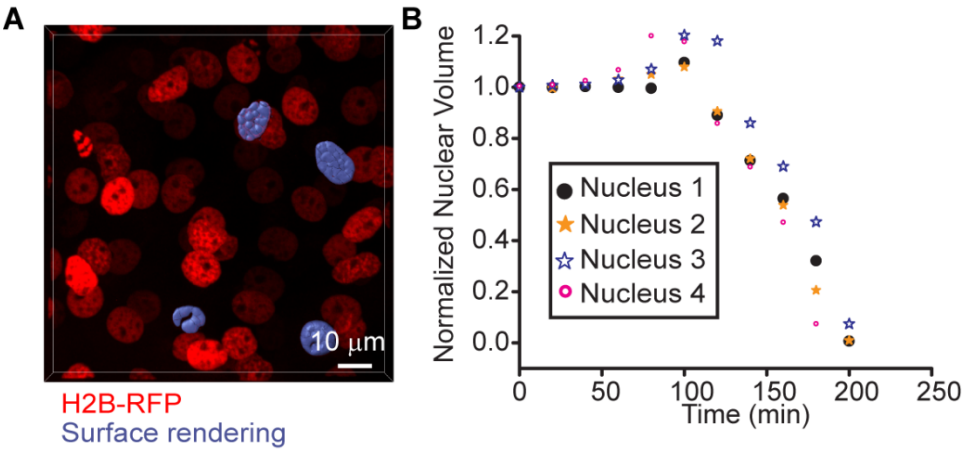

Enucleation dynamics in mouse skin. (A) We studied enucleation through live imaging of E18.5 skin explants taken from an embryo whose epidermal progenitors were transduced *in utero* with a lentivirus harboring a gene encoding H2B-RFP under the control of a constitutive promoter. This approach allowed us to capture a few complete enucleation events per imaging session (~16-20 h). In some instances, nuclei were sufficiently sparse to create high quality surface renderings (shown in purple) of chromatin signal in individual (late) granular cells. (B) Using the imaging and surface rendering approach in (A), we quantified the relative changes in nuclear volume, using chromatin signal as a proxy, through the process of enucleation. Note the stereotypical and rapid decline in nuclear volume (chromatin compaction) over the span of 2 hours.

Fig. S21.

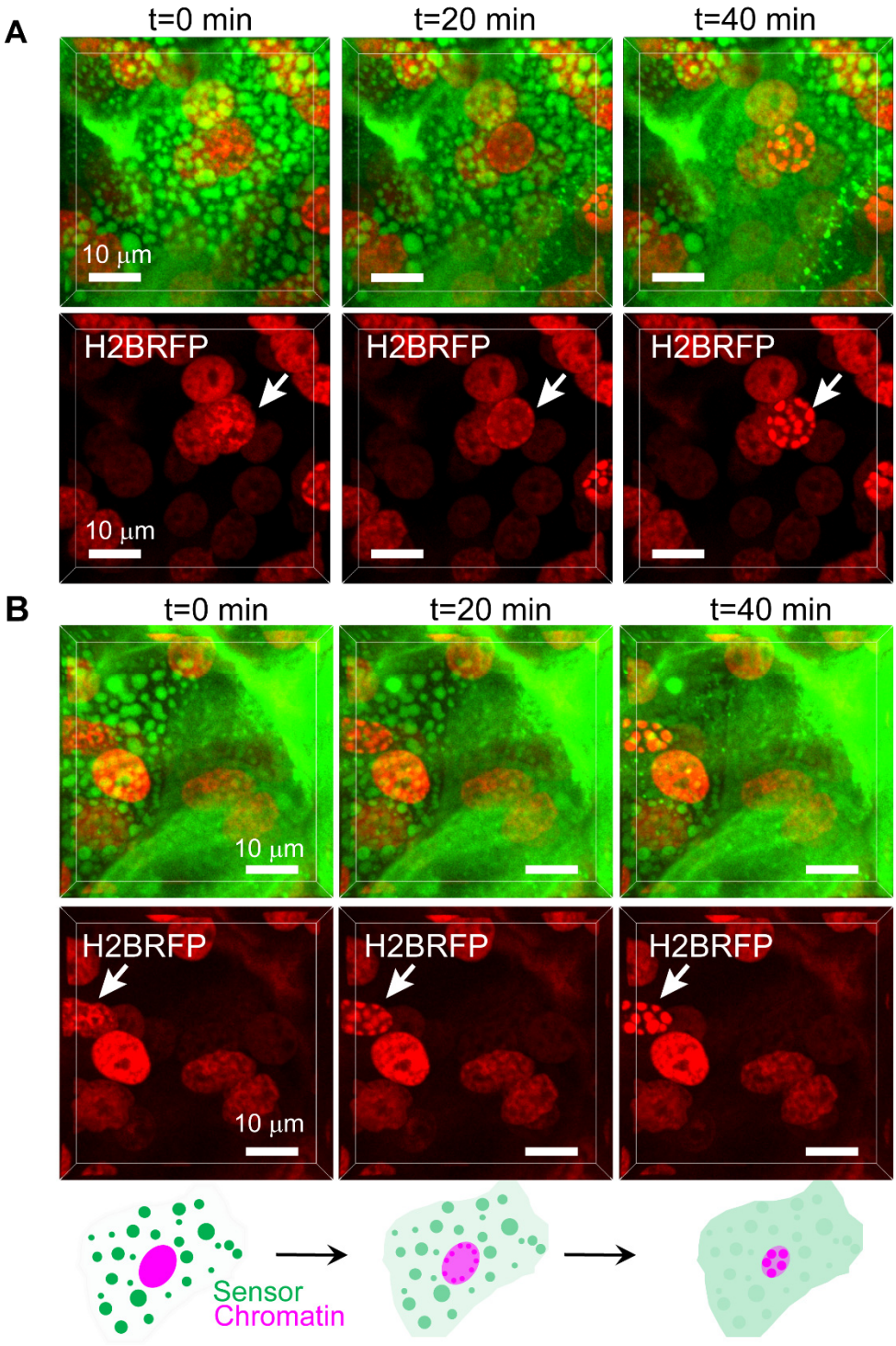

KG dynamics through the initial stages of enucleation. (A-B) Live imaging of the process of enucleation in E18.5 skin explants from embryos whose epidermal progenitors had been transduced *in utero* to enable suprabasal expression of Sensor A and constitutive expression of H2B-RFP (to label chromatin). Similar to the behavior reported in Fig. 7C, we observed a perfect synchronization of release of the sensor from within KGs, concomitant with its accumulation in

the cytoplasm and the initiation of chromatin compaction. Arrows point to nuclei undergoing degeneration/loss. The late stages and completion of these two enucleation events can be seen in Movie S8.

Fig. S22.

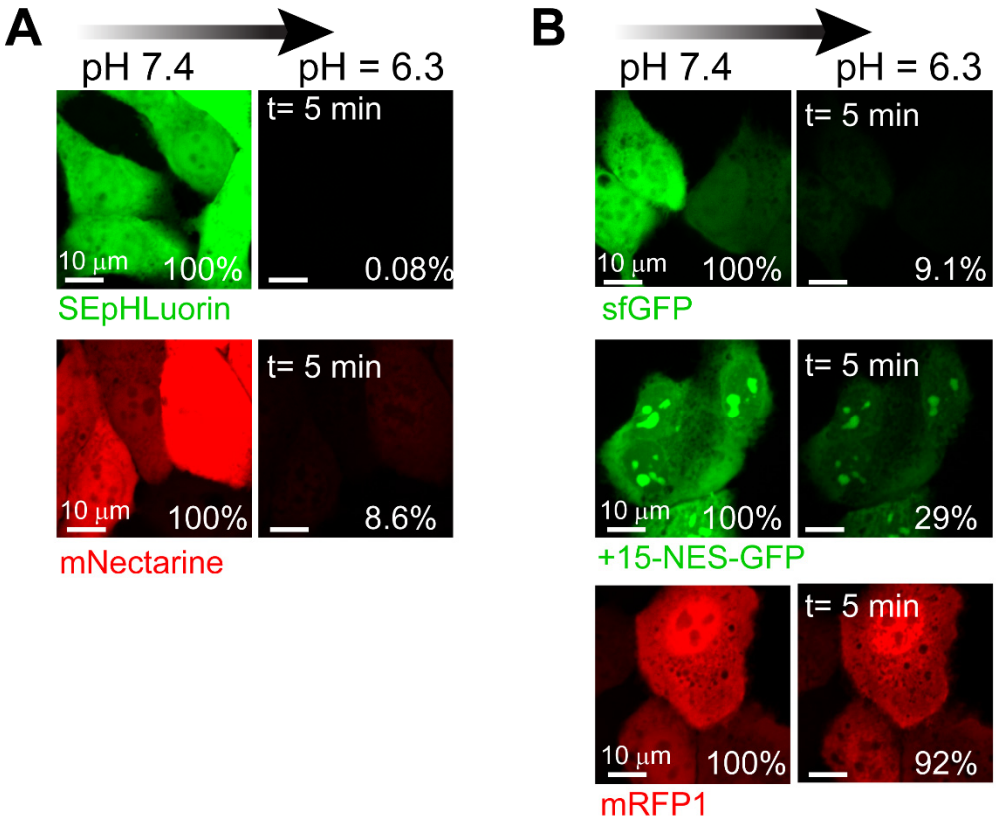

Validation of pH sensors and pH sensitivity of other fluorescent proteins. (A) We transfected HACATs with constructs encoding two published pH reporters that are highly sensitive in our pH range of interest (7.4 to 6.0): SEpHLuorin (*60*), a GFP-based pH reporter, and mNectarine, an RFP-based pH reporter (*61*). Both reporters were designed to lose brightness at low pH (~6.0). When we switched the media pH from 7.4 to 6.3 in the presence of KCl and Nigericin (see methods) to set the intracellular pH to 6.3, both SEpHLuorin and mNectarine exhibited a sharp drop in fluorescence intensity. Average final fluorescence (relative to pH 7.4) is shown (average of 10-30 cells in each case). While sfGFP (as well as EGFP and those closely-related variants) are known to be pH sensitive at pH values approaching 6.5, which we verify here for sfGFP (drop in signal to 9.1%), +15-NES-GFP is only mildly pH sensitive and remains highly fluorescent at pH 6.3. mRFP1 is known to be pH insensitive in this pH range and our experiments confirm its pH insensitivity.

Fig. S23.

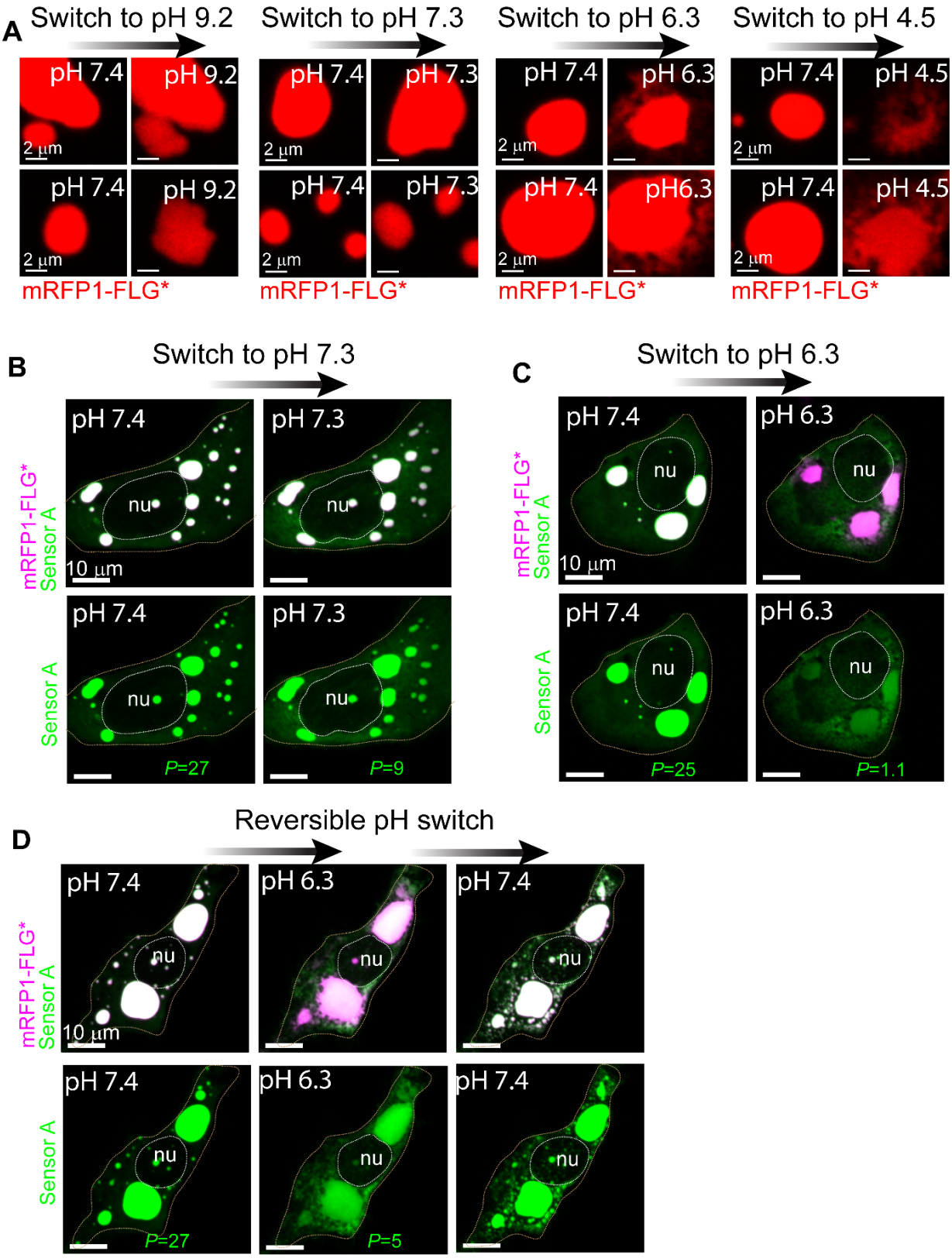
A
Switch to pH 9.2
Switch to pH 7.3
Switch to pH 6.3
Switch to pH 4.5
pH 7.4
pH 9.2
pH 7.3
pH 6.3
pH6.3
pH 4.5
2 μm
mRFP1-FLG*
B
Switch to pH 7.3
mRFP1-FLG*
Sensor A
nu
10 μm
P=27
P=9
C
Switch to pH 6.3
P=25
P=1.1
D
Reversible pH switch
P=5

pH-responsiveness of tagged-KGs. (A) Response of tagged-KGs in HaCATs expressing FLG* [mRFP1-(r8)8-Tail] when the intracellular pH was buffered (with KCl and Nigericin, see methods) to different pH values. We show detailed views of individual tagged-KGs (within cells), soon after (t= 5 min) they were exposed to the pH shifts. Note that starting a ~pH 6.3, the phase separation capacity of FLG* was drastically reduced and mRFP-FLG* began to leak/dissolve into the cytoplasm, resulting in the progressive shrinkage of KGs (32% ± 19% decrease in volume five minutes after the pH shift). This effect was more prominent at pH values below the pKa of His (see data at pH of 4.5) and for small KGs (e.g. Top panel at pH 4.5). In contrast, at alkaline (pH 9.2) or neutral pH, we only saw swelling of tagged-KGs without release/dissolution of FLG* into the cytoplasm. These subtle pH-independent changes represent the contribution of our intracellular pH buffer (KCl + ionophore). (B-C) Response of tagged-KGs in HaCATs co-expressing FLG* [mRFP1-(r8)8-Tail] and Sensor A (granules appear white in the merged image due to the high enrichment of Sensor A within mRFP-tagged KGs) to our intracellular pH buffering media when pH was kept at ~7.4 (B) or lowered to pH 6.3 (C). Lower panels exclusively show Sensor A data (with adjusted contrast settings) to facilitate visualization of Sensor A enrichment within KGs. The partition coefficients shown in the images correspond to data for Sensor A in those specific cells. The average partition coefficient for Sensor A across 3 to 4 cells prior to pH change was ~P=25.1 ± 6.8, which dropped to P=12.2 ± 4.3 when buffering at pH 7.3 and to P=3.2 ± 1.8 at pH 6.3. Note that under intracellular pH buffering but in the absence of a pH shift, Sensor A showed a small decrease in partition coefficient, which was reflective of the subtle effect of our intracellular pH buffers on the phase separation capacity of FLG. In contrast, the prominent decrease of phase separation capacity that FLG experienced when buffering at pH 6.3 (as shown in panel A) was mirrored by a large reduction in the partition coefficient of Sensor A, which nonetheless remained enriched within KGs as they shrank. (C) Similar to (B) but followed by reversal (within 5 min) of the intracellular pH from 6.3 to ~7.4. This experiment demonstrates that the effects of pH on both FLG* and Sensor A are dynamic and reversible. Moreover, data in (B-D) show that the changes in the partition coefficient of Sensor A reflect the relative impact of environmental stimuli on the ultra-weak forces that drive and sustain the liquid-liquid phase separation of FLG. In (B-D), dotted lines mark approximate cell boundaries. All images are maximum intensity projections.

Fig. S24.

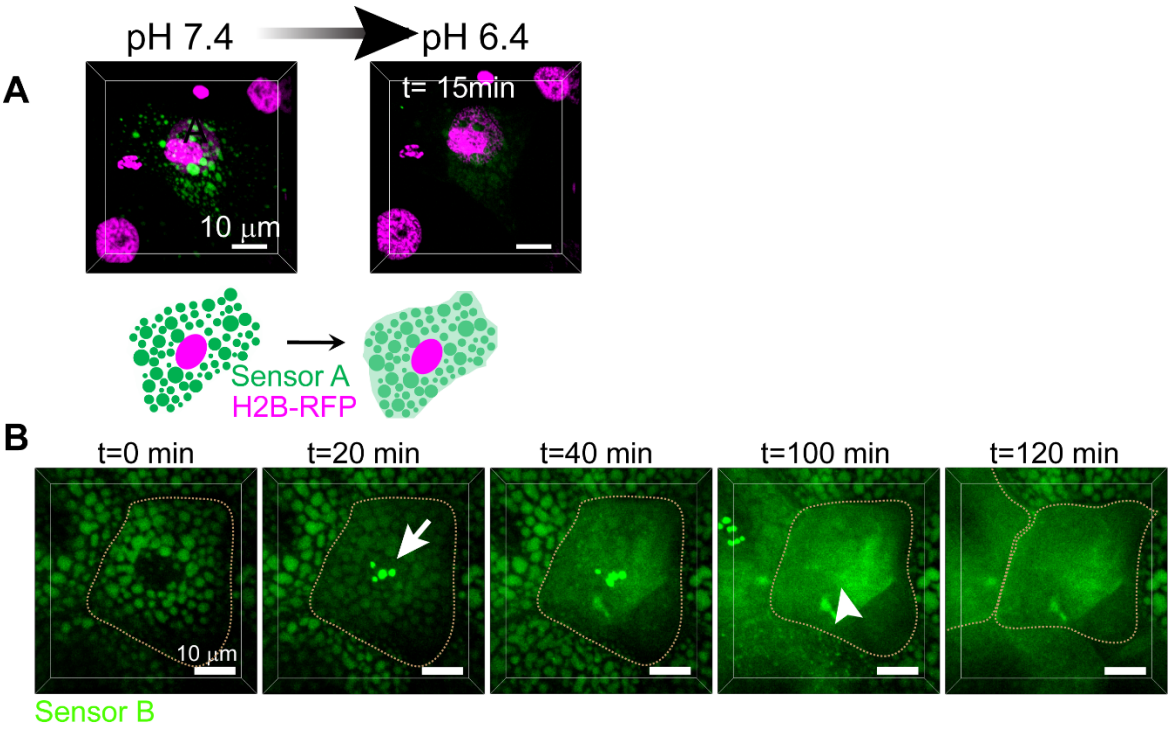

pH-triggered and pH-like changes in human and murine granular cells. (A) Direct manipulation of pH in human granular cells in culture leads to a rapid reduction in the partitioning of Sensor A into endogenous KGs. Its dilution into the cytoplasm as well as the progressive dissolution of KGs are consistent with the pH-triggered dynamics observed for mRFP-tagged KGs (Fig. 7E). Primary human keratinocytes were transduced to drive expression of Sensor A and H2B-RFP and induced to differentiate over 7 days to drive their stratification and *FLG* expression (see methods). (B) Live imaging of the process of enucleation and cornification in mouse epidermis *in utero* transduced to drive suprabasal expression of Sensor B, which is smaller than Sensor A and can upon loss of nuclear integrity enter the nucleus. Note that a late granular cell with abundant and large KGs first shows signs indicative of the endogenouse pH shift (Fig. 7F top panels), becoming increasingly abundant in the cytoplasm and followed by rapid entry of Sensor B into the nuclear compartment (see arrow at t=20 min). Twenty minutes after the initiation of KG dissolution (at t=40 min), Sensor B is equally partitioned between the cytoplasm and leftover KGs (similar to what we observe for Sensor A in response to the endogenous pH shift). Starting at t=100 min, the nuclear compartment is no longer visible and the cell has acquired squame-like features (arrowheads). In the last snapshot (t=120 min), a second cell (adjoined to the first squame) has transitioned to a squame.

Table S1.

Sequence information for FLG and paralogs in all mammalian species considered in Fig. 1E and fig. S1D. Curated gene assemblies are available upon request.

Protein	Species	Accession number*	Curation notes
FLG	Mouse (C57B6)		Curated from genomic DNA and mRNA sequences (available sequence, XP_017175331.1 is low quality)
FLG	Human	NP_002007.1	
FLG	Naked mole rat	EHB05610.1	
FLG	Chimpanzee	H2R8N0	Updated in Feb 2018
FLG	Northern white-cheeked gibbon	XM_012511601.1	Curated to include all of Exon3 and Exon2 (predicted form includes up to a partial B domain)
FLG	Sumatran orangutan	XM_003780333.2	
FLG	Golden snub-nosed monkey	XM_010352972.1	
FLG	Common marmoset	XP_008982649.1	
FLG	Gorilla	BAT51076.1	Sequence reported by Romero et al. lacked part of the B domain and the S-100 domain.
FLG	Bornean orangutan	BAT51075.1	Sequence reported by Romero et al. lacked part of the B domain and the S-100 domain.
FLG2	Human	NP_001014364.1	(Based on GRCh38.p2)
FLG2	Dog	XM_014120745.1	Entry updated to XP_013976221.1
FLG2	Mouse (Balbc)	NP_001013826.1	
FLG2	Mouse (C57B6)		Different from NP_001013826.1. Sequence directly curated from high quality gDNA available from GRCm38.p4 (current transcript annotation appears to be wrong as they attempted to map mRNA for the Balbc variant, which is much shorter)
FLG2	Cheetah	XP_014943408.1	
FLG2	Chimpanzee	XP_016782784.1	
FLG2	Drill	XP_011829043.1	
FLG2	Crab-eating macaque	XP_015312597.1	
FLG2	Northern white-cheeked gibbon	XP_012366375.1	
RPTN	Mouse (C57B6)	NP_033126.2	
RPTN	Human	NP_001116437.1	
RPTN	Rhesus macaque	XP_015006569.1	

Protein	Species	Accession number*	Curation notes
RPTN	Cow	XP_010801377.1	
RPTN	Dog	XP_003432327.1	Updated to XP_022260085.1
RPTN	Norway rat	XP_227371.1	
RPTN	Naked mole rat	XP_004854195.1	Updated to XP_004854195.2
RPTN	Chimpanzee	XP_016782772.1	Updated to XP_016782772.2
RPTN	Western lowland gorilla	XP_004026730.1	
HRNR	Human	NP_001009931.1	
HRNR	Mouse (C57B6)	NP_598459.2	
HRNR	Goat	XP_013817836.1	
HRNR	Bactrian camel	XP_010956837.1	
HRNR	Cow	XP_010801374.1	
HRNR	Rhesus monkey	XP_015007852.1	
HRNR	Dog	XP_005630887.1	
HRNR	Alpine marmot	XP_015358148.1	
TCHH	Human	NP_009044.2	
TCHH	Mouse (C57B6)	NP_001156570.1	
TCHH	Norway rat	XP_006232882.1	
TCHH	Cow	XP_002686080.3	
TCHH	Degu	XP_012370438.1	

.*NCBI, GenBank or Uniprot accession numbers.

Table S2.

Sequence information for synthesized FLG variants that appear in the main manuscript. We do not include the full sequence for the following mRFP1-based filaggrin variants: mRFP1-(r8)4, mRFP1-(r8)8, mRFP1-(r8)12 and mRFP1-(r8)8-Tail as their sequence can be easily derived from the equivalent sfGFP-based variants. We include two mRFP1-based constructs as reference (mRFP1-(r8)16 and S100-mRFP1-(r8)8-Tail).

Construct	Sequence
sfGFP-(r8)	MGSKGEELFTGVVPILVELDGDVNGHKFSVRGEGEGDATNGKLTLKFI CTTGKLPVPWPTLVTTLGYGVQCFSRYPDHMKRHDFFKSAMPEGYVQ ERTISFKDDGTYKTRAEVKFEGDTLVNRIELKGIDFKEDGNILGHKLEY NFNSHNVYITADKQKNGIKANFKIRHNVEDGSVQLADHYQQNTPIGDG PVLLPDNHYLSTQSVLSKDPNEKRDHMVLLEFVTAAGITHGMDELYKS PGGQVSTHEQSESSHGWTGPSTRGRQGSRHEQAQDSSRHSASQDGQDT IRGHPGSSRGGRQGYHHEHSVDSSGHSGSHHSHTTSQGRSDASRGQSGS RSASRTTRNEEQSGDGSRHSGSRHHEASTHADISRHSQAVQGQSEGSRR SRRQGSSVSQDSDSEGHSEDSERWSGSASRNHHGSAQEQLRDGSRHPR SHQEDRAGHGHSADSSRQSGTRHTQTSSGGQAASSHEQARSSAGERHG SHHQQSADSSRHSGIGHGQASSAVRDSGHRGYSGSQASDNEGHSEDSD TQSVSAHGQAGSHQQSHQESARGRSGETSGHSGSFLYG
sfGFP-(r8)2	MGSKGEELFTGVVPILVELDGDVNGHKFSVRGEGEGDATNGKLTLKFI CTTGKLPVPWPTLVTTLGYGVQCFSRYPDHMKRHDFFKSAMPEGYVQ ERTISFKDDGTYKTRAEVKFEGDTLVNRIELKGIDFKEDGNILGHKLEY NFNSHNVYITADKQKNGIKANFKIRHNVEDGSVQLADHYQQNTPIGDG PVLLPDNHYLSTQSVLSKDPNEKRDHMVLLEFVTAAGITHGMDELYKS PGGQVSTHEQSESSHGWTGPSTRGRQGSRHEQAQDSSRHSASQDGQDT IRGHPGSSRGGRQGYHHEHSVDSSGHSGSHHSHTTSQGRSDASRGQSGS RSASRTTRNEEQSGDGSRHSGSRHHEASTHADISRHSQAVQGQSEGSRR SRRQGSSVSQDSDSEGHSEDSERWSGSASRNHHGSAQEQLRDGSRHPR SHQEDRAGHGHSADSSRQSGTRHTQTSSGGQAASSHEQARSSAGERHG SHHQQSADSSRHSGIGHGQASSAVRDSGHRGYSGSQASDNEGHSEDSD TQSVSAHGQAGSHQQSHQESARGRSGETSGHSGSFLYGQVSTHEQSESS HGWTGPSTRGRQGSRHEQAQDSSRHSASQDGQDTIRGHPGSSRGGRQG YHHEHSVDSSGHSGSHHSHTTSQGRSDASRGQSGSRSASRTTRNEEQSG DGSRHSGSRHHEASTHADISRHSQAVQGQSEGSRRSRRQGSSVSQDSDS EGHSEDSERWSGSASRNHHGSAQEQLRDGSRHPRSHQEDRAGHGHSA DSSRQSGTRHTQTSSGGQAASSHEQARSSAGERHGSHHQQSADSSRHS GIGHGQASSAVRDSGHRGYSGSQASDNEGHSEDSDTQSVSAHGQAGSH QQSHQESARGRSGETSGHSGSFLYG

Construct	Sequence
sfGFP-(r8)4	MGSKGEELFTGVVPILVELDGDVNGHKFSVRGEGEGDATNGKLTLKFI CTTGKLPVPWPTLVTTLGYGVQCFSRYPDHMKRHDFFKSAMPEGYVQ ERTISFKDDGTYKTRAEVKFEGDTLVNRIELKGIDFKEDGNILGHKLEY NFNSHNVYITADKQKNGIKANFKIRHNVEDGSVQLADHYQQNTPIGDG PVLLPDNHYLSTQSVLSKDPNEKRDHMVLLEFVTAAGITHGMDELYKS PGGQVSTHEQSESSHGWTGPSTRGRQGSRHEQAQDSSRHSASQDGQDT IRGHPGSSRGGRQGYHHEHSVDSSGHSGSHHSHTTSQGRSDASRGQSGS RSASRTTRNEEQSGDGSRHSGSRHHEASTHADISRHSQAVQGQSEGSRR SRRQGSSVSQDSDSEGHSEDSERWSGSASRNHHGSAQEQLRDGSRHPR SHQEDRAGHGHSADSSRQSGTRHTQTSSGGQAASSHEQARSSAGERHG SHHQQSADSSRHSGIGHGQASSAVRDSGHRGYSGSQASDNEGHSEDSD TQSVSAHGQAGSHQQSHQESARGRSGETSGHSGSFLYGQVSTHEQSESS HGWTGPSTRGRQGSRHEQAQDSSRHSASQDGQDTIRGHPGSSRGGRQG YHHEHSVDSSGHSGSHHSHTTSQGRSDASRGQSGSRSASRTTRNEEQSG DGSRHSGSRHHEASTHADISRHSQAVQGQSEGSRRSRRQGSSVSQDSDS EGHSEDSERWSGSASRNHHGSAQEQLRDGSRHPRSHQEDRAGHGHSA DSSRQSGTRHTQTSSGGQAASSHEQARSSAGERHGSHHQQSADSSRHS GIGHGQASSAVRDSGHRGYSGSQASDNEGHSEDSDTQSVSAHGQAGSH QQSHQESARGRSGETSGHSGSFLYGQVSTHEQSESSHGWTGPSTRGRQ GSRHEQAQDSSRHSASQDGQDTIRGHPGSSRGGRQGYHHEHSVDSSGH SGSHHSHTTSQGRSDASRGQSGSRSASRTTRNEEQSGDGSRHSGSRHHE ASTHADISRHSQAVQGQSEGSRRSRRQGSSVSQDSDSEGHSEDSERWSG SASRNHHGSAQEQLRDGSRHPRSHQEDRAGHGHSADSSRQSGTRHTQT SSGGQAASSHEQARSSAGERHGSHHQQSADSSRHSGIGHGQASSAVRD SGHRGYSGSQASDNEGHSEDSDTQSVSAHGQAGSHQQSHQESARGRSG ETSGHSGSFLYGQVSTHEQSESSHGWTGPSTRGRQGSRHEQAQDSSRHS ASQDGQDTIRGHPGSSRGGRQGYHHEHSVDSSGHSGSHHSHTTSQGRS DASRGQSGSRSASRTTRNEEQSGDGSRHSGSRHHEASTHADISRHSQAV QGQSEGSRRSRRQGSSVSQDSDSEGHSEDSERWSGSASRNHHGSAQEQ LRDGSRHPRSHQEDRAGHGHSADSSRQSGTRHTQTSSGGQAASSHEQA RSSAGERHGSHHQQSADSSRHSGIGHGQASSAVRDSGHRGYSGSQASD NEGHSEDSDTQSVSAHGQAGSHQQSHQESARGRSGETSGHSGSFLYG

Construct	Sequence
sfGFP-(r8)8	MGSKGEELFTGVVPILVELDGDVNGHKFSVRGEGEGDATNGKLTLKFI CTTGKLPVPWPTLVTTLGYGVQCFSRYPDHMKRHDFFKSAMPEGYVQ ERTISFKDDGTYKTRAEVKFEGDTLVNRIELKGIDFKEDGNILGHKLEY NFNSHNVYITADKQKNGIKANFKIRHNVEDGSVQLADHYQQNTPIGDG PVLLPDNHYLSTQSVLSKDPNEKRDHMVLLEFVTAAGITHGMDELYKS PGGQVSTHEQSESSHGWTGPSTRGRQGSRHEQAQDSSRHSASQDGQDT IRGHPGSSRGGRQGYHHEHSVDSSGHSGSHHSHTTSQGRSDASRGQSGS RSASRTTRNEEQSGDGSRHSGSRHHEASTHADISRHSQAVQGQSEGSRR SRRQGSSVSQDSDSEGHSEDSERWSGSASRNHHGSAQEQLRDGSRHPR SHQEDRAGHGHSADSSRQSGTRHTQTSSGGQAASSHEQARSSAGERHG SHHQQSADSSRHSGIGHGQASSAVRDSGHRGYSGSQASDNEGHSEDSD TQSVSAHGQAGSHQQSHQESARGRSGETSGHSGSFLYGQVSTHEQSESS HGWTGPSTRGRQGSRHEQAQDSSRHSASQDGQDTIRGHPGSSRGGRQG YHHEHSVDSSGHSGSHHSHTTSQGRSDASRGQSGSRSASRTTRNEEQSG DGSRHSGSRHHEASTHADISRHSQAVQGQSEGSRRSRRQGSSVSQDSDS EGHSEDSERWSGSASRNHHGSAQEQLRDGSRHPRSHQEDRAGHGHSA DSSRQSGTRHTQTSSGGQAASSHEQARSSAGERHGSHHQQSADSSRHS GIGHGQASSAVRDSGHRGYSGSQASDNEGHSEDSDTQSVSAHGQAGSH QQSHQESARGRSGETSGHSGSFLYGQVSTHEQSESSHGWTGPSTRGRQ GSRHEQAQDSSRHSASQDGQDTIRGHPGSSRGGRQGYHHEHSVDSSGH SGSHHSHTTSQGRSDASRGQSGSRSASRTTRNEEQSGDGSRHSGSRHHE ASTHADISRHSQAVQGQSEGSRRSRRQGSSVSQDSDSEGHSEDSERWSG SASRNHHGSAQEQLRDGSRHPRSHQEDRAGHGHSADSSRQSGTRHTQT SSGGQAASSHEQARSSAGERHGSHHQQSADSSRHSGIGHGQASSAVRD SGHRGYSGSQASDNEGHSEDSDTQSVSAHGQAGSHQQSHQESARGRSG ETSGHSGSFLYGQVSTHEQSESSHGWTGPSTRGRQGSRHEQAQDSSRHS ASQDGQDTIRGHPGSSRGGRQGYHHEHSVDSSGHSGSHHSHTTSQGRS DASRGQSGSRSASRTTRNEEQSGDGSRHSGSRHHEASTHADISRHSQAV QGQSEGSRRSRRQGSSVSQDSDSEGHSEDSERWSGSASRNHHGSAQEQ LRDGSRHPRSHQEDRAGHGHSADSSRQSGTRHTQTSSGGQAASSHEQA RSSAGERHGSHHQQSADSSRHSGIGHGQASSAVRDSGHRGYSGSQASD NEGHSEDSDTQSVSAHGQAGSHQQSHQESARGRSGETSGHSGSFLYGQ VSTHEQSESSHGWTGPSTRGRQGSRHEQAQDSSRHSASQDGQDTIRGH PGSSRGGRQGYHHEHSVDSSGHSGSHHSHTTSQGRSDASRGQSGSRSA SRTTRNEEQSGDGSRHSGSRHHEASTHADISRHSQAVQGQSEGSRRSRR QGSSVSQDSDSEGHSEDSERWSGSASRNHHGSAQEQLRDGSRHPRSHQ EDRAGHGHSADSSRQSGTRHTQTSSGGQAASSHEQARSSAGERHGSHH QQSADSSRHSGIGHGQASSAVRDSGHRGYSGSQASDNEGHSEDSDTQS VSAHGQAGSHQQSHQESARGRSGETSGHSGSFLYGQVSTHEQSESSHG WTGPSTRGRQGSRHEQAQDSSRHSASQDGQDTIRGHPGSSRGGRQGYH HEHSVDSSGHSGSHHSHTTSQGRSDASRGQSGSRSASRTTRNEEQSGDG SRHSGSRHHEASTHADISRHSQAVQGQSEGSRRSRRQGSSVSQDSDSEG HSEDSERWSGSASRNHHGSAQEQLRDGSRHPRSHQEDRAGHGHSADSS RQSGTRHTQTSSGGQAASSHEQARSSAGERHGSHHQQSADSSRHSGIG HGQASSAVRDSGHRGYSGSQASDNEGHSEDSDTQSVSAHGQAGSHQQ

Construct	Sequence
	SHQESARGRSGETSGHSGSFLYGQVSTHEQSESSHGWTGPSTRGRQGSR HEQAQDSSRHSASQDGQDTIRGHPGSSRGGRQGYHHEHSVDSSGHSGS HHSHTTSQGRSDASRGQSGSRSASRTTRNEEQSGDGSRHSGSRHHEAST HADISRHSQAVQGQSEGSRRSRRQGSSVSQDSDSEGHSEDSERWSGSAS RNHHGSAQEQLRDGSRHPRSHQEDRAGHGHSADSSRQSGTRHTQTSSG GQAASSHEQARSSAGERHGSHHQQSADSSRHSGIGHGQASSAVRDSGH RGYSGSQASDNEGHSEDSDTQSVSAHGQAGSHQQSHQESARGRSGETS GHSGSFLYGQVSTHEQSESSHGWTGPSTRGRQGSRHEQAQDSSRHSAS QDGQDTIRGHPGSSRGGRQGYHHEHSVDSSGHSGSHHSHTTSQGRSDA SRGQSGSRSASRTTRNEEQSGDGSRHSGSRHHEASTHADISRHSQAVQG QSEGSRRSRRQGSSVSQDSDSEGHSEDSERWSGSASRNHHGSAQEQLR DGSRHPRSHQEDRAGHGHSADSSRQSGTRHTQTSSGGQAASSHEQARS SAGERHGSHHQQSADSSRHSGIGHGQASSAVRDSGHRGYSGSQASDNE GHSEDSDTQSVSAHGQAGSHQQSHQESARGRSGETSGHSGSFLYG

Construct	Sequence
sfGFP-(r8)10	MGSKGEELFTGVVPILVELDGDVNGHKFSVRGEGEGDATNGKLTLKFI CTTGKLPVPWPTLVTTLGYGVQCFSRYPDHMKRHDFFKSAMPEGYVQ ERTISFKDDGTYKTRAEVKFEGDTLVNRIELKGIDFKEDGNILGHKLEY NFNSHNVYITADKQKNGIKANFKIRHNVEDGSVQLADHYQQNTPIGDG PVLLPDNHYLSTQSVLSKDPNEKRDHMVLLEFVTAAGITHGMDELYKS PGGQVSTHEQSESSHGWTGPSTRGRQGSRHEQAQDSSRHSASQDGQDT IRGHPGSSRGGRQGYHHEHSVDSSGHSGSHHSHTTSQGRSDASRGQSGS RSASRTTRNEEQSGDGSRHSGSRHHEASTHADISRHSQAVQGQSEGSRR SRRQGSSVSQDSDSEGHSEDSERWSGSASRNHHGSAQEQLRDGSRHPR SHQEDRAGHGHSADSSRQSGTRHTQTSSGGQAASSHEQARSSAGERHG SHHQQSADSSRHSGIGHGQASSAVRDSGHRGYSGSQASDNEGHSEDSD TQSVSAHGQAGSHQQSHQESARGRSGETSGHSGSFLYGQVSTHEQSESS HGWTGPSTRGRQGSRHEQAQDSSRHSASQDGQDTIRGHPGSSRGGRQG YHHEHSVDSSGHSGSHHSHTTSQGRSDASRGQSGSRSASRTTRNEEQSG DGSRHSGSRHHEASTHADISRHSQAVQGQSEGSRRSRRQGSSVSQDSDS EGHSEDSERWSGSASRNHHGSAQEQLRDGSRHPRSHQEDRAGHGHSA DSSRQSGTRHTQTSSGGQAASSHEQARSSAGERHGSHHQQSADSSRHS GIGHGQASSAVRDSGHRGYSGSQASDNEGHSEDSDTQSVSAHGQAGSH QQSHQESARGRSGETSGHSGSFLYGQVSTHEQSESSHGWTGPSTRGRQ GSRHEQAQDSSRHSASQDGQDTIRGHPGSSRGGRQGYHHEHSVDSSGH SGSHHSHTTSQGRSDASRGQSGSRSASRTTRNEEQSGDGSRHSGSRHHE ASTHADISRHSQAVQGQSEGSRRSRRQGSSVSQDSDSEGHSEDSERWSG SASRNHHGSAQEQLRDGSRHPRSHQEDRAGHGHSADSSRQSGTRHTQT SSGGQAASSHEQARSSAGERHGSHHQQSADSSRHSGIGHGQASSAVRD SGHRGYSGSQASDNEGHSEDSDTQSVSAHGQAGSHQQSHQESARGRSG ETSGHSGSFLYGQVSTHEQSESSHGWTGPSTRGRQGSRHEQAQDSSRHS ASQDGQDTIRGHPGSSRGGRQGYHHEHSVDSSGHSGSHHSHTTSQGRS DASRGQSGSRSASRTTRNEEQSGDGSRHSGSRHHEASTHADISRHSQAV QGQSEGSRRSRRQGSSVSQDSDSEGHSEDSERWSGSASRNHHGSAQEQ LRDGSRHPRSHQEDRAGHGHSADSSRQSGTRHTQTSSGGQAASSHEQA RSSAGERHGSHHQQSADSSRHSGIGHGQASSAVRDSGHRGYSGSQASD NEGHSEDSDTQSVSAHGQAGSHQQSHQESARGRSGETSGHSGSFLYGQ VSTHEQSESSHGWTGPSTRGRQGSRHEQAQDSSRHSASQDGQDTIRGH PGSSRGGRQGYHHEHSVDSSGHSGSHHSHTTSQGRSDASRGQSGSRSA SRTTRNEEQSGDGSRHSGSRHHEASTHADISRHSQAVQGQSEGSRRSRR QGSSVSQDSDSEGHSEDSERWSGSASRNHHGSAQEQLRDGSRHPRSHQ EDRAGHGHSADSSRQSGTRHTQTSSGGQAASSHEQARSSAGERHGSHH QQSADSSRHSGIGHGQASSAVRDSGHRGYSGSQASDNEGHSEDSDTQS VSAHGQAGSHQQSHQESARGRSGETSGHSGSFLYGQVSTHEQSESSHG WTGPSTRGRQGSRHEQAQDSSRHSASQDGQDTIRGHPGSSRGGRQGYH HEHSVDSSGHSGSHHSHTTSQGRSDASRGQSGSRSASRTTRNEEQSGDG SRHSGSRHHEASTHADISRHSQAVQGQSEGSRRSRRQGSSVSQDSDSEG HSEDSERWSGSASRNHHGSAQEQLRDGSRHPRSHQEDRAGHGHSADSS RQSGTRHTQTSSGGQAASSHEQARSSAGERHGSHHQQSADSSRHSGIG HGQASSAVRDSGHRGYSGSQASDNEGHSEDSDTQSVSAHGQAGSHQQ

Construct	Sequence
	SHQESARGRSGETSGHSGSFLYGGQVSTHEQSESSHGWTGPSTRGRQGSR HEQAQDSSRHSASQDGQDTIRGHPGSSRGGRQGYHHEHSVDSSGHSGS HHSHTTSQGRSDASRGQSGSRSASRTTRNEEQSGDGSRHSGSRHHEAST HADISRHSQAVQGQSEGSRRSRRQGSSVSQDSDSEGHSEDSERWSGSAS RNHHGSAQEQLRDGSRHPRSHQEDRAGHGHSADSSRQSGTRHTQTSSG GQAASSHEQARSSAGERHGSHHQQSADSSRHSGIGHGQASSAVRDSGH RGYSGSQASDNEGHSEDSDTQSVSAHGQAGSHQQSHQESARGRSGETS GHSGSFLYGGQVSTHEQSESSHGWTGPSTRGRQGSRHEQAQDSSRHSAS QDGQDTIRGHPGSSRGGRQGYHHEHSVDSSGHSGSHHSHTTSQGRSDA SRGQSGSRSASRTTRNEEQSGDGSRHSGSRHHEASTHADISRHSQAVQG QSEGSRRSRRQGSSVSQDSDSEGHSEDSERWSGSASRNHHGSAQEQLR DGSRHPRSHQEDRAGHGHSADSSRQSGTRHTQTSSGGQAASSHEQARS SAGERHGSHHQQSADSSRHSGIGHGQASSAVRDSGHRGYSGSQASDNE GHSEDSDTQSVSAHGQAGSHQQSHQESARGRSGETSGHSGSFLYGGQVS THEQSESSHGWTGPSTRGRQGSRHEQAQDSSRHSASQDGQDTIRGHPG SSRGGRQGYHHEHSVDSSGHSGSHHSHTTSQGRSDASRGQSGSRSASR TTRNEEQSGDGSRHSGSRHHEASTHADISRHSQAVQGQSEGSRRSRRQ GSSVSQDSDSEGHSEDSERWSGSASRNHHGSAQEQLRDGSRHPRSHQE DRAGHGHSADSSRQSGTRHTQTSSGGQAASSHEQARSSAGERHGSHHQ QSADSSRHSGIGHGQASSAVRDSGHRGYSGSQASDNEGHSEDSDTQSV SAHGQAGSHQQSHQESARGRSGETSGHSGSFLYGGQVSTHEQSESSHGW TGPSTRGRQGSRHEQAQDSSRHSASQDGQDTIRGHPGSSRGGRQGYHH EHSVDSSGHSGSHHSHTTSQGRSDASRGQSGSRSASRTTRNEEQSGDGS RHSGSRHHEASTHADISRHSQAVQGQSEGSRRSRRQGSSVSQDSDSEGH SEDSERWSGSASRNHHGSAQEQLRDGSRHPRSHQEDRAGHGHSADSSR QSGTRHTQTSSGGQAASSHEQARSSAGERHGSHHQQSADSSRHSGIGH GQASSAVRDSGHRGYSGSQASDNEGHSEDSDTQSVSAHGQAGSHQQS HQESARGRSGETSGHSGSFLYG

Construct	Sequence
sfGFP-(r8)12	MGSKGEELFTGVVPILVELDGDVNGHKFSVRGEGEGDATNGKLTLKFI CTTGKLPVPWPTLVTTLGYGVQCFSRYPDHMKRHDFFKSAMPEGYVQ ERTISFKDDGTYKTRAEVKFEGDTLVNRIELKGIDFKEDGNILGHKLEY NFNSHNVYITADKQKNGIKANFKIRHNVEDGSVQLADHYQQNTPIGDG PVLLPDNHYLSTQSVLSKDPNEKRDHMVLLEFVTAAGITHGMDELYKS PGGQVSTHEQSESSHGWTGPSTRGRQGSRHEQAQDSSRHSASQDGQDT IRGHPGSSRGGRQGYHHEHSVDSSGHSGSHHSHTTSQGRSDASRGQSGS RSASRTTRNEEQSGDGSRHSGSRHHEASTHADISRHSQAVQGQSEGSRR SRRQGSSVSQDSDSEGHSEDSERWSGSASRNHHGSAQEQLRDGSRHPR SHQEDRAGHGHSADSSRQSGTRHTQTSSGGQAASSHEQARSSAGERHG SHHQQSADSSRHSGIGHGQASSAVRDSGHRGYSGSQASDNEGHSEDSD TQSVSAHGQAGSHQQSHQESARGRSGETSGHSGSFLYGQVSTHEQSESS HGWTGPSTRGRQGSRHEQAQDSSRHSASQDGQDTIRGHPGSSRGGRQG YHHEHSVDSSGHSGSHHSHTTSQGRSDASRGQSGSRSASRTTRNEEQSG DGSRHSGSRHHEASTHADISRHSQAVQGQSEGSRRSRRQGSSVSQDSDS EGHSEDSERWSGSASRNHHGSAQEQLRDGSRHPRSHQEDRAGHGHSA DSSRQSGTRHTQTSSGGQAASSHEQARSSAGERHGSHHQQSADSSRHS GIGHGQASSAVRDSGHRGYSGSQASDNEGHSEDSDTQSVSAHGQAGSH QQSHQESARGRSGETSGHSGSFLYGQVSTHEQSESSHGWTGPSTRGRQ GSRHEQAQDSSRHSASQDGQDTIRGHPGSSRGGRQGYHHEHSVDSSGH SGSHHSHTTSQGRSDASRGQSGSRSASRTTRNEEQSGDGSRHSGSRHHE ASTHADISRHSQAVQGQSEGSRRSRRQGSSVSQDSDSEGHSEDSERWSG SASRNHHGSAQEQLRDGSRHPRSHQEDRAGHGHSADSSRQSGTRHTQT SSGGQAASSHEQARSSAGERHGSHHQQSADSSRHSGIGHGQASSAVRD SGHRGYSGSQASDNEGHSEDSDTQSVSAHGQAGSHQQSHQESARGRSG ETSGHSGSFLYGQVSTHEQSESSHGWTGPSTRGRQGSRHEQAQDSSRHS ASQDGQDTIRGHPGSSRGGRQGYHHEHSVDSSGHSGSHHSHTTSQGRS DASRGQSGSRSASRTTRNEEQSGDGSRHSGSRHHEASTHADISRHSQAV QGQSEGSRRSRRQGSSVSQDSDSEGHSEDSERWSGSASRNHHGSAQEQ LRDGSRHPRSHQEDRAGHGHSADSSRQSGTRHTQTSSGGQAASSHEQA RSSAGERHGSHHQQSADSSRHSGIGHGQASSAVRDSGHRGYSGSQASD NEGHSEDSDTQSVSAHGQAGSHQQSHQESARGRSGETSGHSGSFLYGQ VSTHEQSESSHGWTGPSTRGRQGSRHEQAQDSSRHSASQDGQDTIRGH PGSSRGGRQGYHHEHSVDSSGHSGSHHSHTTSQGRSDASRGQSGSRSA SRTTRNEEQSGDGSRHSGSRHHEASTHADISRHSQAVQGQSEGSRRSRR QGSSVSQDSDSEGHSEDSERWSGSASRNHHGSAQEQLRDGSRHPRSHQ EDRAGHGHSADSSRQSGTRHTQTSSGGQAASSHEQARSSAGERHGSHH QQSADSSRHSGIGHGQASSAVRDSGHRGYSGSQASDNEGHSEDSDTQS VSAHGQAGSHQQSHQESARGRSGETSGHSGSFLYGQVSTHEQSESSHG WTGPSTRGRQGSRHEQAQDSSRHSASQDGQDTIRGHPGSSRGGRQGYH HEHSVDSSGHSGSHHSHTTSQGRSDASRGQSGSRSASRTTRNEEQSGDG SRHSGSRHHEASTHADISRHSQAVQGQSEGSRRSRRQGSSVSQDSDSEG HSEDSERWSGSASRNHHGSAQEQLRDGSRHPRSHQEDRAGHGHSADSS RQSGTRHTQTSSGGQAASSHEQARSSAGERHGSHHQQSADSSRHSGIG HGQASSAVRDSGHRGYSGSQASDNEGHSEDSDTQSVSAHGQAGSHQQ

Construct	Sequence
	SHQESARGRSGETSGHSGSFLYGQVSTHEQSESSHGWTGPSTRGRQGSR HEQAQDSSRHSASQDGQDTIRGHPGSSRGGRQGYHHEHSVDSSGHSGS HHSHTTSQGRSDASRGQSGSRSASRTTRNEEQSGDGSRHSGSRHHEAST HADISRHSQAVQGQSEGSRRSRRQGSSVSQDSDSEGHSEDSERWSGSAS RNHHGSAQEQLRDGSRHPRSHQEDRAGHGHSADSSRQSGTRHTQTSSG GQAASSHEQARSSAGERHGSHHQQSADSSRHSGIGHGQASSAVRDSGH RGYSGSQASDNEGHSEDSDTQSVSAHGQAGSHQQSHQESARGRSGETS GHSGSFLYGQVSTHEQSESSHGWTGPSTRGRQGSRHEQAQDSSRHSAS QDGQDTIRGHPGSSRGGRQGYHHEHSVDSSGHSGSHHSHTTSQGRSDA SRGQSGSRSASRTTRNEEQSGDGSRHSGSRHHEASTHADISRHSQAVQG QSEGSRRSRRQGSSVSQDSDSEGHSEDSERWSGSASRNHHGSAQEQLR DGSRHPRSHQEDRAGHGHSADSSRQSGTRHTQTSSGGQAASSHEQARS SAGERHGSHHQQSADSSRHSGIGHGQASSAVRDSGHRGYSGSQASDNE GHSEDSDTQSVSAHGQAGSHQQSHQESARGRSGETSGHSGSFLYGQVS THEQSESSHGWTGPSTRGRQGSRHEQAQDSSRHSASQDGQDTIRGHPG SSRGGRQGYHHEHSVDSSGHSGSHHSHTTSQGRSDASRGQSGSRSASR TTRNEEQSGDGSRHSGSRHHEASTHADISRHSQAVQGQSEGSRRSRRQ GSSVSQDSDSEGHSEDSERWSGSASRNHHGSAQEQLRDGSRHPRSHQE DRAGHGHSADSSRQSGTRHTQTSSGGQAASSHEQARSSAGERHGSHHQ QSADSSRHSGIGHGQASSAVRDSGHRGYSGSQASDNEGHSEDSDTQSV SAHGQAGSHQQSHQESARGRSGETSGHSGSFLYGQVSTHEQSESSHGW TGPSTRGRQGSRHEQAQDSSRHSASQDGQDTIRGHPGSSRGGRQGYHH EHSVDSSGHSGSHHSHTTSQGRSDASRGQSGSRSASRTTRNEEQSGDGS RHSGSRHHEASTHADISRHSQAVQGQSEGSRRSRRQGSSVSQDSDSEGH SEDSERWSGSASRNHHGSAQEQLRDGSRHPRSHQEDRAGHGHSADSSR QSGTRHTQTSSGGQAASSHEQARSSAGERHGSHHQQSADSSRHSGIGH GQASSAVRDSGHRGYSGSQASDNEGHSEDSDTQSVSAHGQAGSHQQS HQESARGRSGETSGHSGSFLYGQVSTHEQSESSHGWTGPSTRGRQGSR HEQAQDSSRHSASQDGQDTIRGHPGSSRGGRQGYHHEHSVDSSGHSGS HHSHTTSQGRSDASRGQSGSRSASRTTRNEEQSGDGSRHSGSRHHEAST HADISRHSQAVQGQSEGSRRSRRQGSSVSQDSDSEGHSEDSERWSGSAS RNHHGSAQEQLRDGSRHPRSHQEDRAGHGHSADSSRQSGTRHTQTSSG GQAASSHEQARSSAGERHGSHHQQSADSSRHSGIGHGQASSAVRDSGH RGYSGSQASDNEGHSEDSDTQSVSAHGQAGSHQQSHQESARGRSGETS GHSGSFLYGQVSTHEQSESSHGWTGPSTRGRQGSRHEQAQDSSRHSAS QDGQDTIRGHPGSSRGGRQGYHHEHSVDSSGHSGSHHSHTTSQGRSDA SRGQSGSRSASRTTRNEEQSGDGSRHSGSRHHEASTHADISRHSQAVQG QSEGSRRSRRQGSSVSQDSDSEGHSEDSERWSGSASRNHHGSAQEQLR DGSRHPRSHQEDRAGHGHSADSSRQSGTRHTQTSSGGQAASSHEQARS SAGERHGSHHQQSADSSRHSGIGHGQASSAVRDSGHRGYSGSQASDNE GHSEDSDTQSVSAHGQAGSHQQSHQESARGRSGETSGHSGSFLYG

Construct	Sequence
sfGFP-(r8)8-Tail	MGSKGEELFTGVVPILVELDGDVNGHKFSVRGEGEGDATNGKLTLKFI CTTGKLPVPWPTLVTTLGYGVQCFSRYPDHMKRHDFFKSAMPEGYVQ ERTISFKDDGTYKTRAEVKFEGDTLVNRIELKGIDFKEDGNILGHKLEY NFNSHNVYITADKQKNGIKANFKIRHNVEDGSVQLADHYQQNTPIGDG PVLLPDNHYLSTQSVLSKDPNEKRDHMVLLEFVTAAGITHGMDELYKS PGGQVSTHEQSESSHGWTGPSTRGRQGSRHEQAQDSSRHSASQDGQDT IRGHPGSSRGGRQGYHHEHSVDSSGHSGSHHSHTTSQGRSDASRGQSGS RSASRTTRNEEQSGDGSRHSGSRHHEASTHADISRHSQAVQGQSEGSRR SRRQGSSVSQDSDSEGHSEDSERWSGSASRNHHGSAQEQLRDGSRHPR SHQEDRAGHGHSADSSRQSGTRHTQTSSGGQAASSHEQARSSAGERHG SHHQQSADSSRHSGIGHGQASSAVRDSGHRGYSGSQASDNEGHSEDSD TQSVSAHGQAGSHQQSHQESARGRSGETSGHSGSFLYGQVSTHEQSESS HGWTGPSTRGRQGSRHEQAQDSSRHSASQDGQDTIRGHPGSSRGGRQG YHHEHSVDSSGHSGSHHSHTTSQGRSDASRGQSGSRSASRTTRNEEQSG DGSRHSGSRHHEASTHADISRHSQAVQGQSEGSRRSRRQGSSVSQDSDS EGHSEDSERWSGSASRNHHGSAQEQLRDGSRHPRSHQEDRAGHGHSA DSSRQSGTRHTQTSSGGQAASSHEQARSSAGERHGSHHQQSADSSRHS GIGHGQASSAVRDSGHRGYSGSQASDNEGHSEDSDTQSVSAHGQAGSH QQSHQESARGRSGETSGHSGSFLYGQVSTHEQSESSHGWTGPSTRGRQ GSRHEQAQDSSRHSASQDGQDTIRGHPGSSRGGRQGYHHEHSVDSSGH SGSHHSHTTSQGRSDASRGQSGSRSASRTTRNEEQSGDGSRHSGSRHHE ASTHADISRHSQAVQGQSEGSRRSRRQGSSVSQDSDSEGHSEDSERWSG SASRNHHGSAQEQLRDGSRHPRSHQEDRAGHGHSADSSRQSGTRHTQT SSGGQAASSHEQARSSAGERHGSHHQQSADSSRHSGIGHGQASSAVRD SGHRGYSGSQASDNEGHSEDSDTQSVSAHGQAGSHQQSHQESARGRSG ETSGHSGSFLYGQVSTHEQSESSHGWTGPSTRGRQGSRHEQAQDSSRHS ASQDGQDTIRGHPGSSRGGRQGYHHEHSVDSSGHSGSHHSHTTSQGRS DASRGQSGSRSASRTTRNEEQSGDGSRHSGSRHHEASTHADISRHSQAV QGQSEGSRRSRRQGSSVSQDSDSEGHSEDSERWSGSASRNHHGSAQEQ LRDGSRHPRSHQEDRAGHGHSADSSRQSGTRHTQTSSGGQAASSHEQA RSSAGERHGSHHQQSADSSRHSGIGHGQASSAVRDSGHRGYSGSQASD NEGHSEDSDTQSVSAHGQAGSHQQSHQESARGRSGETSGHSGSFLYGQ VSTHEQSESSHGWTGPSTRGRQGSRHEQAQDSSRHSASQDGQDTIRGH PGSSRGGRQGYHHEHSVDSSGHSGSHHSHTTSQGRSDASRGQSGSRSA SRTTRNEEQSGDGSRHSGSRHHEASTHADISRHSQAVQGQSEGSRRSRR QGSSVSQDSDSEGHSEDSERWSGSASRNHHGSAQEQLRDGSRHPRSHQ EDRAGHGHSADSSRQSGTRHTQTSSGGQAASSHEQARSSAGERHGSHH QQSADSSRHSGIGHGQASSAVRDSGHRGYSGSQASDNEGHSEDSDTQS VSAHGQAGSHQQSHQESARGRSGETSGHSGSFLYGQVSTHEQSESSHG WTGPSTRGRQGSRHEQAQDSSRHSASQDGQDTIRGHPGSSRGGRQGYH HEHSVDSSGHSGSHHSHTTSQGRSDASRGQSGSRSASRTTRNEEQSGDG SRHSGSRHHEASTHADISRHSQAVQGQSEGSRRSRRQGSSVSQDSDSEG HSEDSERWSGSASRNHHGSAQEQLRDGSRHPRSHQEDRAGHGHSADSS RQSGTRHTQTSSGGQAASSHEQARSSAGERHGSHHQQSADSSRHSGIG HGQASSAVRDSGHRGYSGSQASDNEGHSEDSDTQSVSAHGQAGSHQQ

Construct	Sequence
	SHQESARGRSGETSGHSGSFLYGQVSTHEQSESSHGWTGPSTRGRQGSR HEQAQDSSRHSASQDGQDTIRGHPGSSRGGRQGYHHEHSVDSSGHSGS HHSHTTSQGRSDASRGQSGSRSASRTTRNEEQSGDGSRHSGSRHHEAST HADISRHSQAVQGQSEGSRRSRRQGSSVSQDSDSEGHSEDSERWSGSAS RNHHGSAQEQLRDGSRHPRSHQEDRAGHGHSADSSRQSGTRHTQTSSG GQAASSHEQARSSAGERHGSHHQQSADSSRHSGIGHGQASSAVRDSGH RGYSGSQASDNEGHSEDSDTQSVSAHGQAGSHQQSHQESARGRSGETS GHSGSFLYGQVSTHEQSESSHGWTGPSTRGRQGSRHEQAQDSSRHSAS QDGQDTIRGHPGSSRGGRQGYHHEHSVDSSGHSGSHHSHTTSQGRSDA SRGQSGSRSASRTTRNEEQSGDGSRHSGSRHHEASTHADISRHSQAVQG QSEGSRRSRRQGSSVSQDSDSEGHSEDSERWSGSASRNHHGSAQEQLR DGSRHPRSHQEDRAGHGHSADSSRQSGTRHTQTSSGGQAASSHEQARS SAGERHGSHHQQSADSSRHSGIGHGQASSAVRDSGHRGYSGSQASDNE GHSEDSDTQSVSAHGQAGSHQQSHQESARGRSGETSGHSGSFLYGPGL CGHSSDISKQLGFSQSQRYYYYEG

Construct	Sequence
sfGFP-(r8)10-Tail	MGSKGEELFTGVVPILVELDGDVNGHKFSVRGEGEGDATNGKLTLKFI CTTGKLPVPWPTLVTTLGYGVQCFSRYPDHMKRHDFFKSAMPEGYVQ ERTISFKDDGTYKTRAEVKFEGDTLVNRIELKGIDFKEDGNILGHKLEY NFNSHNVYITADKQKNGIKANFKIRHNVEDGSVQLADHYQQNTPIGDG PVLLPDNHYLSTQSVLSKDPNEKRDHMVLLEFVTAAGITHGMDELYKS PGGQVSTHEQSESSHGWTGPSTRGRQGSRHEQAQDSSRHSASQDGQDT IRGHPGSSRGGRQGYHHEHSVDSSGHSGSHHSHTTSQGRSDASRGQSGS RSASRTTRNEEQSGDGSRHSGSRHHEASTHADISRHSQAVQGQSEGSRR SRRQGSSVSQDSDSEGHSEDSERWSGSASRNHHGSAQEQLRDGSRHPR SHQEDRAGHGHSADSSRQSGTRHTQTSSGGQAASSHEQARSSAGERHG SHHQQSADSSRHSGIGHGQASSAVRDSGHRGYSGSQASDNEGHSEDSD TQSVSAHGQAGSHQQSHQESARGRSGETSGHSGSFLYGQVSTHEQSESS HGWTGPSTRGRQGSRHEQAQDSSRHSASQDGQDTIRGHPGSSRGGRQG YHHEHSVDSSGHSGSHHSHTTSQGRSDASRGQSGSRSASRTTRNEEQSG DGSRHSGSRHHEASTHADISRHSQAVQGQSEGSRRSRRQGSSVSQDSDS EGHSEDSERWSGSASRNHHGSAQEQLRDGSRHPRSHQEDRAGHGHSA DSSRQSGTRHTQTSSGGQAASSHEQARSSAGERHGSHHQQSADSSRHS GIGHGQASSAVRDSGHRGYSGSQASDNEGHSEDSDTQSVSAHGQAGSH QQSHQESARGRSGETSGHSGSFLYGQVSTHEQSESSHGWTGPSTRGRQ GSRHEQAQDSSRHSASQDGQDTIRGHPGSSRGGRQGYHHEHSVDSSGH SGSHHSHTTSQGRSDASRGQSGSRSASRTTRNEEQSGDGSRHSGSRHHE ASTHADISRHSQAVQGQSEGSRRSRRQGSSVSQDSDSEGHSEDSERWSG SASRNHHGSAQEQLRDGSRHPRSHQEDRAGHGHSADSSRQSGTRHTQT SSGGQAASSHEQARSSAGERHGSHHQQSADSSRHSGIGHGQASSAVRD SGHRGYSGSQASDNEGHSEDSDTQSVSAHGQAGSHQQSHQESARGRSG ETSGHSGSFLYGQVSTHEQSESSHGWTGPSTRGRQGSRHEQAQDSSRHS ASQDGQDTIRGHPGSSRGGRQGYHHEHSVDSSGHSGSHHSHTTSQGRS DASRGQSGSRSASRTTRNEEQSGDGSRHSGSRHHEASTHADISRHSQAV QGQSEGSRRSRRQGSSVSQDSDSEGHSEDSERWSGSASRNHHGSAQEQ LRDGSRHPRSHQEDRAGHGHSADSSRQSGTRHTQTSSGGQAASSHEQA RSSAGERHGSHHQQSADSSRHSGIGHGQASSAVRDSGHRGYSGSQASD NEGHSEDSDTQSVSAHGQAGSHQQSHQESARGRSGETSGHSGSFLYGQ VSTHEQSESSHGWTGPSTRGRQGSRHEQAQDSSRHSASQDGQDTIRGH PGSSRGGRQGYHHEHSVDSSGHSGSHHSHTTSQGRSDASRGQSGSRSA SRTTRNEEQSGDGSRHSGSRHHEASTHADISRHSQAVQGQSEGSRRSRR QGSSVSQDSDSEGHSEDSERWSGSASRNHHGSAQEQLRDGSRHPRSHQ EDRAGHGHSADSSRQSGTRHTQTSSGGQAASSHEQARSSAGERHGSHH QQSADSSRHSGIGHGQASSAVRDSGHRGYSGSQASDNEGHSEDSDTQS VSAHGQAGSHQQSHQESARGRSGETSGHSGSFLYGQVSTHEQSESSHG WTGPSTRGRQGSRHEQAQDSSRHSASQDGQDTIRGHPGSSRGGRQGYH HEHSVDSSGHSGSHHSHTTSQGRSDASRGQSGSRSASRTTRNEEQSGDG SRHSGSRHHEASTHADISRHSQAVQGQSEGSRRSRRQGSSVSQDSDSEG HSEDSERWSGSASRNHHGSAQEQLRDGSRHPRSHQEDRAGHGHSADSS RQSGTRHTQTSSGGQAASSHEQARSSAGERHGSHHQQSADSSRHSGIG HGQASSAVRDSGHRGYSGSQASDNEGHSEDSDTQSVSAHGQAGSHQQ

Construct	Sequence
	SHQESARGRSGETSGHSGSFLYGGQVSTHEQSESSHGWTGPSTRGRQGSR HEQAQDSSRHSASQDGQDTIRGHPGSSRGGRQGYHHEHSVDSSGHSGS HHSHTTSQGRSDASRGQSGSRSASRTTRNEEQSGDGSRHSGSRHHEAST HADISRHSQAVQGQSEGSRRSRRQGSSVSQDSDSEGHSEDSERWSGSAS RNHHGSAQEQLRDGSRHPRSHQEDRAGHGHSADSSRQSGTRHTQTSSG GQAASSHEQARSSAGERHGSHHQQSADSSRHSGIGHGQASSAVRDSGH RGYSGSQASDNEGHSEDSDTQSVSAHGQAGSHQQSHQESARGRSGETS GHSGSFLYGGQVSTHEQSESSHGWTGPSTRGRQGSRHEQAQDSSRHSAS QDGQDTIRGHPGSSRGGRQGYHHEHSVDSSGHSGSHHSHTTSQGRSDA SRGQSGSRSASRTTRNEEQSGDGSRHSGSRHHEASTHADISRHSQAVQG QSEGSRRSRRQGSSVSQDSDSEGHSEDSERWSGSASRNHHGSAQEQLR DGSRHPRSHQEDRAGHGHSADSSRQSGTRHTQTSSGGQAASSHEQARS SAGERHGSHHQQSADSSRHSGIGHGQASSAVRDSGHRGYSGSQASDNE GHSEDSDTQSVSAHGQAGSHQQSHQESARGRSGETSGHSGSFLYGGQVS THEQSESSHGWTGPSTRGRQGSRHEQAQDSSRHSASQDGQDTIRGHPG SSRGGRQGYHHEHSVDSSGHSGSHHSHTTSQGRSDASRGQSGSRSASR TTRNEEQSGDGSRHSGSRHHEASTHADISRHSQAVQGQSEGSRRSRRQ GSSVSQDSDSEGHSEDSERWSGSASRNHHGSAQEQLRDGSRHPRSHQE DRAGHGHSADSSRQSGTRHTQTSSGGQAASSHEQARSSAGERHGSHHQ QSADSSRHSGIGHGQASSAVRDSGHRGYSGSQASDNEGHSEDSDTQSV SAHGQAGSHQQSHQESARGRSGETSGHSGSFLYGGQVSTHEQSESSHGW TGPSTRGRQGSRHEQAQDSSRHSASQDGQDTIRGHPGSSRGGRQGYHH EHSVDSSGHSGSHHSHTTSQGRSDASRGQSGSRSASRTTRNEEQSGDGS RHSGSRHHEASTHADISRHSQAVQGQSEGSRRSRRQGSSVSQDSDSEGH SEDSERWSGSASRNHHGSAQEQLRDGSRHPRSHQEDRAGHGHSADSSR QSGTRHTQTSSGGQAASSHEQARSSAGERHGSHHQQSADSSRHSGIGH GQASSAVRDSGHRGYSGSQASDNEGHSEDSDTQSVSAHGQAGSHQQS HQESARGRSGETSGHSGSFLYGPGLCGHSSDISKQLGFSQSQRYYYYEG

Construct	Sequence
sfGFP-(r8)12-Tail	MGSKGEELFTGVVPILVELDGDVNGHKFSVRGEGEGDATNGKLTLKFI CTTGKLPVPWPTLVTTLGYGVQCFSRYPDHMKRHDFFKSAMPEGYVQ ERTISFKDDGTYKTRAEVKFEGDTLVNRIELKGIDFKEDGNILGHKLEY NFNSHNVYITADKQKNGIKANFKIRHNVEDGSVQLADHYQQNTPIGDG PVLLPDNHYLSTQSVLSKDPNEKRDHMVLLEFVTAAGITHGMDELYKS PGGQVSTHEQSESSHGWTGPSTRGRQGSRHEQAQDSSRHSASQDGQDT IRGHPGSSRGGRQGYHHEHSVDSSGHSGSHHSHTTSQGRSDASRGQSGS RSASRTTRNEEQSGDGSRHSGSRHHEASTHADISRHSQAVQGQSEGSRR SRRQGSSVSQDSDSEGHSEDSERWSGSASRNHHGSAQEQLRDGSRHPR SHQEDRAGHGHSADSSRQSGTRHTQTSSGGQAASSHEQARSSAGERHG SHHQQSADSSRHSGIGHGQASSAVRDSGHRGYSGSQASDNEGHSEDSD TQSVSAHGQAGSHQQSHQESARGRSGETSGHSGSFLYGQVSTHEQSESS HGWTGPSTRGRQGSRHEQAQDSSRHSASQDGQDTIRGHPGSSRGGRQG YHHEHSVDSSGHSGSHHSHTTSQGRSDASRGQSGSRSASRTTRNEEQSG DGSRHSGSRHHEASTHADISRHSQAVQGQSEGSRRSRRQGSSVSQDSDS EGHSEDSERWSGSASRNHHGSAQEQLRDGSRHPRSHQEDRAGHGHSA DSSRQSGTRHTQTSSGGQAASSHEQARSSAGERHGSHHQQSADSSRHS GIGHGQASSAVRDSGHRGYSGSQASDNEGHSEDSDTQSVSAHGQAGSH QQSHQESARGRSGETSGHSGSFLYGQVSTHEQSESSHGWTGPSTRGRQ GSRHEQAQDSSRHSASQDGQDTIRGHPGSSRGGRQGYHHEHSVDSSGH SGSHHSHTTSQGRSDASRGQSGSRSASRTTRNEEQSGDGSRHSGSRHHE ASTHADISRHSQAVQGQSEGSRRSRRQGSSVSQDSDSEGHSEDSERWSG SASRNHHGSAQEQLRDGSRHPRSHQEDRAGHGHSADSSRQSGTRHTQT SSGGQAASSHEQARSSAGERHGSHHQQSADSSRHSGIGHGQASSAVRD SGHRGYSGSQASDNEGHSEDSDTQSVSAHGQAGSHQQSHQESARGRSG ETSGHSGSFLYGQVSTHEQSESSHGWTGPSTRGRQGSRHEQAQDSSRHS ASQDGQDTIRGHPGSSRGGRQGYHHEHSVDSSGHSGSHHSHTTSQGRS DASRGQSGSRSASRTTRNEEQSGDGSRHSGSRHHEASTHADISRHSQAV QGQSEGSRRSRRQGSSVSQDSDSEGHSEDSERWSGSASRNHHGSAQEQ LRDGSRHPRSHQEDRAGHGHSADSSRQSGTRHTQTSSGGQAASSHEQA RSSAGERHGSHHQQSADSSRHSGIGHGQASSAVRDSGHRGYSGSQASD NEGHSEDSDTQSVSAHGQAGSHQQSHQESARGRSGETSGHSGSFLYGQ VSTHEQSESSHGWTGPSTRGRQGSRHEQAQDSSRHSASQDGQDTIRGH PGSSRGGRQGYHHEHSVDSSGHSGSHHSHTTSQGRSDASRGQSGSRSA SRTTRNEEQSGDGSRHSGSRHHEASTHADISRHSQAVQGQSEGSRRSRR QGSSVSQDSDSEGHSEDSERWSGSASRNHHGSAQEQLRDGSRHPRSHQ EDRAGHGHSADSSRQSGTRHTQTSSGGQAASSHEQARSSAGERHGSHH QQSADSSRHSGIGHGQASSAVRDSGHRGYSGSQASDNEGHSEDSDTQS VSAHGQAGSHQQSHQESARGRSGETSGHSGSFLYGQVSTHEQSESSHG WTGPSTRGRQGSRHEQAQDSSRHSASQDGQDTIRGHPGSSRGGRQGYH HEHSVDSSGHSGSHHSHTTSQGRSDASRGQSGSRSASRTTRNEEQSGDG SRHSGSRHHEASTHADISRHSQAVQGQSEGSRRSRRQGSSVSQDSDSEG HSEDSERWSGSASRNHHGSAQEQLRDGSRHPRSHQEDRAGHGHSADSS RQSGTRHTQTSSGGQAASSHEQARSSAGERHGSHHQQSADSSRHSGIG HGQASSAVRDSGHRGYSGSQASDNEGHSEDSDTQSVSAHGQAGSHQQ

Construct	Sequence
	SHQESARGRSGETSGHSGSFLYGGQVSTHEQSESSHGWTGPSTRGRQGSR HEQAQDSSRHSASQDGQDTIRGHPGSSRGGRQGYHHEHSVDSSGHSGS HHSHTTSQGRSDASRGQSGSRSASRTTRNEEQSGDGSRHSGSRHHEAST HADISRHSQAVQGQSEGSRRSRRQGSSVSQDSDSEGHSEDSERWSGSAS RNHHGSAQEQLRDGSRHPRSHQEDRAGHGHSADSSRQSGTRHTQTSSG GQAASSHEQARSSAGERHGSHHQQSADSSRHSGIGHGQASSAVRDSGH RGYSGSQASDNEGHSEDSDTQSVSAHGQAGSHQQSHQESARGRSGETS GHSGSFLYGGQVSTHEQSESSHGWTGPSTRGRQGSRHEQAQDSSRHSAS QDGQDTIRGHPGSSRGGRQGYHHEHSVDSSGHSGSHHSHTTSQGRSDA SRGQSGSRSASRTTRNEEQSGDGSRHSGSRHHEASTHADISRHSQAVQG QSEGSRRSRRQGSSVSQDSDSEGHSEDSERWSGSASRNHHGSAQEQLR DGSRHPRSHQEDRAGHGHSADSSRQSGTRHTQTSSGGQAASSHEQARS SAGERHGSHHQQSADSSRHSGIGHGQASSAVRDSGHRGYSGSQASDNE GHSEDSDTQSVSAHGQAGSHQQSHQESARGRSGETSGHSGSFLYGGQVS THEQSESSHGWTGPSTRGRQGSRHEQAQDSSRHSASQDGQDTIRGHPG SSRGGRQGYHHEHSVDSSGHSGSHHSHTTSQGRSDASRGQSGSRSASR TTRNEEQSGDGSRHSGSRHHEASTHADISRHSQAVQGQSEGSRRSRRQ GSSVSQDSDSEGHSEDSERWSGSASRNHHGSAQEQLRDGSRHPRSHQE DRAGHGHSADSSRQSGTRHTQTSSGGQAASSHEQARSSAGERHGSHHQ QSADSSRHSGIGHGQASSAVRDSGHRGYSGSQASDNEGHSEDSDTQSV SAHGQAGSHQQSHQESARGRSGETSGHSGSFLYGGQVSTHEQSESSHGW TGPSTRGRQGSRHEQAQDSSRHSASQDGQDTIRGHPGSSRGGRQGYHH EHSVDSSGHSGSHHSHTTSQGRSDASRGQSGSRSASRTTRNEEQSGDGS RHSGSRHHEASTHADISRHSQAVQGQSEGSRRSRRQGSSVSQDSDSEGH SEDSERWSGSASRNHHGSAQEQLRDGSRHPRSHQEDRAGHGHSADSSR QSGTRHTQTSSGGQAASSHEQARSSAGERHGSHHQQSADSSRHSGIGH GQASSAVRDSGHRGYSGSQASDNEGHSEDSDTQSVSAHGQAGSHQQS HQESARGRSGETSGHSGSFLYGGQVSTHEQSESSHGWTGPSTRGRQGSR HEQAQDSSRHSASQDGQDTIRGHPGSSRGGRQGYHHEHSVDSSGHSGS HHSHTTSQGRSDASRGQSGSRSASRTTRNEEQSGDGSRHSGSRHHEAST HADISRHSQAVQGQSEGSRRSRRQGSSVSQDSDSEGHSEDSERWSGSAS RNHHGSAQEQLRDGSRHPRSHQEDRAGHGHSADSSRQSGTRHTQTSSG GQAASSHEQARSSAGERHGSHHQQSADSSRHSGIGHGQASSAVRDSGH RGYSGSQASDNEGHSEDSDTQSVSAHGQAGSHQQSHQESARGRSGETS GHSGSFLYGGQVSTHEQSESSHGWTGPSTRGRQGSRHEQAQDSSRHSAS QDGQDTIRGHPGSSRGGRQGYHHEHSVDSSGHSGSHHSHTTSQGRSDA SRGQSGSRSASRTTRNEEQSGDGSRHSGSRHHEASTHADISRHSQAVQG QSEGSRRSRRQGSSVSQDSDSEGHSEDSERWSGSASRNHHGSAQEQLR DGSRHPRSHQEDRAGHGHSADSSRQSGTRHTQTSSGGQAASSHEQARS SAGERHGSHHQQSADSSRHSGIGHGQASSAVRDSGHRGYSGSQASDNE GHSEDSDTQSVSAHGQAGSHQQSHQESARGRSGETSGHSGSFLYGPGL CGHSSDISKQLGFSQSQRYYYYEG

Construct	Sequence
S100-sfGFP-(r8)8-Tail	MSTLLENIFAIINLFKQYSKKDKNTDTLSKKELKELLEKEFRQILKNPDD PDMVDVFMDHLDIDHNKKIDFTEFLLMVFKLAQAYYESTRKEGVPGSG VPGAGVPGSRSDGSKGEELFTGVVPILVELDGDVNGHKFSVRGEGEGD ATNGKLTLKFICTTGKLPVPWPTLVTTLGYGVQCFSRYPDHMKRHDFF KSAMPEGYVQERTISFKDDGTYKTRAEVKFEGDTLVNRIELKGIDFKED GNILGHKLEYNFNSHNVYITADKQKNGIKANFKIRHNVEDGSVQLADH YQQNTPIGDGPVLLPDNHYLSTQSVLSKDPNEKRDHMVLLEFVTAAGIT HGMDELYKSPGGQVSTHEQSESSHGWTGPSTRGRQGSRHEQAQDSSR HSASQDGQDTIRGHPGSSRGGRQGYHHEHSVDSSGHSGSHHSHTTSQG RSDASRGQSGSRSASRTTRNEEQSGDGSRHSGSRHHEASTHADISRHSQ AVQGQSEGSRRSRRQGSSVSQDSDSEGHSEDSERWSGSASRNHHGSAQ EQLRDGSRHPRSHQEDRAGHGHSADSSRQSGTRHTQTSSGGQAASSHE QARSSAGERHGSHHQQSADSSRHSGIGHGQASSAVRDSGHRGYSGSQA SDNEGHSEDSDTQSVSAHGQAGSHQQSHQESARGRSGETSGHSGSFLY GQVSTHEQSESSHGWTGPSTRGRQGSRHEQAQDSSRHSASQDGQDTIR GHPGSSRGGRQGYHHEHSVDSSGHSGSHHSHTTSQGRSDASRGQSGSR SASRTTRNEEQSGDGSRHSGSRHHEASTHADISRHSQAVQGQSEGSRRS RRQGSSVSQDSDSEGHSEDSERWSGSASRNHHGSAQEQLRDGSRHPRS HQEDRAGHGHSADSSRQSGTRHTQTSSGGQAASSHEQARSSAGERHGS HHQQSADSSRHSGIGHGQASSAVRDSGHRGYSGSQASDNEGHSEDSDT QSVSAHGQAGSHQQSHQESARGRSGETSGHSGSFLYGQVSTHEQSESS HGWTGPSTRGRQGSRHEQAQDSSRHSASQDGQDTIRGHPGSSRGGRQG YHHEHSVDSSGHSGSHHSHTTSQGRSDASRGQSGSRSASRTTRNEEQSG DGSRHSGSRHHEASTHADISRHSQAVQGQSEGSRRSRRQGSSVSQDSDS EGHSEDSERWSGSASRNHHGSAQEQLRDGSRHPRSHQEDRAGHGHSA DSSRQSGTRHTQTSSGGQAASSHEQARSSAGERHGSHHQQSADSSRHS GIGHGQASSAVRDSGHRGYSGSQASDNEGHSEDSDTQSVSAHGQAGSH QQSHQESARGRSGETSGHSGSFLYGQVSTHEQSESSHGWTGPSTRGRQ GSRHEQAQDSSRHSASQDGQDTIRGHPGSSRGGRQGYHHEHSVDSSGH SGSHHSHTTSQGRSDASRGQSGSRSASRTTRNEEQSGDGSRHSGSRHHE ASTHADISRHSQAVQGQSEGSRRSRRQGSSVSQDSDSEGHSEDSERWSG SASRNHHGSAQEQLRDGSRHPRSHQEDRAGHGHSADSSRQSGTRHTQT SSGGQAASSHEQARSSAGERHGSHHQQSADSSRHSGIGHGQASSAVRD SGHRGYSGSQASDNEGHSEDSDTQSVSAHGQAGSHQQSHQESARGRSG ETSGHSGSFLYGQVSTHEQSESSHGWTGPSTRGRQGSRHEQAQDSSRHS ASQDGQDTIRGHPGSSRGGRQGYHHEHSVDSSGHSGSHHSHTTSQGRS DASRGQSGSRSASRTTRNEEQSGDGSRHSGSRHHEASTHADISRHSQAV QGQSEGSRRSRRQGSSVSQDSDSEGHSEDSERWSGSASRNHHGSAQEQ LRDGSRHPRSHQEDRAGHGHSADSSRQSGTRHTQTSSGGQAASSHEQA RSSAGERHGSHHQQSADSSRHSGIGHGQASSAVRDSGHRGYSGSQASD NEGHSEDSDTQSVSAHGQAGSHQQSHQESARGRSGETSGHSGSFLYGQ VSTHEQSESSHGWTGPSTRGRQGSRHEQAQDSSRHSASQDGQDTIRGH PGSSRGGRQGYHHEHSVDSSGHSGSHHSHTTSQGRSDASRGQSGSRSA SRTTRNEEQSGDGSRHSGSRHHEASTHADISRHSQAVQGQSEGSRRSRR QGSSVSQDSDSEGHSEDSERWSGSASRNHHGSAQEQLRDGSRHPRSHQ

Construct	Sequence
	EDRAGHGHSADSSRQSGTRHTQTSSGGQAASSHEQARSSAGERHGSHH QQSADSSRHSGIGHGQASSAVRDSGHRGYSGSQASDNEGHSEDSDTQS VSAHGQAGSHQQSHQESARGRSGETSGHSGSFLYGQVSTHEQSESSHG WTGPSTRGRQGSRHEQAQDSSRHSASQDGQDTIRGHPGSSRGGRQGYH HEHSVDSSGHSGSHHSHTTSQGRSDASRGQSGSRSASRTTRNEEQSGDG SRHSGSRHHEASTHADISRHSQAVQGQSEGSRRSRRQGSSVSQDSDSEG HSEDSERWSGSASRNHHGSAQEQLRDGSRHPRSHQEDRAGHGHSADSS RQSGTRHTQTSSGGQAASSHEQARSSAGERHGSHHQQSADSSRHSGIG HGQASSAVRDSGHRGYSGSQASDNEGHSEDSDTQSVSAHGQAGSHQQ SHQESARGRSGETSGHSGSFLYGQVSTHEQSESSHGWTGPSTRGRQGSR HEQAQDSSRHSASQDGQDTIRGHPGSSRGGRQGYHHEHSVDSSGHSGS HHSHTTSQGRSDASRGQSGSRSASRTTRNEEQSGDGSRHSGSRHHEAST HADISRHSQAVQGQSEGSRRSRRQGSSVSQDSDSEGHSEDSERWSGSAS RNHHGSAQEQLRDGSRHPRSHQEDRAGHGHSADSSRQSGTRHTQTSSG GQAASSHEQARSSAGERHGSHHQQSADSSRHSGIGHGQASSAVRDSGH RGYSGSQASDNEGHSEDSDTQSVSAHGQAGSHQQSHQESARGRSGETS GHSGSFLYGPGLCGHSSDISKQLGFSQSQRYYYYEG

Construct	Sequence
mRFP1-(r8)16	MASSEDVIKEFMRFKVRMEGSVNGHEFEIEGEGEGRPYEGTQTAKLKV TKGGPLPFAWDILSPQFQYGSKAYVKHPADIPDYLKLSFPEGFKWERV MNFEDGGVVTVTQDSSLQDGEFIYKVKLRGTNFPSDGPVMQKKTMGW EASTERMYPEDGALKGEIKMRLKLKDGGHYDAEVKTTYMAKKPVQLP GAYKTDIKLDITSHNEDYTIVEQYERAEGRHSTGASPGGQVSTHEQSES SHGWTGPSTRGRQGSRHEQAQDSSRHSASQDGQDTIRGHPGSSRGGRQ GYHHEHSVDSSGHSGSHHSHTTSQGRSDASRGQSGSRSASRTTRNEEQS GDGSRHSGSRHHEASTHADISRHSQAVQGQSEGSRRSRRQGSSVSQDS DSEGHSEDSERWSGSASRNHHGSAQEQLRDGSRHPRSHQEDRAGHGHS ADSSRQSGTRHTQTSSGGQAASSHEQARSSAGERHGSHHQQSADSSRH SGIGHGQASSAVRDSGHRGYSGSQASDNEGHSEDSDTQSVSAHGQAGS HQQSHQESARGRSGETSGHSGSFLYGQVSTHEQSESSHGWTGPSTRGR QGSRHEQAQDSSRHSASQDGQDTIRGHPGSSRGGRQGYHHEHSVDSSG HSGSHHSHTTSQGRSDASRGQSGSRSASRTTRNEEQSGDGSRHSGSRHH EASTHADISRHSQAVQGQSEGSRRSRRQGSSVSQDSDSEGHSEDSERWS GSASRNHHGSAQEQLRDGSRHPRSHQEDRAGHGHSADSSRQSGTRHTQ TSSGGQAASSHEQARSSAGERHGSHHQQSADSSRHSGIGHGQASSAVR DSGHRGYSGSQASDNEGHSEDSDTQSVSAHGQAGSHQQSHQESARGRS GETSGHSGSFLYGQVSTHEQSESSHGWTGPSTRGRQGSRHEQAQDSSR HSASQDGQDTIRGHPGSSRGGRQGYHHEHSVDSSGHSGSHHSHTTSQG RSDASRGQSGSRSASRTTRNEEQSGDGSRHSGSRHHEASTHADISRHSQ AVQGQSEGSRRSRRQGSSVSQDSDSEGHSEDSERWSGSASRNHHGSAQ EQLRDGSRHPRSHQEDRAGHGHSADSSRQSGTRHTQTSSGGQAASSHE QARSSAGERHGSHHQQSADSSRHSGIGHGQASSAVRDSGHRGYSGSQA SDNEGHSEDSDTQSVSAHGQAGSHQQSHQESARGRSGETSGHSGSFLY GQVSTHEQSESSHGWTGPSTRGRQGSRHEQAQDSSRHSASQDGQDTIR GHPGSSRGGRQGYHHEHSVDSSGHSGSHHSHTTSQGRSDASRGQSGSR SASRTTRNEEQSGDGSRHSGSRHHEASTHADISRHSQAVQGQSEGSRRS RRQGSSVSQDSDSEGHSEDSERWSGSASRNHHGSAQEQLRDGSRHPRS HQEDRAGHGHSADSSRQSGTRHTQTSSGGQAASSHEQARSSAGERHGS HHQQSADSSRHSGIGHGQASSAVRDSGHRGYSGSQASDNEGHSEDSDT QSVSAHGQAGSHQQSHQESARGRSGETSGHSGSFLYGQVSTHEQSESS HGWTGPSTRGRQGSRHEQAQDSSRHSASQDGQDTIRGHPGSSRGGRQG YHHEHSVDSSGHSGSHHSHTTSQGRSDASRGQSGSRSASRTTRNEEQSG DGSRHSGSRHHEASTHADISRHSQAVQGQSEGSRRSRRQGSSVSQDSDS EGHSEDSERWSGSASRNHHGSAQEQLRDGSRHPRSHQEDRAGHGHSA DSSRQSGTRHTQTSSGGQAASSHEQARSSAGERHGSHHQQSADSSRHS GIGHGQASSAVRDSGHRGYSGSQASDNEGHSEDSDTQSVSAHGQAGSH QQSHQESARGRSGETSGHSGSFLYGQVSTHEQSESSHGWTGPSTRGRQ GSRHEQAQDSSRHSASQDGQDTIRGHPGSSRGGRQGYHHEHSVDSSGH SGSHHSHTTSQGRSDASRGQSGSRSASRTTRNEEQSGDGSRHSGSRHHE ASTHADISRHSQAVQGQSEGSRRSRRQGSSVSQDSDSEGHSEDSERWSG SASRNHHGSAQEQLRDGSRHPRSHQEDRAGHGHSADSSRQSGTRHTQT SSGGQAASSHEQARSSAGERHGSHHQQSADSSRHSGIGHGQASSAVRD SGHRGYSGSQASDNEGHSEDSDTQSVSAHGQAGSHQQSHQESARGRSG

Construct	Sequence
	ETSGHSGSFLYGQVSTHEQSESSHGWTGPSTRGRQGSRHEQAQDSSRHS ASQDGQDTIRGHPGSSRGGRQGYHHEHSVDSSGHSGSHHSHTTSQGRS DASRGQSGSRSASRTTRNEEQSGDGSRHSGSRHHEASTHADISRHSQAV QGQSEGSRRSRRQGSSVSQDSDSEGHSEDSERWSGSASRNHHGSAQEQ LRDGSRHPRSHQEDRAGHGHSADSSRQSGTRHTQTSSGGQAASSHEQA RSSAGERHGSHHQQSADSSRHSGIGHGQASSAVRDSGHRGYSGSQASD NEGHSEDSDTQSVSAHGQAGSHQQSHQESARGRSGETSGHSGSFLYGQ VSTHEQSESSHGWTGPSTRGRQGSRHEQAQDSSRHSASQDGQDTIRGH PGSSRGGRQGYHHEHSVDSSGHSGSHHSHTTSQGRSDASRGQSGSRSA SRTTRNEEQSGDGSRHSGSRHHEASTHADISRHSQAVQGQSEGSRRSRR QGSSVSQDSDSEGHSEDSERWSGSASRNHHGSAQEQLRDGSRHPRSHQ EDRAGHGHSADSSRQSGTRHTQTSSGGQAASSHEQARSSAGERHGSHH QQSADSSRHSGIGHGQASSAVRDSGHRGYSGSQASDNEGHSEDSDTQS VSAHGQAGSHQQSHQESARGRSGETSGHSGSFLYGQVSTHEQSESSHG WTGPSTRGRQGSRHEQAQDSSRHSASQDGQDTIRGHPGSSRGGRQGYH HEHSVDSSGHSGSHHSHTTSQGRSDASRGQSGSRSASRTTRNEEQSGDG SRHSGSRHHEASTHADISRHSQAVQGQSEGSRRSRRQGSSVSQDSDSEG HSEDSERWSGSASRNHHGSAQEQLRDGSRHPRSHQEDRAGHGHSADSS RQSGTRHTQTSSGGQAASSHEQARSSAGERHGSHHQQSADSSRHSGIG HGQASSAVRDSGHRGYSGSQASDNEGHSEDSDTQSVSAHGQAGSHQQ SHQESARGRSGETSGHSGSFLYGQVSTHEQSESSHGWTGPSTRGRQGSR HEQAQDSSRHSASQDGQDTIRGHPGSSRGGRQGYHHEHSVDSSGHSGS HHSHTTSQGRSDASRGQSGSRSASRTTRNEEQSGDGSRHSGSRHHEAST HADISRHSQAVQGQSEGSRRSRRQGSSVSQDSDSEGHSEDSERWSGSAS RNHHGSAQEQLRDGSRHPRSHQEDRAGHGHSADSSRQSGTRHTQTSSG GQAASSHEQARSSAGERHGSHHQQSADSSRHSGIGHGQASSAVRDSGH RGYSGSQASDNEGHSEDSDTQSVSAHGQAGSHQQSHQESARGRSGETS GHSGSFLYGQVSTHEQSESSHGWTGPSTRGRQGSRHEQAQDSSRHSAS QDGQDTIRGHPGSSRGGRQGYHHEHSVDSSGHSGSHHSHTTSQGRSDA SRGQSGSRSASRTTRNEEQSGDGSRHSGSRHHEASTHADISRHSQAVQG QSEGSRRSRRQGSSVSQDSDSEGHSEDSERWSGSASRNHHGSAQEQLR DGSRHPRSHQEDRAGHGHSADSSRQSGTRHTQTSSGGQAASSHEQARS SAGERHGSHHQQSADSSRHSGIGHGQASSAVRDSGHRGYSGSQASDNE GHSEDSDTQSVSAHGQAGSHQQSHQESARGRSGETSGHSGSFLYGQVS THEQSESSHGWTGPSTRGRQGSRHEQAQDSSRHSASQDGQDTIRGHPG SSRGGRQGYHHEHSVDSSGHSGSHHSHTTSQGRSDASRGQSGSRSASR TTRNEEQSGDGSRHSGSRHHEASTHADISRHSQAVQGQSEGSRRSRRQ GSSVSQDSDSEGHSEDSERWSGSASRNHHGSAQEQLRDGSRHPRSHQE DRAGHGHSADSSRQSGTRHTQTSSGGQAASSHEQARSSAGERHGSHHQ QSADSSRHSGIGHGQASSAVRDSGHRGYSGSQASDNEGHSEDSDTQSV SAHGQAGSHQQSHQESARGRSGETSGHSGSFLYGQVSTHEQSESSHGW TGPSTRGRQGSRHEQAQDSSRHSASQDGQDTIRGHPGSSRGGRQGYHH EHSVDSSGHSGSHHSHTTSQGRSDASRGQSGSRSASRTTRNEEQSGDGS RHSGSRHHEASTHADISRHSQAVQGQSEGSRRSRRQGSSVSQDSDSEGH SEDSERWSGSASRNHHGSAQEQLRDGSRHPRSHQEDRAGHGHSADSSR

Construct	Sequence
	QSGTRHTQTSSGGQAASSHEQARSSAGERHGSHHQQSADSSRHSGIGH GQASSAVRDSGHRGYSGSQASDNEGHSEDSDTQSVSAHGQAGSHQQS HQESARGRSGETSGHSGSFLYGQVSTHEQSESSHGWTGPSTRGRQGSR HEQAQDSSRHSASQDGQDTIRGHPGSSRGGRQGYHHEHSVDSSGHSGS HHSHTTSQGRSDASRGQSGSRSASRTTRNEEQSGDGSRHSGSRHHEAST HADISRHSQAVQGQSEGSRRSRRQGSSVSQDSDSEGHSEDSERWSGSAS RNHHGSAQEQLRDGSRHPRSHQEDRAGHGHSADSSRQSGTRHTQTSSG GQAASSHEQARSSAGERHGSHHQQSADSSRHSGIGHGQASSAVRDSGH RGYSGSQASDNEGHSEDSDTQSVSAHGQAGSHQQSHQESARGRSGETS GHSGSFLYGQVSTHEQSESSHGWTGPSTRGRQGSRHEQAQDSSRHSAS QDGQDTIRGHPGSSRGGRQGYHHEHSVDSSGHSGSHHSHTTSQGRSDA SRGQSGSRSASRTTRNEEQSGDGSRHSGSRHHEASTHADISRHSQAVQG QSEGSRRSRRQGSSVSQDSDSEGHSEDSERWSGSASRNHHGSAQEQLR DGSRHPRSHQEDRAGHGHSADSSRQSGTRHTQTSSGGQAASSHEQARS SAGERHGSHHQQSADSSRHSGIGHGQASSAVRDSGHRGYSGSQASDNE GHSEDSDTQSVSAHGQAGSHQQSHQESARGRSGETSGHSGSFLYGQVS THEQSESSHGWTGPSTRGRQGSRHEQAQDSSRHSASQDGQDTIRGHPG SSRGGRQGYHHEHSVDSSGHSGSHHSHTTSQGRSDASRGQSGSRSASR TTRNEEQSGDGSRHSGSRHHEASTHADISRHSQAVQGQSEGSRRSRRQ GSSVSQDSDSEGHSEDSERWSGSASRNHHGSAQEQLRDGSRHPRSHQE DRAGHGHSADSSRQSGTRHTQTSSGGQAASSHEQARSSAGERHGSHHQ QSADSSRHSGIGHGQASSAVRDSGHRGYSGSQASDNEGHSEDSDTQSV SAHGQAGSHQQSHQESARGRSGETSGHSGSFLYG

Construct	Sequence
S100-mRFP1-(r8)8-Tail	MSTLLENIFAIINLFKQYSKKDKNTDTLSKKELKELLEKEFRQILKNPDD PDMVDVFMDHLDIDHNKKIDFTEFLLMVFKLAQAYYESTRKEGVPGSG VPGAGVPGSRSDASSEDVIKEFMRFKVRMEGSVNGHEFEIEGEGEGRPY EGTQTAKLKVTKGGPLPFAWDILSPQFQYGSKAYVKHPADIPDYLKLSF PEGFKWERVMNFEDGGVVTVTQDSSLQDGEFIYKVKLRGTNFPSDGPV MQKKTMGWEASTERMYPEDGALKGEIKMRLKLKDGGHYDAEVKTTY MAKKPVQLPGAYKTDIKLDITSHNEDYTIVEQYERAEGRHSTGASPGG QVSTHEQSESSHGWTGPSTRGRQGSRHEQAQDSSRHSASQDGQDTIRG HPGSSRGGRQGYHHEHSVDSSGHSGSHHSHTTSQGRSDASRGQSGSRS ASRTTRNEEQSGDGSRHSGSRHHEASTHADISRHSQAVQGQSEGSRRSR RQGSSVSQDSDSEGHSEDSERWSGSASRNHHGSAQEQLRDGSRHPRSH QEDRAGHGHSADSSRQSGTRHTQTSSGGQAASSHEQARSSAGERHGSH HQQSADSSRHSGIGHGQASSAVRDSGHRGYSGSQASDNEGHSEDSDTQ SVSAHGQAGSHQQSHQESARGRSGETSGHSGSFLYGQVSTHEQSESSH GWTGPSTRGRQGSRHEQAQDSSRHSASQDGQDTIRGHPGSSRGGRQGY HHEHSVDSSGHSGSHHSHTTSQGRSDASRGQSGSRSASRTTRNEEQSGD GSRHSGSRHHEASTHADISRHSQAVQGQSEGSRRSRRQGSSVSQDSDSE GHSEDSERWSGSASRNHHGSAQEQLRDGSRHPRSHQEDRAGHGHSAD SSRQSGTRHTQTSSGGQAASSHEQARSSAGERHGSHHQQSADSSRHSGI GHGQASSAVRDSGHRGYSGSQASDNEGHSEDSDTQSVSAHGQAGSHQ QSHQESARGRSGETSGHSGSFLYGQVSTHEQSESSHGWTGPSTRGRQGS RHEQAQDSSRHSASQDGQDTIRGHPGSSRGGRQGYHHEHSVDSSGHSG SHHSHTTSQGRSDASRGQSGSRSASRTTRNEEQSGDGSRHSGSRHHEAS THADISRHSQAVQGQSEGSRRSRRQGSSVSQDSDSEGHSEDSERWSGSA SRNHHGSAQEQLRDGSRHPRSHQEDRAGHGHSADSSRQSGTRHTQTSS GGQAASSHEQARSSAGERHGSHHQQSADSSRHSGIGHGQASSAVRDSG HRGYSGSQASDNEGHSEDSDTQSVSAHGQAGSHQQSHQESARGRSGET SGHSGSFLYGQVSTHEQSESSHGWTGPSTRGRQGSRHEQAQDSSRHSA SQDGQDTIRGHPGSSRGGRQGYHHEHSVDSSGHSGSHHSHTTSQGRSD ASRGQSGSRSASRTTRNEEQSGDGSRHSGSRHHEASTHADISRHSQAVQ GQSEGSRRSRRQGSSVSQDSDSEGHSEDSERWSGSASRNHHGSAQEQL RDGSRHPRSHQEDRAGHGHSADSSRQSGTRHTQTSSGGQAASSHEQAR SSAGERHGSHHQQSADSSRHSGIGHGQASSAVRDSGHRGYSGSQASDN EGHSEDSDTQSVSAHGQAGSHQQSHQESARGRSGETSGHSGSFLYGQV STHEQSESSHGWTGPSTRGRQGSRHEQAQDSSRHSASQDGQDTIRGHP GSSRGGRQGYHHEHSVDSSGHSGSHHSHTTSQGRSDASRGQSGSRSAS RTTRNEEQSGDGSRHSGSRHHEASTHADISRHSQAVQGQSEGSRRSRRQ GSSVSQDSDSEGHSEDSERWSGSASRNHHGSAQEQLRDGSRHPRSHQE DRAGHGHSADSSRQSGTRHTQTSSGGQAASSHEQARSSAGERHGSHHQ QSADSSRHSGIGHGQASSAVRDSGHRGYSGSQASDNEGHSEDSDTQSV SAHGQAGSHQQSHQESARGRSGETSGHSGSFLYGQVSTHEQSESSHGW TGPSTRGRQGSRHEQAQDSSRHSASQDGQDTIRGHPGSSRGGRQGYHH EHSVDSSGHSGSHHSHTTSQGRSDASRGQSGSRSASRTTRNEEQSGDGS RHSGSRHHEASTHADISRHSQAVQGQSEGSRRSRRQGSSVSQDSDSEGH SEDSERWSGSASRNHHGSAQEQLRDGSRHPRSHQEDRAGHGHSADSSR

Construct	Sequence
	QSGTRHTQTSSGGQAASSHEQARSSAGERHGSHHQQSADSSRHSGIGH GQASSAVRDSGHRGYSGSQASDNEGHSEDSDTQSVSAHGQAGSHQQS HQESARGRSGETSGHSGSFLYGQVSTHEQSESSHGWTGPSTRGRQGSR HEQAQDSSRHSASQDGQDTIRGHPGSSRGGRQGYHHEHSVDSSGHSGS HHSHTTSQGRSDASRGQSGSRSASRTTRNEEQSGDGSRHSGSRHHEAST HADISRHSQAVQGQSEGSRRSRRQGSSVSQDSDSEGHSEDSERWSGSAS RNHHGSAQEQLRDGSRHPRSHQEDRAGHGHSADSSRQSGTRHTQTSSG GQAASSHEQARSSAGERHGSHHQQSADSSRHSGIGHGQASSAVRDSGH RGYSGSQASDNEGHSEDSDTQSVSAHGQAGSHQQSHQESARGRSGETS GHSGSFLYGQVSTHEQSESSHGWTGPSTRGRQGSRHEQAQDSSRHSAS QDGQDTIRGHPGSSRGGRQGYHHEHSVDSSGHSGSHHSHTTSQGRSDA SRGQSGSRSASRTTRNEEQSGDGSRHSGSRHHEASTHADISRHSQAVQG QSEGSRRSRRQGSSVSQDSDSEGHSEDSERWSGSASRNHHGSAQEQLR DGSRHPRSHQEDRAGHGHSADSSRQSGTRHTQTSSGGQAASSHEQARS SAGERHGSHHQQSADSSRHSGIGHGQASSAVRDSGHRGYSGSQASDNE GHSEDSDTQSVSAHGQAGSHQQSHQESARGRSGETSGHSGSFLYGPGL CGHSSDISKQLGFSQSQRYYYYEG

Table S3.

Sequence information for synthesized phase separation sensors.

Construct	Sequence
r8 (WT repeat in human FLG)	QVSTHEQSESSHGWTGPSTRGRQGSRHEQAQDSSRHSASQDGQDTIRG HPGSSRGGRQGYHHEHSVDSSGHSGSHHSHTTSQGRSDASRGQSGSRS ASRTTRNEEQSGDGSRHSGSRHHEASTHADISRHSQAVQGQSEGSRRSR RQGSSVSQDSDSEGHSEDSERWSGSASRNHHGSAQEQLRDGSRHPRSH QEDRAGHGHSADSSRQSGTRHTQTSSGGQAASSHEQARSSAGERHGSH HQQSADSSRHSGIGHGQASSAVRDSGHRGYSGSQASDNEGHSEDSDTQ SVSAHGQAGSHQQSHQESARGRSGETSGHSGSFLY
r8H1	QVSTHEQSESSHGWTGPSTRGRQGSRYEQAQDSSRYSASQDGQDTIRG YPGSSRGGRQGYHHEHSVDSSGYSGSHHSHTTSQGRSDASRGQSGSRS ASRTTRNEEQSGDGSRYSGSRHHEASTHADISRYSQAVQGQSEGSRRSR RQGSSVSQDSDSEGHSEDSERWSGSASRNHHGSAQEQLRDGSRHPRSH QEDRAGHGYSADSSRQSGTRHTQTSSGGQAASSHEQARSSAGERHGSH YQQSADSSRHSGIGHGQASSAVRDSGHRGYSGSQASDNEGHSEDSDTQ SVSAHGQAGSHQQSHQESARGRSGETSGHSGSFLY
r8H2	QVSTYEQSESSYGWTGPSTRGRQGSRYEQAQDSSRYSASQDGQDTIRG YPGSSRGGRQGYYYEHSVDSSGYSGSYHSHTTSQGRSDASRGQSGSRS ASRTTRNEEQSGDGSRYSGSRHYEASTHADISRYSQAVQGQSEGSRRSR RQGSSVSQDSDSEGHSEDSERWSGSASRNHHGSAQEQLRDGSRYPRSH QEDRAGHGYSADSSRQSGTRYTQTSSGGQAASSHEQARSSAGERYGSH YQQSADSSRHSGIGHGQASSAVRDSGHRGYSGSQASDNEGHSEDSDTQ SVSAHGQAGSHQQSYQESARGRSGETSGHSGSFLY
ir8H2	YLFSGSHGSTEGSRGRASEQYSQQHSGAQGHASVSQTDSDESHGENDS AQSGSYGRHGSDRVASSAQGHGIGSHRSSDASQQYHSGYREGASSRAQ EHSSAAQGGSSTQTYRTGSQRSSDASYGHGARDEQHSRPYRSGDRLQE QASGHHNRSASGSWRESDESHGESDSDQSVSSGQRRSRRSGESQGQVA QSYRSIDAHTSAEYHRSGSYRSGDGSQEENRTTRSASRSGSQGRSADSR GQSTTHSHYSGSYGSSDVSHEYYYGQRGGRSSGPYGRITDQGDQSASY RSSDQAQEYRSGQRGRTSPGTWGYSSESQEYTSVQ
pr8H2	TRNHQGDQRSSHSSSQSYQRYPSRIHEEREDAYEHEGGSSRGGRSGGQS GGSTREQHSASAVGSATRQSEGGYTSYYIASQSSDSHSYGQRSSYSVGS QDQRTDGNAYDGTSQHDRSSASGYRGEFEQSRSAVPGASGGQDHERES QSRSRHTEWHDGDIGSGGSSESRASSGQEGARSSEDRERGAGSSSGGSR QSSTDRQHRYGGAEGSGSQGRSGSHQDDSNHQYAGQGRASYHLGYSP ARQHSSSYSTRHDRYTTQYQSGQAAGSRYHSQLYTQSTDQSAASSEQA DSVQVSTSSQSYRGRSWDSSGEVRRSHSYGASSH
eFlg1	GRDGSHSYQGDRSGHSHQRQGYHEQSDRAGHGDSGHRGYSGRDGSHS YQGDRSGHSHQRQGYHEQSDRAGHGDSGHRGYSGRDGSHSYQGDRS GHSHQRQGYHEQSDRAGHGDSGHRGYSGRDGSHSYQGDRSGHSHQR QGYHEQSDRAGHGDSGHRGYSGRDGSHSYQGDRSGHSHQRQGYHEQ SDRAGHGDSGHRGYS

Construct	Sequence
ieFlg1	SYGRHGSDGHGARDSQEHYGQRQHSHGSRDGQYSHSGDRGSYGRHGS DGHGARDSQEHYGQRQHSHGSRDGQYSHSGDRGSYGRHGSDGHGAR DSQEHYGQRQHSHGSRDGQYSHSGDRGSYGRHGSDGHGARDSQEHY GQRQHSHGSRDGQYSHSGDRGSYGRHGSDGHGARDSQEHYGQRQHS HGSRDGQYSHSGDRG
eFlg2	GRDGSHSYQGDRSGHSHQRQGYHEQSDRAGHGDSGHRGYSGRDGSHS YQGDRSGHSHQRQGYHEQSDRAGHGDSGHRGYSGRDGSHSYQGDRS GHSHQRQGYHEQSDRAGHGDSGHRGYSGRDGSHSYQGDRSGHSHQR QGYHEQSDRAGHGDSGHRGYSSYGRHGSDGHGARDSQEHYGQRQHS HGSRDGQYSHSGDRGSYGRHGSDGHGARDSQEHYGQRQHSHGSRDG QYSHSGDRGSYGRHGSDGHGARDSQEHYGQRQHSHGSRDGQYSHSGD RGSYGRHGSDGHGARDSQEHYGQRQHSHGSRDGQYSHSGDRG
sfGFP-NES	MGASKGEELFTGVVPILVELDGDVNGHKFSVRGEGEGDATNGKLTLKF ICTTGKLPVPWPTLVTTLGYGVQCFSRYPDHMKRHDFFKSAMPEGYVQ ERTISFKDDGTYKTRAEVKFEGDTLVNRIELKGIDFKEDGNILGHKLEY NFNSHNVYITADKQKNGIKANFKIRHNVEDGSVQLADHYQQNTPIGDG PVLLPDNHYLSTQSVLSKDPNEKRDHMVLLEFVTAAGITHGMDELYKS GLELLEDLTLGSP
-20sfGFP-NES	MGASKGEELFTGVVPILVELDGDVNGHKFSVRGEGEGDATNGKLTLKF ICTTGKLPVPWPTLVTTLTYGVQCFSRYPDHMDQHDFFKSAMPEGYVQ ERTISFKDDGTYKTRAEVKFEGDTLVNRIELKGIDFKEDGNILGHKLEY NFNSHDVYITADKQENGIKAEFEIRHNVEDGSVQLADHYQQNTPIGDGP VLLPDDHYLSTESALSKDPNEDRDHMVLLEFVTAAGIDHGMDELYKSG LELLEDLTLGSPG
+15sfGFP-NES	MGASKGERLFTGVVPILVELDGDVNGHKFSVRGEGEGDATRGKLTLKF ICTTGKLPVPWPTLVTTLTYGVQCFSRYPKHMKRHDFFKSAMPEGYVQ ERTISFKKDGTYKTRAEVKFEGRTLVNRIELKGRDFKEKGNILGHKLEY NFNSHNVYITADKRKNGIKANFKIRHNVKDGSVQLADHYQQNTPIGRG PVLLPRNHYLSTRSALSKDPKEKRDHMVLLEFVTAAGITHGMDELYKS GLELLEDLTLGSP
+15sfGFPK-NES	MGASKGEKLFTGVVPILVELDGDVNGHKFSVRGEGEGDATKGKLTLKF ICTTGKLPVPWPTLVTTLTYGVQCFSRYPKHMKRHDFFKSAMPEGYVQ ERTISFKKDGTYKTRAEVKFEGKTLVNRIELKGKDFKEKGNILGHKLEY NFNSHNVYITADKKKNGIKANFKIRHNVKDGSVQLADHYQQNTPIGKG PVLLPKNHYLSTKSALSKDPKEKRDHMVLLEFVTAAGITHGMDELYKS GLELLEDLTLGSPG

Construct	Sequence
Sensor A (full sequence)	MGASKGERLFTGVVPILVELDGDVNGHKFSVRGEGEGDATRGKLTLKF ICTTGKLPVPWPTLVTTLTYGVQCFSRYPKHMKRHDFFKSAMPEGYVQ ERTISFKKDGTYKTRAEVKFEGRTLVNRIELKGRDFKEKGNILGHKLEY NFNSHNVYITADKRKNGIKANFKIRHNVKDGSVQLADHYQQNTPIGRG PVLLPRNHYLSTRSALSKDPKEKRDHMVLLEFVTAAGITHGMDELYKS GLELLEDLTLGSPGYLFSGSHGSTEGSRGRASEQYSQQHSGAQGHASVS QTDSDESHGENDSAQSGSYGRHGSDRVASSAQGHGIGSHRSSDASQQY HSGYREGASSRAQEHSSAAQGGSSTQTYRTGSQRSSDASYGHGARDEQ HSRPYRSGDRLQEQASGHHNRSASGSWRESDESHGESDSDQSVSSGQR RSRRSGESQGQVAQSYRSIDAHTSAEYHRSGSYRSGDGSQEENRTTRSA SRSGSQGRSADSRGQSTTHSHYSGSYGSSDVSHEYYYGQRGGRSSGPY GRITDQGDQSASYRSSDQAQEYRSGQRGRTSPGTWGYSSESQEYTSVQ GS
Sensor B (full sequence)	MGASKGERLFTGVVPILVELDGDVNGHKFSVRGEGEGDATRGKLTLKF ICTTGKLPVPWPTLVTTLTYGVQCFSRYPKHMKRHDFFKSAMPEGYVQ ERTISFKKDGTYKTRAEVKFEGRTLVNRIELKGRDFKEKGNILGHKLEY NFNSHNVYITADKRKNGIKANFKIRHNVKDGSVQLADHYQQNTPIGRG PVLLPRNHYLSTRSALSKDPKEKRDHMVLLEFVTAAGITHGMDELYKS GLELLEDLTLGSPGSYGRHGSDGHGARDSQEHYGQRQHSHGSRDGQY SHSGDRGSYGRHGSDGHGARDSQEHYGQRQHSHGSRDGQYSHSGDRG SYGRHGSDGHGARDSQEHYGQRQHSHGSRDGQYSHSGDRGSYGRHGS DGHGARDSQEHYGQRQHSHGSRDGQYSHSGDRGSYGRHGSDGHGAR DSQEHYGQRQHSHGSRDGQYSHSGDRGGS

Table S4.

Sequence information for K10-related sequences. The underlined protein sequence is also underlined in the name of the construct to facilitate the identification of domains.

Construct	Sequence
mRFP1-K10	MASSEDVIKEFMRFKVRMEGSVNGHEFEIEGEGEGRPYEGTQTAKL KVTKGGPLPFAWDILSPQFQYGSKAYVKHPADIPDYLKLSFPEGFK WERVMNFEDGGVVTVTQDSSLQDGEFIYKVKLRGTNFPSDGPVMQ KKTMGWEASTERMYPEDGALKGEIKMRLKLKDGGHYDAEVKTTY MAKKPVQLPGAYKTDIKLDITSHNEDYTIVEQYERAEGRHSTGASG LELLEDLTLGRSDGSVRYSSSKHYSSSRSGGGGGGGGCGGGGGVSS LRISSSKGSLGGGFSSGGFSGGSFSRGSSGGGCFGGSSGGYGGLGGF GGGSFRGSYGSSSFGGSYGGSFGGGSFGGGSFGGGSFGGGGFGGGG FGGGFGGGFGGDGGLLSGNEKVTMQNLNDRLASYLDKVRALEESN YELEGKIKEWYEKHGNSHQGEPRDYSKYYKTIDDLKNQILNLTTDN ANILLQIDNARLAADDFRLKYENEVALRQSVEADINGLRRVLDELT LTKADLEMQIESLTEELAYLKKNHEEEMKDLRNVSTGDVNVEMNA APGVDLTQLLNNMRSQYEQLAEQNRKDAEAWFNEKSKELTTEIDN NIEQISSYKSEITELRRNVQALEIELQSQLALKQSLEASLAETEGRYC VQLSQIQAQISALEEQLQQIRAETECQNTEYQQLLDIKIRLENEIQTY RSLLEGEGSGSSGGGGRGGGSFGGGYGGGSSGGGSSGGGHGGGHG GSSGGGYGGGSSGGGSSGGGYGGGSSSGGHGGSSSGGYGGGSSGG GGGGYGGGSSGGGSSSGGGYGGGSSSGGHKSSSSGSVGESSSKGPR Y
N-LC(K10)-mCherry	MSVRYSSSKHYSSSRSGGGGGGGGCGGGGGVSSLRISSSKGSLGGG FSSGGFSGGSFSRGSSGGGCFGGSSGGYGGLGGFGGGSFRGSYGSSS FGGSYGGIFGGGSFGGGSFGGGSFGGGGFGGGGFGGGFGGGFGGD GGLLSGNSPGVSKGEEDNMAIIKEFMRFKVHMEGSVNGHEFEIEGE GEGRPYEGTQTAKLKVTKGGPLPFAWDILSPQFMYGSKAYVKHPA DIPDYLKLSFPEGFKWERVMNFEDGGVVTVTQDSSLQDGEFIYKVK LRGTNFPSDGPVMQKKTMGWEASSERMYPEDGALKGEIKQRLKLK DGGHYDAEVKTTYKAKKPVQLPGAYNVNIKLDITSHNEDYTIVEQY ERAEGRHSTGGMDELYKGS
mCherry-C-LC(K10)	MSVRYSSSKHYSSSRSGGGGGGGGCGGGGGVSSLRISSSKGSLGGG FSSGGFSGGSFSRGSSGGGCFGGSSGGYGGLGGFGGGSFRGSYGSSS FGGSYGGIFGGGSFGGGSFGGGSFGGGGFGGGGFGGGFGGGFGGD GGLLSGNSPGVSKGEEDNMAIIKEFMRFKVHMEGSVNGHEFEIEGE GEGRPYEGTQTAKLKVTKGGPLPFAWDILSPQFMYGSKAYVKHPA DIPDYLKLSFPEGFKWERVMNFEDGGVVTVTQDSSLQDGEFIYKVK LRGTNFPSDGPVMQKKTMGWEASSERMYPEDGALKGEIKQRLKLK DGGHYDAEVKTTYKAKKPVQLPGAYNVNIKLDITSHNEDYTIVEQY ERAEGRHSTGGMDELYKGSGSSSGGGGRGGGSFGGGYGGGSSGGGS SGGGHGGGHGGSSGGGYGGGSSGGGSSGGGYGGGSSSGGHGGSSS GGYGGGSSGGGGGGYGGGSSGGGSSSGGGYGGGSSSGGHKSSSSG SVGESSSKGPRY

Construct	Sequence
mCherry	MVSKGEEDNMAIIKEFMRFKVHMEGSVNGHEFEIEGEGEGRPYEGT QTAKLKVTKGGPLPFAWDILSPQFMYGSKAYVKHPADIPDYLKLSF PEGFKWERVMNFEDGGVVTVTQDSSLQDGEFIYKVKLRGTNFPSD GPVMQKKTMGWEASSERMYPEDGALKGEIKQRLKLKDGGHYDAE VKTTYKAKKPVQLPGAYNVNIKLDITSHNEDYTIVEQYERAEGRHS TGGMDELYKSPG

Table S5.

Sequence information for FLG variants recognized by conventional clients and sequence details for their corresponding clients. For FLG constructs, we underline the domain that is specifically bound by the client.

Construct	Sequence
mRFP1- ENLYFQS- (r8)8-Tail	MASSEDVIKEFMRFKVRMEGSVNGHEFEIEGEGEGRPYEGTQTAKL KVTKGGPLPFAWDILSPQFQYGSKAYVKHPADIPDYLKLSFPEGFK WERVMNFEDGGVVTVTQDSSLQDGEFIYKVKLRGTNFPSDGPVMQ KKTMGWEASTERMYPEDGALKGEIKMRLKLKDGGHYDAEVKTTY MAKKPVQLPGAYKTDIKLDITSHNEDYTIVEQYERAEGRHSTGASG SENLYFQSGPGGQVSTHEQSESSHGWTGPSTRGRQGSRHEQAQDSS RHSASQDGQDTIRGHPGSSRGGRQGYHHEHSVDSSGHSGSHHSHTT SQGRSDASRGQSGSRSASRTTRNEEQSGDGSRHSGSRHHEASTHADI SRHSQAVQGQSEGSRRSRRQGSSVSQDSDSEGHSEDSERWSGSASR NHHGSAQEQLRDGSRHPRSHQEDRAGHGHSADSSRQSGTRHTQTSS GGQAASSHEQARSSAGERHGSHHQQSADSSRHSGIGHGQASSAVRD SGHRGYSGSQASDNEGHSEDSDTQSVSAHGQAGSHQQSHQESARG RSGETSGHSGSFLYGQVSTHEQSESSHGWTGPSTRGRQGSRHEQAQ DSSRHSASQDGQDTIRGHPGSSRGGRQGYHHEHSVDSSGHSGSHHS HTTSQGRSDASRGQSGSRSASRTTRNEEQSGDGSRHSGSRHHEAST HADISRHSQAVQGQSEGSRRSRRQGSSVSQDSDSEGHSEDSERWSG SASRNHHGSAQEQLRDGSRHPRSHQEDRAGHGHSADSSRQSGTRH TQTSSGGQAASSHEQARSSAGERHGSHHQQSADSSRHSGIGHGQAS SAVRDSGHRGYSGSQASDNEGHSEDSDTQSVSAHGQAGSHQQSHQ ESARGRSGETSGHSGSFLYGQVSTHEQSESSHGWTGPSTRGRQGSR HEQAQDSSRHSASQDGQDTIRGHPGSSRGGRQGYHHEHSVDSSGHS GSHHSHTTSQGRSDASRGQSGSRSASRTTRNEEQSGDGSRHSGSRH HEASTHADISRHSQAVQGQSEGSRRSRRQGSSVSQDSDSEGHSEDSE RWSGSASRNHHGSAQEQLRDGSRHPRSHQEDRAGHGHSADSSRQS GTRHTQTSSGGQAASSHEQARSSAGERHGSHHQQSADSSRHSGIGH GQASSAVRDSGHRGYSGSQASDNEGHSEDSDTQSVSAHGQAGSHQ QSHQESARGRSGETSGHSGSFLYGQVSTHEQSESSHGWTGPSTRGR QGSRHEQAQDSSRHSASQDGQDTIRGHPGSSRGGRQGYHHEHSVDS SGHSGSHHSHTTSQGRSDASRGQSGSRSASRTTRNEEQSGDGSRHS GSRHHEASTHADISRHSQAVQGQSEGSRRSRRQGSSVSQDSDSEGH SEDSERWSGSASRNHHGSAQEQLRDGSRHPRSHQEDRAGHGHSAD SSRQSGTRHTQTSSGGQAASSHEQARSSAGERHGSHHQQSADSSRH SGIGHGQASSAVRDSGHRGYSGSQASDNEGHSEDSDTQSVSAHGQA GSHQQSHQESARGRSGETSGHSGSFLYGQVSTHEQSESSHGWTGPS TRGRQGSRHEQAQDSSRHSASQDGQDTIRGHPGSSRGGRQGYHHE HSVDSSGHSGSHHSHTTSQGRSDASRGQSGSRSASRTTRNEEQSGD GSRHSGSRHHEASTHADISRHSQAVQGQSEGSRRSRRQGSSVSQDS DSEGHSEDSERWSGSASRNHHGSAQEQLRDGSRHPRSHQEDRAGH GHSADSSRQSGTRHTQTSSGGQAASSHEQARSSAGERHGSHHQQSA DSSRHSGIGHGQASSAVRDSGHRGYSGSQASDNEGHSEDSDTQSVS

	AHGQAGSHQQSHQESARGRSGETSGHSGSFLYGQVSTHEQSESSHG WTGPSTRGRQGSRHEQAQDSSRHSASQDGQDTIRGHPGSSRGGRQG YHHEHSVDSSGHSGSHHSHTTSQGRSDASRGQSGSRSASRTTRNEE QSGDGSRHSGSRHHEASTHADISRHSQAVQGQSEGSRRSRRQGSSV SQDSDSEGHSEDSERWSGSASRNHHGSAQEQLRDGSRHPRSHQEDR AGHGHSADSSRQSGTRHTQTSSGGQAASSHEQARSSAGERHGSHH QQSADSSRHSGIGHGQASSAVRDSGHRGYSGSQASDNEGHSEDSDT QSVSAHGQAGSHQQSHQESARGRSGETSGHSGSFLYGQVSTHEQSE SSHGWTGPSTRGRQGSRHEQAQDSSRHSASQDGQDTIRGHPGSSRG GRQGYHHEHSVDSSGHSGSHHSHTTSQGRSDASRGQSGSRSASRTT RNEEQSGDGSRHSGSRHHEASTHADISRHSQAVQGQSEGSRRSRRQ GSSVSQDSDSEGHSEDSERWSGSASRNHHGSAQEQLRDGSRHPRSH QEDRAGHGHSADSSRQSGTRHTQTSSGGQAASSHEQARSSAGERH GSHHQQSADSSRHSGIGHGQASSAVRDSGHRGYSGSQASDNEGHSE DSDTQSVSAHGQAGSHQQSHQESARGRSGETSGHSGSFLYGQVSTH EQSESSHGWTGPSTRGRQGSRHEQAQDSSRHSASQDGQDTIRGHPG SSRGGRQGYHHEHSVDSSGHSGSHHSHTTSQGRSDASRGQSGSRSA SRTTRNEEQSGDGSRHSGSRHHEASTHADISRHSQAVQGQSEGSRRS RRQGSSVSQDSDSEGHSEDSERWSGSASRNHHGSAQEQLRDGSRHP RSHQEDRAGHGHSADSSRQSGTRHTQTSSGGQAASSHEQARSSAGE RHGSHHQQSADSSRHSGIGHGQASSAVRDSGHRGYSGSQASDNEG HSEDSDTQSVSAHGQAGSHQQSHQESARGRSGETSGHSGSFLYGPG LCGHSSDISKQLGFSQSQRYYYYEG
mRFP1- ENLYFQR- (r8)8-Tail	Same as above but with a single S to R mutation as shown in red.
mS100-mRFP1- (r8)4-Tail	MSALLESITSMIEIFQQYSTSDKEEETLSKEELKELLEGQLQAVLKNP DDQDIAEVFMQMLDVDHDDKLDFAEYLLLVLKLAKAYYEASKNE GVPGSGVPGAGVPGSRSDASSEDVIKEFMRFKVRMEGSVNGHEFEI EGEGEGRPYEGTQTAKLKVTKGGPLPFAWDILSPQFQYGSKAYVKH PADIPDYLKLSFPEGFKWERVMNFEDGGVVTVTQDSSLQDGEFIYK VKLRGTNFPSDGPVMQKKTMGWEASTERMYPEDGALKGEIKMRL KLKDGGHYDAEVKTTYMAKKPVQLPGAYKTDIKLDITSHNEDYTI VEQYERAEGRHSTGASPGGQVSTHEQSESSHGWTGPSTRGRQGSRH EQAQDSSRHSASQDGQDTIRGHPGSSRGGRQGYHHEHSVDSSGHSG SHHSHTTSQGRSDASRGQSGSRSASRTTRNEEQSGDGSRHSGSRHH EASTHADISRHSQAVQGQSEGSRRSRRQGSSVSQDSDSEGHSEDSER WSGSASRNHHGSAQEQLRDGSRHPRSHQEDRAGHGHSADSSRQSG TRHTQTSSGGQAASSHEQARSSAGERHGSHHQQSADSSRHSGIGHG QASSAVRDSGHRGYSGSQASDNEGHSEDSDTQSVSAHGQAGSHQQ SHQESARGRSGETSGHSGSFLYGQVSTHEQSESSHGWTGPSTRGRQ GSRHEQAQDSSRHSASQDGQDTIRGHPGSSRGGRQGYHHEHSVDSS GHSGSHHSHTTSQGRSDASRGQSGSRSASRTTRNEEQSGDGSRHSG SRHHEASTHADISRHSQAVQGQSEGSRRSRRQGSSVSQDSDSEGHSE DSERWSGSASRNHHGSAQEQLRDGSRHPRSHQEDRAGHGHSADSS RQSGTRHTQTSSGGQAASSHEQARSSAGERHGSHHQQSADSSRHSG

	IGHGQASSAVRDSGHRGYSGSQASDNEGHSEDSDTQSVSAHGQAGS HQQSHQESARGRSGETSGHSGSFLYGQVSTHEQSESSHGWTGPSTR GRQGSRHEQAQDSSRHSASQDGQDTIRGHPGSSRGGRQGYHHEHS VDSSGHSGSHHSHTTSQGRSDASRGQSGSRSASRTTRNEEQSGDGS RHSGSRHHEASTHADISRHSQAVQGQSEGSRRSRRQGSSVSQDSDSE GHSEDSERWSGSASRNHHGSAQEQLRDGSRHPRSHQEDRAGHGHS ADSSRQSGTRHTQTSSGGQAASSHEQARSSAGERHGSHHQQSADSS RHSGIGHGQASSAVRDSGHRGYSGSQASDNEGHSEDSDTQSVSAHG QAGSHQQSHQESARGRSGETSGHSGSFLYGQVSTHEQSESSHGWTG PSTRGRQGSRHEQAQDSSRHSASQDGQDTIRGHPGSSRGGRQGYHH EHSVDSSGHSGSHHSHTTSQGRSDASRGQSGSRSASRTTRNEEQSGD GSRHSGSRHHEASTHADISRHSQAVQGQSEGSRRSRRQGSSVSQDS DSEGHSEDSERWSGSASRNHHGSAQEQLRDGSRHPRSHQEDRAGH GHSADSSRQSGTRHTQTSSGGQAASSHEQARSSAGERHGSHHQQSA DSSRHSGIGHGQASSAVRDSGHRGYSGSQASDNEGHSEDSDTQSVS AHGQAGSHQQSHQESARGRSGETSGHSGSFLYGPGLCGHSSDISKQ LGFSQSQRYYYYEG
sfGFP-dTEVP	MGSKGEELFTGVVPILVELDGDVNGHKFSVRGEGEGDATNGKLTL KFICTTGKLPVPWPTLVTTLGYGVQCFSRYPDHMKRHDFFKSAMPE GYVQERTISFKDDGTYKTRAEVKFEGDTLVNRIELKGIDFKEDGNIL GHKLEYNFNSHNVYITADKQKNGIKANFKIRHNVEDGSVQLADHY QQNTPIGDGPVLLPDNHYLSTQSVLSKDPNEKRDHMVLLEFVTAAG ITHGMDELYKSPGSPGSGESLFKGPRDYNPISSTICHLTNESDGHTTS LYGIGFGPFIITNKHLFRRNNGTLLVQSLHGVFKVKNTTTLQQHLID GRDMIIIRMPKDFPPFPQKLKFREPQREERICLVTTNFQTKSMSSMVS DTSCTFPSSDGIFWKHWIQTKDGQAGSPLVSTRDGFIVGIHSASNFT NTNNYFTSVPKNFMELLTNQEAQQWVSGWRLNADSVLWGGHKVF MVKPEEPFQPVKEATQLMNELVYSQ
mS100-n20GFP	MSALLESITSMIEIFQQYSTSDKEEETLSKEELKELLEGQLQAVLKNP DDQDIAEVFMQMLDVDHDDKLDFAEYLLLVLKLAKAYYEASKNE GVPGSGVPGAGVPGSRSDGASKGEELFTGVVPILVELDGDVNGHKF SVRGEGEGDATNGKLTLKFICTTGKLPVPWPTLVTTLTYGVQCFSR YPDHMDQHDFFKSAMPEGYVQERTISFKDDGTYKTRAEVKFEGDT LVNRIELKGIDFKEDGNILGHKLEYNFNSHDVYITADKQENGIKAEF EIRHNVEDGSVQLADHYQQNTPIGDGPVLLPDDHYLSTESALSKDP NEDRDHMVLLEFVTAAGIDHGMDELYKSGLELLEDLTL

Movie S1.

FLG granules undergo liquid-like fusion events in the cell. Live imaging of HaCATs expressing WT(p) FLG [sfGFP-(r8)12-Ctail] (shown in green) and a cytoplasmic marker (mCherry; shown in magenta). Z stacks were acquired every 2 min and are shown as 3D projections. Scale bar is 10 μm. This time-lapse is complementary to still images in Fig 2C.

Movie S2.

Liquid-like fusion events among FLG granules exhibit fast dynamics. Live imaging of HaCATs expressing WT(p) FLG [sfGFP-(r8)10-Ctail]. To capture the rapid dynamics of granule fusion, images were acquired images every 200 ms in a single plane that shows two interacting granules in focus. Scale bar is 5 μm. This time-lapse is complementary to still images in Fig S8.

Movie S3.

Liquid-like streaming of a FLG granule upon deformation with an AFM probe. Live imaging of HaCATs expressing a tail FLG mutant [sfGFP-(r8)8] as we apply pressure with an AFM probe directly on top of one of its FLG granules. The time-lapse was acquired as an overlay of epifluorescence (GFP) and brightfield (DIC) images. Video rate is 30 frames per second (about twice as fast as real time). This time-lapse is complementary to still images in Fig. 3D.

Movie S4.

Mechanically-induced fusion of two WT(up) FLG granules. Live imaging of HaCATs expressing S100-unprocessed FLG [S100-sfGFP-(r8)8-Ctail] as we use the AFM probe to trigger a fusion event by driving two granules into contact. The time-lapse was acquired as an overlay of epifluorescence (GFP) and brightfield (DIC) images. Video rate is 30 frames per second (about twice as fast as real time).

Movie S5.

KGs in skin occasionally fuse as granular cells mature and become crowded with KGs. Live imaging of explanted mouse skin that was *in utero* transduced to drive constitutive expression of Sensor A. Time-lapse shows 3D projections of Z stacks across epidermal layers (with an early granular cell in focus) that were acquired every 20 min over 14 h. Over this period, we observed three KG fusion events as the granular cell matures and its cytoplasm becomes crowded with rapidly growing KGs. One of these fusion events is highlighted in Fig. S17A. Scale bar is 5 μm.

Movie S6.

KG dynamics in living mouse skin. Live imaging of E18.5 explanted mouse skin that was *in utero* transduced to drive suprabasal expression of Sensor A. Time-lapse shows 3D projections of Z stacks across epidermal layers (with prominent granular cells at the top) that were acquired every 20 min over 16 h, showing remarkable maturation of granular cells and their KGs. Note that KGs grow predominantly without undergoing fusion. The time-lapse is shown at 5 frames per second and the video includes a time stamp to indicate real imaging time. Scale bar is 10 μm.

Movie S7.

Keratin fibers cage KGs and oppose their liquid-like fusion. Live imaging of HaCATs with an mRFP-tagged K10 network (magenta) and containing sfGFP-tagged FLG* granules (green). Same cell as in Fig. 6A. Time-lapse corresponds to 3D renderings of mRFP and sfGFP fluorescence in a whole-cell view of insets/snapshots included in Fig. 6B. Scale bar is 10 μm.

Movie S8.

KG and early enucleation dynamics are synced in mouse skin. Live imaging of explanted mouse skin that was *in utero* transduced to drive suprabasal expression of Sensor A (green) and constitutive expression of a chromatin marker (H2B-RFP; magenta). Time-lapse shows 3D projections of Z stacks across epidermal layers (with prominent late granular cells at the top) that were acquired every 20 min over 11 h. Over this period, we capture several enucleation events in which the initiation of chromatin compaction is synced with the partial release of sensor from within KGs and into the cytoplasm. One of these events is highlighted in Fig. 7C. Scale bar is 10 μm.

References and Notes

1. C. P. Brangwynne, C. R. Eckmann, D. S. Courson, A. Rybarska, C. Hoege, J. Gharakhani, F. Jülicher, A. A. Hyman, Germline P granules are liquid droplets that localize by controlled dissolution/condensation. *Science* **324**, 1729–1732 (2009). doi:10.1126/science.1172046 Medline

2. S. F. Banani, H. O. Lee, A. A. Hyman, M. K. Rosen, Biomolecular condensates: Organizers of cellular biochemistry. *Nat. Rev. Mol. Cell Biol.* **18**, 285–298 (2017). doi:10.1038/nrm.2017.7 Medline

3. Y. Shin, C. P. Brangwynne, Liquid phase condensation in cell physiology and disease. *Science* **357**, eaaf4382 (2017). doi:10.1126/science.aaf4382 Medline

4. M. Feric, N. Vaidya, T. S. Harmon, D. M. Mitrea, L. Zhu, T. M. Richardson, R. W. Kriwacki, R. V. Pappu, C. P. Brangwynne, Coexisting liquid phases underlie nucleolar subcompartments. *Cell* **165**, 1686–1697 (2016). doi:10.1016/j.cell.2016.04.047 Medline

5. X. Su, J. A. Ditlev, E. Hui, W. Xing, S. Banjade, J. Okrut, D. S. King, J. Taunton, M. K. Rosen, R. D. Vale, Phase separation of signaling molecules promotes T cell receptor signal transduction. *Science* **352**, 595–599 (2016). doi:10.1126/science.aad9964 Medline

6. J. T. Wang, J. Smith, B.-C. Chen, H. Schmidt, D. Rasoloson, A. Paix, B. G. Lambrus, D. Calidas, E. Betzig, G. Seydoux, Regulation of RNA granule dynamics by phosphorylation of serine-rich, intrinsically disordered proteins in C. elegans. *eLife* **3**, e04591 (2014). doi:10.7554/eLife.04591 Medline

7. A. Molliex, J. Temirov, J. Lee, M. Coughlin, A. P. Kanagaraj, H. J. Kim, T. Mittag, J. P. Taylor, Phase separation by low complexity domains promotes stress granule assembly and drives pathological fibrillization. *Cell* **163**, 123–133 (2015). doi:10.1016/j.cell.2015.09.015 Medline

8. B. R. Sabari, A. Dall'Agnese, A. Boija, I. A. Klein, E. L. Coffey, K. Shrinivas, B. J. Abraham, N. M. Hannett, A. V. Zamudio, J. C. Manteiga, C. H. Li, Y. E. Guo, D. S. Day, J. Schuijers, E. Vasile, S. Malik, D. Hnisz, T. I. Lee, I. I. Cisse, R. G. Roeder, P. A. Sharp, A. K. Chakraborty, R. A. Young, Coactivator condensation at super-enhancers links phase separation and gene control. *Science* **361**, eaar3958 (2018). doi:10.1126/science.aar3958 Medline

9. W.-K. Cho, J.-H. Spille, M. Hecht, C. Lee, C. Li, V. Grube, I. I. Cisse, Mediator and RNA polymerase II clusters associate in transcription-dependent condensates. *Science* **361**, 412–415 (2018). doi:10.1126/science.aar4199 Medline

10. B. A. Gibson, L. K. Doolittle, M. W. G. Schneider, L. E. Jensen, N. Gamarra, L. Henry, D. W. Gerlich, S. Redding, M. K. Rosen, Organization of chromatin by intrinsic and regulated phase separation. *Cell* **179**, 470–484.e21 (2019). doi:10.1016/j.cell.2019.08.037 Medline

11. G. Wan, B. D. Fields, G. Spracklin, A. Shukla, C. M. Phillips, S. Kennedy, Spatiotemporal regulation of liquid-like condensates in epigenetic inheritance. *Nature* **557**, 679–683 (2018). doi:10.1038/s41586-018-0132-0 Medline

12. Y. Lin, D. S. Protter, M. K. Rosen, R. Parker, Formation and maturation of phase-separated liquid droplets by RNA-binding proteins. *Mol. Cell* **60**, 208–219 (2015). doi:10.1016/j.molcel.2015.08.018 Medline

13. H. Jiang, S. Wang, Y. Huang, X. He, H. Cui, X. Zhu, Y. Zheng, Phase transition of spindle-associated protein regulate spindle apparatus assembly. *Cell* **163**, 108–122 (2015). doi:10.1016/j.cell.2015.08.010 Medline

14. A. K. Rai, J.-X. Chen, M. Selbach, L. Pelkmans, Kinase-controlled phase transition of membraneless organelles in mitosis. *Nature* **559**, 211–216 (2018). doi:10.1038/s41586-018-0279-8 Medline

15. O. Beutel, R. Maraspini, K. Pombo-García, C. Martin-Lemaitre, A. Honigmann, Phase Separation of Zonula Occludens Proteins Drives Formation of Tight Junctions. *Cell* **179**, 923–936.e11 (2019). doi:10.1016/j.cell.2019.10.011 Medline

16. E. S. Freeman Rosenzweig, B. Xu, L. Kuhn Cuellar, A. Martinez-Sanchez, M. Schaffer, M. Strauss, H. N. Cartwright, P. Ronceray, J. M. Plitzko, F. Förster, N. S. Wingreen, B. D. Engel, L. C. M. Mackinder, M. C. Jonikas, The eukaryotic CO2-concentrating organelle is liquid-like and exhibits dynamic reorganization. *Cell* **171**, 148–162.e19 (2017). doi:10.1016/j.cell.2017.08.008 Medline

17. S. Alberti, A. Gladfelter, T. Mittag, Considerations and Challenges in Studying Liquid-Liquid Phase Separation and Biomolecular Condensates. *Cell* **176**, 419–434 (2019). doi:10.1016/j.cell.2018.12.035 Medline

18. H. B. Schmidt, A. Barreau, R. Rohatgi, Phase separation-deficient TDP43 remains functional in splicing. *Nat. Commun.* **10**, 4890 (2019). doi:10.1038/s41467-019-12740-2 Medline

19. D. Bracha, M. T. Walls, M.-T. Wei, L. Zhu, M. Kurian, J. L. Avalos, J. E. Toettcher, C. P. Brangwynne, Mapping Local and Global Liquid Phase Behavior in Living Cells Using Photo-Oligomerizable Seeds. *Cell* **175**, 1467–1480.e13 (2018). doi:10.1016/j.cell.2018.10.048 Medline

20. J. A. Segre, Epidermal barrier formation and recovery in skin disorders. *J. Clin. Invest.* **116**, 1150–1158 (2006). doi:10.1172/JCI28521 Medline

21. B. A. Dale, K. A. Resing, R. B. Presland, in *The Keratinocyte Handbook*, I. Leigh, E. B. Lane, F. M. Watt, Eds. (Cambridge Univ. Press, 1994), chap. 17, pp. 323–350.

22. F. G. Quiroz, A. Chilkoti, Sequence heuristics to encode phase behaviour in intrinsically disordered protein polymers. *Nat. Mater.* **14**, 1164–1171 (2015). doi:10.1038/nmat4418 Medline

23. C. N. Palmer, A. D. Irvine, A. Terron-Kwiatkowski, Y. Zhao, H. Liao, S. P. Lee, D. R. Goudie, A. Sandilands, L. E. Campbell, F. J. D. Smith, G. M. O'Regan, R. M. Watson, J. E. Cecil, S. J. Bale, J. G. Compton, J. J. DiGiovanna, P. Fleckman, S. Lewis-Jones, G. Arseculeratne, A. Sergeant, C. S. Munro, B. El Houate, K. McElreavey, L. B. Halkjaer, H. Bisgaard, S. Mukhopadhyay, W. H. I. McLean, Common loss-of-function variants of the epidermal barrier protein filaggrin are a major predisposing factor for atopic dermatitis. *Nat. Genet.* **38**, 441–446 (2006). doi:10.1038/ng1767 Medline

24. S. J. Brown, W. H. McLean, One remarkable molecule: Filaggrin. *J. Invest. Dermatol.* **132**, 751–762 (2012). doi:10.1038/jid.2011.393 Medline

25. D. J. Margolis, J. Gupta, A. J. Apter, T. Ganguly, O. Hoffstad, M. Papadopoulos, T. R. Rebbeck, N. Mitra, Filaggrin-2 variation is associated with more persistent atopic dermatitis in African American subjects. *J. Allergy Clin. Immunol.* **133**, 784–789 (2014). doi:10.1016/j.jaci.2013.09.015 Medline

26. S. Rahrig, J. M. Dettmann, B. Brauns, V. N. Lorenz, T. Buhl, S. Kezic, P. M. Elias, S. Weidinger, M. Mempel, M. P. Schön, A. Braun, Transient epidermal barrier deficiency and lowered allergic threshold in filaggrin-hornerin ($FlgHrnr^{-/-}$) double-deficient mice. *Allergy* **74**, 1327–1339 (2019). doi:10.1111/all.13756 Medline

27. X. F. C. C. Wong, S. L. I. J. Denil, J. N. Foo, H. Chen, A. S. L. Tay, R. L. Haines, M. B. Y. Tang, W. H. I. McLean, A. Sandilands, F. J. D. Smith, E. B. Lane, J. Liu, J. E. A. Common, Array-based sequencing of filaggrin gene for comprehensive detection of disease-associated variants. *J. Allergy Clin. Immunol.* **141**, 814–816 (2018). doi:10.1016/j.jaci.2017.10.001 Medline

28. C.-A. Lo, I. Kays, F. Emran, T.-J. Lin, V. Cvetkovska, B. E. Chen, Quantification of protein levels in single living cells. *Cell Rep.* **13**, 2634–2644 (2015). doi:10.1016/j.celrep.2015.11.048 Medline

29. C. G. Bunick, R. B. Presland, O. T. Lawrence, D. J. Pearton, L. M. Milstone, T. A. Steitz, Crystal structure of human profilaggrin S100 domain and identification of target proteins annexin II, stratifin, and HSP27. *J. Invest. Dermatol.* **135**, 1801–1809 (2015). doi:10.1038/jid.2015.102 Medline

30. S. F. Banani, A. M. Rice, W. B. Peeples, Y. Lin, S. Jain, R. Parker, M. K. Rosen, Compositional control of phase-separated cellular bodies. *Cell* **166**, 651–663 (2016). doi:10.1016/j.cell.2016.06.010 Medline

31. B. S. Schuster, E. H. Reed, R. Parthasarathy, C. N. Jahnke, R. M. Caldwell, J. G. Bermudez, H. Ramage, M. C. Good, D. A. Hammer, Controllable protein phase separation and modular recruitment to form responsive membraneless organelles. *Nat. Commun.* **9**, 2985 (2018). doi:10.1038/s41467-018-05403-1 Medline

32. T. Christensen, W. Hassouneh, K. Trabbic-Carlson, A. Chilkoti, Predicting transition temperatures of elastin-like polypeptide fusion proteins. *Biomacromolecules* **14**, 1514–1519 (2013). doi:10.1021/bm400167h Medline

33. B. R. McNaughton, J. J. Cronican, D. B. Thompson, D. R. Liu, Mammalian cell penetration, siRNA transfection, and DNA transfection by supercharged proteins. *Proc. Natl. Acad. Sci. U.S.A.* **106**, 6111–6116 (2009). doi:10.1073/pnas.0807883106 Medline

34. J. Jaubert, S. Patel, J. Cheng, J. A. Segre, Tetracycline-regulated transactivators driven by the involucrin promoter to achieve epidermal conditional gene expression. *J. Invest. Dermatol.* **123**, 313–318 (2004). doi:10.1111/j.0022-202X.2004.23203.x Medline

35. C. Bonnart, C. Deraison, M. Lacroix, Y. Uchida, C. Besson, A. Robin, A. Briot, M. Gonthier, L. Lamant, P. Dubus, B. Monsarrat, A. Hovnanian, Elastase 2 is expressed in human and mouse epidermis and impairs skin barrier function in Netherton syndrome through

filaggrin and lipid misprocessing. *J. Clin. Invest.* **120**, 871–882 (2010). doi:10.1172/JCI41440 Medline

36. P. Rompolas, K. R. Mesa, K. Kawaguchi, S. Park, D. Gonzalez, S. Brown, J. Boucher, A. M. Klein, V. Greco, Spatiotemporal coordination of stem cell commitment during epidermal homeostasis. *Science* **352**, 1471–1474 (2016). doi:10.1126/science.aaf7012 Medline

37. T. Kartasova, D. R. Roop, K. A. Holbrook, S. H. Yuspa, Mouse differentiation-specific keratins 1 and 10 require a preexisting keratin scaffold to form a filament network. *J. Cell Biol.* **120**, 1251–1261 (1993). doi:10.1083/jcb.120.5.1251 Medline

38. V. Kumar, J.-E. Bouameur, J. Bär, R. H. Rice, H.-T. Hornig-Do, D. R. Roop, N. Schwarz, S. Brodesser, S. Thiering, R. E. Leube, R. J. Wiesner, P. Vijayaraj, C. B. Brazel, S. Heller, H. Binder, H. Löffler-Wirth, P. Seibel, T. M. Magin, A keratin scaffold regulates epidermal barrier formation, mitochondrial lipid composition, and activity. *J. Cell Biol.* **211**, 1057–1075 (2015). doi:10.1083/jcb.201404147 Medline

39. C.-H. Lee, M.-S. Kim, B. M. Chung, D. J. Leahy, P. A. Coulombe, Structural basis for heteromeric assembly and perinuclear organization of keratin filaments. *Nat. Struct. Mol. Biol.* **19**, 707–715 (2012). doi:10.1038/nsmb.2330 Medline

40. M. P. Hughes, M. R. Sawaya, D. R. Boyer, L. Goldschmidt, J. A. Rodriguez, D. Cascio, L. Chong, T. Gonen, D. S. Eisenberg, Atomic structures of low-complexity protein segments reveal kinked β sheets that assemble networks. *Science* **359**, 698–701 (2018). doi:10.1126/science.aan6398 Medline

41. S. Noda, M. Suárez-Fariñas, B. Ungar, S. J. Kim, C. de Guzman Strong, H. Xu, X. Peng, Y. D. Estrada, S. Nakajima, T. Honda, J. U. Shin, H. Lee, J. G. Krueger, K.-H. Lee, K. Kabashima, E. Guttman-Yassky, The Asian atopic dermatitis phenotype combines features of atopic dermatitis and psoriasis with increased TH17 polarization. *J. Allergy Clin. Immunol.* **136**, 1254–1264 (2015). doi:10.1016/j.jaci.2015.08.015 Medline

42. T. J. Nott, E. Petsalaki, P. Farber, D. Jervis, E. Fussner, A. Plochowietz, T. D. Craggs, D. P. Bazett-Jones, T. Pawson, J. D. Forman-Kay, A. J. Baldwin, Phase transition of a disordered nuage protein generates environmentally responsive membraneless organelles. *Mol. Cell* **57**, 936–947 (2015). doi:10.1016/j.molcel.2015.01.013 Medline

43. M. Dzuricky, S. Roberts, A. Chilkoti, Convergence of artificial protein polymers and intrinsically disordered proteins. *Biochemistry* **57**, 2405–2414 (2018). doi:10.1021/acs.biochem.8b00056 Medline

44. R. Niesner, B. Peker, P. Schlüsche, K.-H. Gericke, C. Hoffmann, D. Hahne, C. Müller-Goymann, 3D-resolved investigation of the pH gradient in artificial skin constructs by means of fluorescence lifetime imaging. *Pharm. Res.* **22**, 1079–1087 (2005). doi:10.1007/s11095-005-5304-6 Medline

45. J. A. Mackay, D. J. Callahan, K. N. Fitzgerald, A. Chilkoti, Quantitative model of the phase behavior of recombinant pH-responsive elastin-like polypeptides. *Biomacromolecules* **11**, 2873–2879 (2010). doi:10.1021/bm100571j Medline

46. S. Alberti, Guilty by association: Mapping out the molecular sociology of droplet compartments. *Mol. Cell* **69**, 349–351 (2018). doi:10.1016/j.molcel.2018.01.020 Medline

47. S. Markmiller, S. Soltanieh, K. L. Server, R. Mak, W. Jin, M. Y. Fang, E.-C. Luo, F. Krach, D. Yang, A. Sen, A. Fulzele, J. M. Wozniak, D. J. Gonzalez, M. W. Kankel, F.-B. Gao, E. J. Bennett, E. Lécuyer, G. W. Yeo, Context-dependent and disease-specific diversity in protein interactions within stress granules. *Cell* **172**, 590–604.e13 (2018). doi:10.1016/j.cell.2017.12.032 Medline

48. I. Brody, An ultrastructural study on the role of the keratohyalin granules in the keratinization process. *J. Ultrastruct. Res.* **3**, 84–104 (1959). doi:10.1016/S0022-5320(59)80018-6 Medline

49. T. Makino, M. Takaishi, M. Morohashi, N. H. Huh, Hornerin, a novel profilaggrin-like protein and differentiation-specific marker isolated from mouse skin. *J. Biol. Chem.* **276**, 47445–47452 (2001). doi:10.1074/jbc.M107512200 Medline

50. P. M. Steinert, D. A. Parry, L. N. Marekov, Trichohyalin mechanically strengthens the hair follicle: Multiple cross-bridging roles in the inner root sheath. *J. Biol. Chem.* **278**, 41409–41419 (2003). doi:10.1074/jbc.M302037200 Medline

51. B. Mészáros, G. Erdős, B. Szabó, É. Schád, Á. Tantos, R. Abukhairan, T. Horváth, N. Murvai, O. P. Kovács, M. Kovács, S. C. E. Tosatto, P. Tompa, Z. Dosztányi, R. Pancsa, PhaSePro: The database of proteins driving liquid–liquid phase separation. *Nucleic Acids Res.* **48**, D360–D367 (2020). doi:10.1093/nar/gkz848 Medline

52. J. Kyte, R. F. Doolittle, A simple method for displaying the hydropathic character of a protein. *J. Mol. Biol.* **157**, 105–132 (1982). doi:10.1016/0022-2836(82)90515-0 Medline

53. J. R. McDaniel, J. A. Mackay, F. G. Quiroz, A. Chilkoti, Recursive directional ligation by plasmid reconstruction allows rapid and seamless cloning of oligomeric genes. *Biomacromolecules* **11**, 944–952 (2010). doi:10.1021/bm901387t Medline

54. A. C. Woerner, F. Frottin, D. Hornburg, L. R. Feng, F. Meissner, M. Patra, J. Tatzelt, M. Mann, K. F. Winklhofer, F. U. Hartl, M. S. Hipp, Cytoplasmic protein aggregates interfere with nucleocytoplasmic transport of protein and RNA. *Science* **351**, 173–176 (2016). doi:10.1126/science.aad2033 Medline

55. S. P. Boudko, T. Sasaki, J. Engel, T. F. Lerch, J. Nix, M. S. Chapman, H. P. Bächinger, Crystal structure of human collagen XVIII trimerization domain: A novel collagen trimerization Fold. *J. Mol. Biol.* **392**, 787–802 (2009). doi:10.1016/j.jmb.2009.07.057 Medline

56. A. Ghoorchian, N. B. Holland, Molecular architecture influences the thermally induced aggregation behavior of elastin-like polypeptides. *Biomacromolecules* **12**, 4022–4029 (2011). doi:10.1021/bm201031m Medline

57. N. Maas-Szabowski, A. Stärker, N. E. Fusenig, Epidermal tissue regeneration and stromal interaction in HaCaT cells is initiated by TGF-α. *J. Cell Sci.* **116**, 2937–2948 (2003). doi:10.1242/jcs.00474 Medline

58. J. A. Nowak, E. Fuchs, in *Stem Cells in Regenerative Medicine*. (Springer, 2009), pp. 215-232.

59. S. Beronja, G. Livshits, S. Williams, E. Fuchs, Rapid functional dissection of genetic networks via tissue-specific transduction and RNAi in mouse embryos. *Nat. Med.* **16**, 821–827 (2010). doi:10.1038/nm.2167 Medline

60. S. Sankaranarayanan, D. De Angelis, J. E. Rothman, T. A. Ryan, The use of pHluorins for optical measurements of presynaptic activity. *Biophys. J.* **79**, 2199–2208 (2000). doi:10.1016/S0006-3495(00)76468-X Medline

61. D. E. Johnson, H. W. Ai, P. Wong, J. D. Young, R. E. Campbell, J. R. Casey, Red fluorescent protein pH biosensor to detect concentrative nucleoside transport. *J. Biol. Chem.* **284**, 20499–20511 (2009). doi:10.1074/jbc.M109.019042 Medline

62. I. Nemoto-Hasebe, M. Akiyama, T. Nomura, A. Sandilands, W. H. I. McLean, H. Shimizu, FLG mutation p.Lys4021X in the C-terminal imperfect filaggrin repeat in Japanese patients with atopic eczema. *Br. J. Dermatol.* **161**, 1387–1390 (2009). doi:10.1111/j.1365-2133.2009.09406.x Medline

63. D. T. Jones, D. Cozzetto, DISOPRED3: Precise disordered region predictions with annotated protein-binding activity. *Bioinformatics* **31**, 857–863 (2015). doi:10.1093/bioinformatics/btu744 Medline

64. D. J. Scott, N. J. Gunn, K. J. Yong, V. C. Wimmer, N. A. Veldhuis, L. M. Challis, M. Haidar, S. Petrou, R. A. D. Bathgate, M. D. W. Griffin, A novel ultra-stable, monomeric green fluorescent protein for direct volumetric imaging of whole organs using clarity. *Sci. Rep.* **8**, 667 (2018). doi:10.1038/s41598-017-18045-y Medline

65. C. M. Nunn, M. Jeeves, M. J. Cliff, G. T. Urquhart, R. R. George, L. H. Chao, Y. Tscuchia, S. Djordjevic, Crystal structure of tobacco etch virus protease shows the protein C terminus bound within the active site. *J. Mol. Biol.* **350**, 145–155 (2005). doi:10.1016/j.jmb.2005.04.013 Medline

66. W. Wang, C. P. Wildes, T. Pattarabanjird, M. I. Sanchez, G. F. Glober, G. A. Matthews, K. M. Tye, A. Y. Ting, A light- and calcium-gated transcription factor for imaging and manipulating activated neurons. *Nat. Biotechnol.* **35**, 864–871 (2017). doi:10.1038/nbt.3909 Medline

67. M.-T. Wei, S. Elbaum-Garfinkle, A. S. Holehouse, C. C.-H. Chen, M. Feric, C. B. Arnold, R. D. Priestley, R. V. Pappu, C. P. Brangwynne, Phase behaviour of disordered proteins underlying low density and high permeability of liquid organelles. *Nat. Chem.* **9**, 1118–1125 (2017). doi:10.1038/nchem.2803 Medline